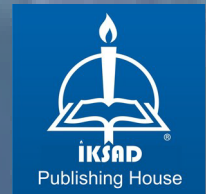# CURRENT STUDIES AT POSITIVE SCIENCES

EDITED BY
Dr. Mehriban EMEK, Dr. E. İlhan ŞAHİN

AUTHORS

Prof. Dr. Ali Fazıl YENİDÜNYA
Prof. Dr. Hüseyin PEKER
Prof. Dr. Mehmet KUL
Prof. Dr. Ömer ŞAHİN
Prof. Dr. Pınar BAŞER
Prof. Dr. Rıdvan EZENTAŞ
Assoc. Prof. Dr. Hilal ÇELİK KAZICI
Assoc. Prof. Dr. Mehmet Sait İZGİ
Assoc. Prof. Dr. Orhan BAYTAR
Assoc. Prof. Dr. Özlem AKSOY
Assoc. Prof. Dr. Rasim Erol DEMİRBATIR
Asst. Prof. Dr. Bülent ÜNAL
Asst. Prof. Dr. Ebru YABAŞ
Asst. Prof. Dr. Elif GÜNEŞ
Asst. Prof. Dr. İpek MEMİKOĞLU
Asst. Prof. Dr. Mustafa DEMİRBİLEK
Dr. Lecturer Hatice ULUSOY
Res. Asst. Dr. Serap ÇETİNKAYA
Dr. Selçuk DUMAN
Dr. Yunus DOĞAN
Lecturer Fırat SALMAN
Lecturer Müge YAYLA
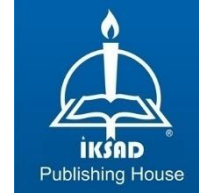Res. Asst. Salih DİKİLİTAŞ
Oğuzhan GİRGİN

İKSAD
Publishing House

CURRENT STUDIES AT POSITIVE SCIENCES

EDITED BY

Dr. Mehriban EMEK, Dr. E. İlhan ŞAHİN

AUTHORS

Prof. Dr. Ali Fazıl YENİDÜNYA
Prof. Dr. Hüseyin PEKER
Prof. Dr. Mehmet KUL
Prof. Dr. Ömer ŞAHİN
Prof. Dr. Pınar BAŞER
Prof. Dr. Rıdvan EZENTAŞ
Assoc. Prof. Dr. Hilal ÇELİK KAZICI
Assoc. Prof. Dr. Mehmet Sait İZGİ
Assoc. Prof. Dr. Orhan BAYTAR
Assoc. Prof. Dr. Özlem AKSOY
Assoc. Prof. Dr. Rasim Erol DEMİRBATIR
Asst. Prof. Dr. Bülent ÜNAL
Asst. Prof. Dr. Ebru YABAŞ
Asst. Prof. Dr. Elif GÜNEŞ
Asst. Prof. Dr. İpek MEMİKOĞLU
Asst. Prof. Dr. Mustafa DEMİRBİLEK
Dr. Lecturer Hatice ULUSOY
Res. Asst. Dr. Serap ÇETİNKAYA
Dr. Selçuk DUMAN
Dr. Yunus DOĞAN
Lecturer Fırat SALMAN
Lecturer Müge YAYLA
Res. Asst. Salih DİKİLİTAŞ
Oğuzhan GİRGİN

CONTENTS

PREFACE

Scientific studies meets with researches in different forms such as articles, proceedings and book chapters. Each forms, each projects reflect the lights of inner knowledges of researches. We proud of being editors of this book which has excellent chapters. It is obvious that authors submit their professional experiences and knowledges' results. In this book there are 13 chapters

At first chapter we read Asst. Prof. Dr. Mustafa DEMİRBİLEK's study entitled A MATHEMATICAL MODEL and HEURISTIC SOLUTION APPROACH FOR VEHICLE ROUTING PROBLEM with SIMULTANEOUS PICKUP and DELIVERY

At second, Assoc. Prof. Dr. Rasim Erol DEMİRBATIR & Prof. Dr. Rıdvan EZENTAŞ shares their chapter with us "A STUDY ON THE 3D GEOMETRIC MODEL OF THE ADNAN SAYGUN' OP. 33 DEMET SUİTE PRELUD SECTİON"

3rd chapter is A NOVEL NAGINI ROBOT DESIGNING written by Oğuzhan GİRGİN and Dr. Yunus DOĞAN

At 4th chapter we read another excellent study AFFORDANCE AND RESTORATIVE DIMENSIONS OF THE BUILT ENVIRONMENT AS SOURCES OF ENVIRONMENTAL STRESSOR of Dr. Bülent ÜNAL, Dr. İpek MEMİKOĞLU, Dr. Elif GÜNEŞ

The next chapter is γ-Al $_2$ O $_3$ -SUPPORTED MATERIALS FOR CATALYZING THE HYDROLYTIC DEHYDROGENATION OF

AMMONIA BORANE written by Assoc Prof. Dr. Mehmet Sait İzgi, Assoc Prof Dr. Orhan BAYTAR, Lecturer Müge YAYLA, Dr. Hilal ÇELİK KAZICI, Prof. Dr. Ömer ŞAHİN

At 6th chapter, Asst. Prof. Dr. Ebru YABAŞ, Prof. Dr. Pınar BAŞER, Prof. Dr. Mehmet KUL's study "New Generation Chemical Materials: Synthesis and Properties for Energy Applications" is also extremely usefull research

At 7th chapter EFFECT OF SOME MORDAN/BORIC ACID IMPREGNATION (DIFFUSION/VACUUM) ON RETENTION / DENSITY ON WOOD is another original research written by Professor Dr. Hüseyin PEKER and Doctor Lecturer Hatice ULUSOY

Professor Dr. Hüseyin PEKER and Doctor Lecturer Hatice ULUSOY's second chapter, but books 8th chapter is IMPREGNATION (STONE WATER) ON WOOD AND VARIOUS PHYSICAL PROPERTIES AT SOME VACUUM/DIFFUSION TIMES

At 9 th chapter THE IMPORTANCE OF DEVELOPING HYDROGEN PEROXIDE SENSOR AND DETERMINATION OF CANDIDATE SENSOR WITH VARIOUS MULTI-METALLIC SUPPORTED CATALYSTS written by Assoc. Prof. Dr. Mehmet Sait İZGİ, Lecturer Fırat SALMAN, Assoc. Prof. Dr. Hilal ÇELİK KAZICI

The next chapter is SPECIES IDENTIFICATION ABILITIES OF NUCLEAR AND PLASTID DNA REGIONS, THEIR IMPORTANCE IN PHYLOGENETIC RELATIONSHIPS AMONG *COLCHICUM* L. SPECIES written by Asst. Prof. Aykut YILMAZ

At 11 th chapter EFFECTS OF PESTICIDES ON HEMATOLOGICAL AND IMMUNOLOGICAL SYSTEM IN FISH written by Dr. Selçuk DUMAN

At 12 th chapter FOOD COLORANTS AND THEIR TOXIC EFFECTS written by Res. Asst. Salih DİKİLİTAŞ and Assoc. Prof. Dr. Özlem AKSOY

Last chapter of book is STRUCTURE AND FUNCTION OF PROTON PUMPS written by Res. Asst. Dr. Serap ÇETİNKAYA and Prof. Dr. Ali Fazıl YENİDÜNYA

We thank to all authors for their contribution on scientific literature

Dr. Mehriban EMEK, Dr. E. İlhan ŞAHİN

CHAPTER 1

A MATHEMATICAL MODEL and HEURISTIC SOLUTION APPROACH FOR VEHICLE ROUTING PROBLEM with SIMULTANEOUS PICKUP and DELIVERY

Asst. Prof. Dr. Mustafa DEMİRBİLEK[1]

[1] Assistant Professor, Gaziantep Islam Science and Technology University, Faculty of Engineering and Natural Sciences, Department of Industrial Engineering, mustafa.demirbilek@gibtu.edu.tr

1. INTRODUCTION

Vehicle Routing Problem (VRP) can be simply defined as finding the shortest route between a depot and geographically scattered points by satisfying a set of constraints. VRP has been attracted many researchers' attentions since the study of Dantzig and Ramster [1], "The Truck Dispatching Problem", published in 1959. They targeted to satisfy demands of fuel stations when minimizing total travel times of a given truck fleet. A linear programming approach is used to solve the problem. Since then, many different types of VRP such as VRP with Time Windows, Stochastic VRP, Multi Depot VRP, Periodic VRP, Dynamic VRP, and different combinations of these have been studied. Not only problem types are evolved, but also a variety of solution methodologies are developed. Exact solution methods such as Branch-and-Bound Algorithms [2], Dynamic Programming [3], Set Partitioning Formulations and Algorithms, Commodity Flow Formulations and Algorithms and heuristic/metaheuristic solution methods such as The Savings Algorithm, Cluster-First-Route-Second Heuristics, Local Search, Population Search algorithms have been proposed over 50 years [4].

VRP with simultaneous pickup and delivery (VRPSPD) is getting attentions among other VRPs due to scarce resources, environmental sensitivities, and regulations. In the VRPSPD, vehicles are delivering as well as collecting goods at the same time. Each day in the planning horizon, a given number of vehicles start their travels from a depot, deliver and pick up goods to/from customers by visiting them only

once, and they return the depot at the end of day. As classical VRPs, the aim is to minimise total distances as well as to maximise total number of visited customers by considering the capacity of each vehicle [5][6]. The online order system of grocery stores is a good example for VRPSPD. Orders are distributed to customers while same vehicles pick up undated goods or empty bottles. Another sector as an example for VRPSPD is the reverse logistics. Because of regulations, some companies are responsible products during their whole life cycles (as in the disposal of laser printers' cartridges) [7].

In this study, we propose a mixed integer linear programming formulation and a heuristic solution method for VRPSPD. The objective is to minimise travelling distances under constraints of working times and capacities of vehicles. Since the classical VRP as well as its extensions (included VRPSPD) are NP-Hard problems [5][6][7], exact solution methods work for small instances. Therefore, the cheapest insertion heuristic is proposed as well. The performance of the insertion heuristic is compared to the exact solution method under different number of customers and capacity of vehicles.

2. SOLUTION METHODOLOGIES

As we mentioned before, we proposed a mixed integer linear programming and a heuristic solution method for the problem. Therefore, the mathematical formulation is explained at first. Next, the heuristic solution method is represented.

2.1. The Mathematical Formulation

We have *n* customers that must be visited by *k* homogeneous vehicles. Each customer has a certain amount of pickup and delivery. When a vehicle visits a customer, the amount of pickup and delivery of a customer cannot exceed capacity of the vehicle. Each vehicle spends 5 minutes for servicing at each customer location. Daily working time (T) for each vehicle is 480 minutes. Vehicles start and return the depot. The mathematical formulation for VRPSPD is mostly taken from the study of Montane and Galvao [7]. Followings show notations and decision variables:

Notations:

V: set of customers

V_0: set of customers and the depot

K: set of vehicles

c_{ij}: distance between locations of customers *i* and *j*

p_j: pickup demand of customer $j, \forall j \in V$

d_j: delivery demand of customer $j, \forall j \in V$

Q: vehicle capacity

T: working time limit for vehicles

S: Service time

Decision Variables:

$x_{ijk} = 1$, if vehicle *k* moves from customer *i* to *j*. 0, otherwise.

$y_{ij} = $ Cumulative amount of pickup at node *i* and transported in arc (*i, j*)

$z_{ij} = $ Cumulative amount of delivery at node i and transported in arc (i, j)

The corresponding mathematical formulation is given by

Minimize:

$$\sum_{k}^{K}\sum_{i}^{V_0}\sum_{j}^{V_0} c_{ij}x_{ijk}, \quad i \neq j$$

Subject to:

$$\sum_{k}^{K}\sum_{i}^{V_0} x_{ijk} = 1, \quad \forall j \in V$$

$$\sum_{i}^{V_0} x_{ijk} - \sum_{i}^{V_0} x_{jik} = 0, \quad \forall j \in V_0, \forall k \in K, i \neq j$$

$$\sum_{j}^{V} x_{0jk} \leq 1, \quad \forall k \in K$$

$$\sum_{i}^{V_0} y_{ij} - \sum_{i}^{V_0} y_{ij} = p_j, \quad \forall j \in V$$

$$\sum_{i}^{V_0} z_{ij} - \sum_{i}^{V_0} z_{ij} = d_j, \quad \forall j \in V$$

$$y_{ij} + z_{ij} \leq Q \sum_{k}^{K} x_{ijk}, \qquad \forall i, \forall j \in V$$

$$\sum_{i}^{V_0} \sum_{j}^{V_0} c_{ij} x_{ijk} + S \sum_{i}^{V_0} \sum_{j}^{V_0} x_{ijk} \leq T, \quad \forall k \in K, i \neq j$$

$$x_{ijk} \in \{0,1\}, \quad \forall i, \forall j \in V_0, \forall k \in K, \ i \neq j$$

$$y_{ij}, z_{ij} \geq 0, \quad \forall i, \forall j \in V_0, \ i \neq j$$

The objective function (1) is to minimize total distance. Constraints (2) make sure that each customer is visited by exactly one vehicle. Constraints (3) ensure that the same vehicle arrives and departs from each customer. Constraints (4) show the maximum number of vehicles allowed. Constraints (5) and (6) are flow equations for pick-up and delivery, respectively; they guarantee that both are satisfied for each customer. Constraints (7) ensure that pickup and delivery demands do not exceed capacity of the vehicle moving from customer *i* to *j*. Constraints (8) show travelling and service times for a vehicle do not exceed the allowed working time. Constraints (9) and (10) demonstrate boundaries of decision variables.

2.2. The Heuristic Algorithm

As we mentioned before, exact solution methods work for small instances since VRP and its extensions are in NP Hard class. When the

number of decision variables and constraints increase, dimension of the problems increase exponentially. After exceeding a certain number of customers and vehicles, finding solutions for problems take so long or impossible [5]. Therefore, metaheuristic and heuristic methods are generally used for solutions of NP Hard class problems if size of the problem is relatively high.

In this study, we propose an insertion heuristic as a solution method. The idea behind the method is to add a node (customer) to the existing tour by increasing overall tour length at minimum level. Thus, the algorithm calculates insertion cost (11) of each candidate node when inserting it into intervals in the tour.

Insertion cost = $C_{12} + C_{23} - C_{13}$

Let us assume that there are two customers, 1 and 3, and Euclidian distance between these two customers is C_{13}. If a new customer, 2, arrives to system and Euclidian distances between customer 1 and 2, and 2 and 3 are represented by C_{12} and C_{23} respectively, the cost of inserting customer 2 between 1 and 3 is calculated with Equation 11. If we have more than one customer, the algorithm calculates insertion cost of each customer, select the customer with the cheapest insertion cost, insert it into the corresponding interval and repeat this procedure for the remaining customers. Note that the algorithm also checks capacity and time constraints for the vehicle before assigning customers into the tour. Pseudo-code for the cheapest insertion heuristic is given in Figure 1.

Each iteration in while loop (3-23), insertion cost of each customer (5-20) is calculated for each vehicle (7-15) and check whether they satisfy capacity and time constraints. Next, the customer with the cheapest insertion cost and satisfying constraints is inserted into the tour of vehicle and same procedure is repeated for the remaining customers.

3. NUMERICAL ANALYSIS AND RESULTS

We use different test instances for both solution methodologies. There are total 45 customers distributed randomly in a coordinate system (X_1=1, Y_1=1, X_2=60, Y_2=60) with delivery demand assigned uniformly between 3 and 9 packages, and pickup demand assigned uniformly between 1 and 8 packages as shown in Table 1. We have different number of vehicles depending on the number of customers with three capacity levels, 50, 80, and 100 packages. The mixed integer linear programming (MILP) is coded with AMPL (A mathematical programming language) IDE 3.5 software and solved with CPLEX 12.9. The cheapest insertion heuristic (CIH) is coded with Python programming language. Both are solved in a PC with Intel i5 7200U 2.5 GHz CPU and 8 GB Ram.

Table 2 shows results of the MILP and CIH under test samples covering different number of customers, vehicles, and capacity of vehicles. We also provide execution times for MILP (MTime) and CIH (HTime) for each test sample. Differences between solutions of MILP and CIH vary between 0.97% and 23.95%. The number of customers exceeds 35, the

execution time for MILP significantly increases. When capacity of vehicles is 50 and the number of

Figure 1. Pseudo-code for the cheapest insertion heuristic

Algorithm 1 The cheapest insertion heuristic

1: Set Customers (V)
2: Set Vehicles (K)
3: **while** Customers list is not empty **do**
4:       MinCustomerCost ← ∞
5:     **for** n= 1 To V **do**
6:         MinVehicleCost ← ∞
7:        **for** k= 1 To K **do**
8:            Calculate insertioncost of Customers[n] for Vehicles[k]
9:            **if** insertionCost =< MinVehicleCost **then**
10:               **if** n satisfies capacity and time constraints for Vehicles[k]
    then
11:                   MinVehicleCost←insertionCost
12:                   Index←k
13:               **end if**
14:           **end if**
15:         **end for**
16:         **if** MinVehicleCost =< MinCustomerCost **then**
17:             MinCustomerCost←MinVehicleCost
18:             CustomerIndex←n
19:         **end if**
20:     **end for**
21:     Vehicles [Index]← Customers[CustomerIndex]
22:     Remove Customers[CustomerIndex] from Customers list
23: **end while**

Table 1. Location and delivery-pickup demands of customers

Customer	X	Y	Delivery	Pickup	Customer	X	Y	Delivery	Pickup
1	25	43	4.81	1.00	24	27	35	4.42	3.86
2	9	6	5.07	2.30	25	54	34	6.70	1.02
3	24	32	7.11	3.93	26	20	32	5.14	7.20
4	13	52	7.02	1.19	27	54	37	8.58	1.11
5	25	33	4.19	1.98	28	41	59	3.82	2.21
6	48	58	7.15	3.19	29	56	42	7.53	1.46
7	52	53	3.23	1.60	30	45	55	3.75	5.98
8	11	52	5.53	1.69	31	2	2	4.48	1.20
9	57	32	4.89	5.84	32	51	32	8.05	4.87
10	41	50	7.50	1.13	33	8	17	8.82	5.10
11	59	45	7.74	2.96	34	34	2	4.40	6.60
12	7	27	4.76	7.36	35	48	23	7.48	7.04
13	17	8	7.07	1.14	36	33	9	3.73	1.42
14	13	16	3.32	4.44	37	3	7	7.28	2.58
15	34	9	7.20	5.13	38	34	1	8.80	1.50
16	7	25	5.49	5.86	39	34	12	7.46	2.77
17	3	32	6.09	5.65	40	12	35	8.08	7.79
18	56	35	3.82	7.32	41	15	30	7.97	5.34
19	9	48	3.99	3.78	42	10	2	5.92	1.49
20	55	21	7.36	6.26	43	36	34	8.93	3.22
21	53	37	5.09	6.26	44	35	23	7.47	4.86
22	16	53	8.79	4.00	45	40	16	5.22	1.46
23	40	37	8.70	1.80					

customers are more than 30, CPLEX cannot find the optimal solution in 7200-second execution time. When the number of customers is 45, CPLEX cannot find optimal solutions in predetermined execution time under all scenarios. Although optimal solution cannot be observed for

MIP when size of customer set increases, solutions provided by CPLEX are still better than solutions of CIH. Another issue is that the gap between results get wider as capacity of vehicles decreases as shown in Figure 1. The possible reason can be that CIH is not good to distribute customers to vehicles since we need more vehicles when capacity of vehicles decreases. Finally, when comparing execution times for both methods, CIH can provide near optimal solution below a second even when the number of customers and vehicles are the highest level in this study.

Table 2. Results of MIP and CIH and execution times under different test settings (* suboptimal, **Etime, Htime**: Executions times for MILP and CIH respectively)

No Customer	No Vehicle	Capacity	MILP Solution	CIH Solution	%	MTime (sec)	HTime (sec)
10	3	50	241.66	283.51	17.32	1.25	0.02
10	2	80	233.46	235.73	0.97	0.62	0.11
10	2	100	233.46	235.73	0.97	0.47	0.02
15	3	50	298.45	303.17	1.58	2.69	0.01
15	2	80	286.20	336.97	17.74	0.79	0.02
15	2	100	279.80	284.57	1.70	1.52	0.04
20	3	50	367.66	440.94	19.93	3.92	0.06
20	2	80	334.78	370.59	10.70	3.27	0.03
20	2	100	334.78	387.87	15.86	1.25	0.02
25	4	50	433.95	529.46	22.01	1549.10	0.27
25	2	80	375.99	434.41	15.54	3.36	0.04
25	2	100	369.85	423.04	14.38	2.31	0.05
30	4	50	483.16	598.89	23.95	319.33	0.30
30	3	80	434.96	518.99	19.32	8.22	0.09

30	2	100	411.09	454.16	10.48	7.59	0.08
35	6	50	593.55*	702.25	18.32	7204.07	0.69
35	3	80	511.23	584.54	14.34	238.19	0.22
35	3	100	491.04	569.95	16.07	101.23	0.25
40	6	50	709.60*	768.10	8.24	7203.95	0.23
40	4	80	564.61	680.87	20.59	7204.37	0.34
40	3	100	538.34	634.11	17.79	470.80	0.31
45	7	50	729.52*	846.32	16.01	7207.73	0.66
45	5	80	620.56*	718.91	15.85	7207.78	0.30
45	4	100	591.46*	707.58	19.63	7206.64	0.83

Figure 1. Results of MILP and CIH under different test settings
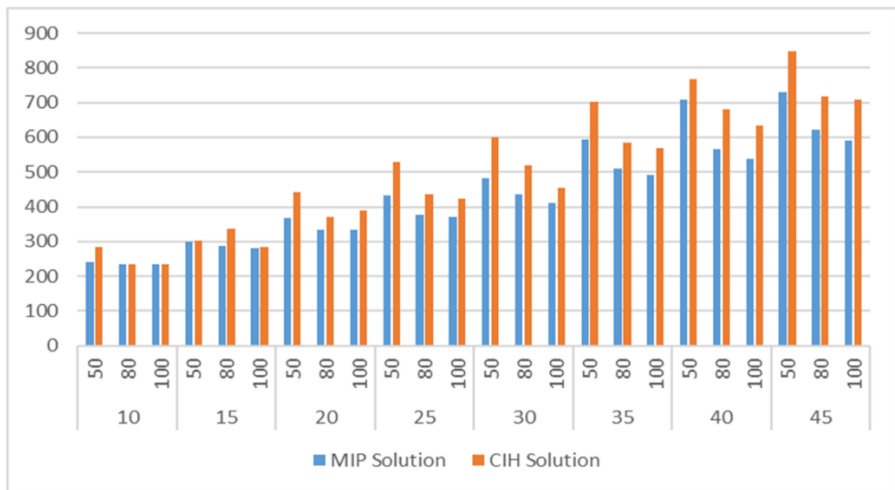
4. CONCLUSION

In this study, we examined Vehicle Routing Problem with Simultaneous Pickup and Delivery (VRPSPD) and two solution methods, the mixed integer linear programming and the cheapest

insertion heuristic. VRPSPD is very important to be able to decrease distribution cost of companies that provide pickup and delivery services for customers at the same time. VRPSPD is in NP Hard class and the exact solution methods work for only small problem instances. For large problem sets, heuristic and metaheuristic methods are used to find optimal/near optimal solutions. To be able to compare two solution methods, first we provide mathematical formulation. The mathematical model is coded in AMPL ide and solved by CPLEX 12.9. Next, the cheapest insertion heuristic is coded by considering capacity and time constraints. Both methods are evaluated by considering different number of customers, 10 to 45, vehicles, 2 to 7, and capacity levels, 50, 80, and 100. According to results, MILP provides up to 24% shorter travel distances compared to CIH even though some its results are suboptimal. Note that MILP does not find optimal solution when the number of customers starts to exceed 40. CIH can find near optimal solutions below one second in each scenario while it takes around 2 hours for MILP.

Although CIH is a good greedy algorithm to solve VRP and its extensions, it is highly possible that CIH as other greedy algorithms do gets stuck at local optima. Therefore, some metaheuristic algorithms can be examined in future studies. Since CIH is an effective construction heuristic, it can be used as an initial solution for a prospective metaheuristic algorithm.

REFERENCES

[1] G. B. Dantzig and J. H. Ramser, "The Truck Dispatching Problem." 1959.

[2] J.-L. Beuchat, M. Shirase, T. Takagi, and E. Okamoto, "An Algorithm for the η," *IACR Cryptol. ePrint Arch.*, vol. 2006, no. c, p. 327, 2006.

[3] B. Columbus, "Book Reviews," no. September, pp. 558–559, 1972.

[4] G. Laporte, "Fifty years of vehicle routing," *Transp. Sci.*, vol. 43, no. 4, pp. 408–416, 2009.

[5] F. P. Goksal, I. Karaoglan, and F. Altiparmak, "A hybrid discrete particle swarm optimization for vehicle routing problem with simultaneous pickup and delivery," *Comput. Ind. Eng.*, vol. 65, no. 1, pp. 39–53, 2013.

[6] J. F. Chen and T. H. Wu, "Vehicle routing problem with simultaneous deliveries and pickups," *J. Oper. Res. Soc.*, vol. 57, no. 5, pp. 579–587, 2006.

[7] F. A. T. Montané and R. D. Galvão, "A tabu search algorithm for the vehicle routing problem with simultaneous pick-up and delivery service," *Comput. Oper. Res.*, vol. 33, no. 3, pp. 595–619, 2006.

CHAPTER 2

A STUDY ON THE 3D GEOMETRIC MODEL OF THE ADNAN SAYGUN' OP. 33 DEMET SUİTE PRELUD SECTİON

Assoc. Prof. Dr. Rasim Erol DEMİRBATIR [1],
Prof. Dr. Rıdvan EZENTAŞ [2]

[1] Bursa Uludağ Üniversitesi, Eğitim Fakültesi Müzik Eğitimi ABD, Bursa, Turkey. redemir@uludag.edu.tr
[2] Bursa Uludağ Üniversitesi, Eğitim Fakültesi Matematik Eğitimi ABD, Bursa, Turkey. rezentas@uludag.edu.tr

INTRODUCTION

It is believed that it was the Ancient Greeks who developed the first theories of music. In Ancient Greece, where music and dance played an important role in people's lives, it is known that poets sing epics accompanied by lyre. The word music is derived from the name of the Musees, believed to be the goddesses of art in ancient Greece. In the meantime, the word mousike was defined as a general term used for every branch of art or science under the protection of Muses (Mann & Newsom, 2000). Music is an aesthetic whole consisting of sounds combined with a certain purpose and method and processed according to a certain understanding of beauty (Uçan, 1994).

Mathematics, on the other hand, parallel to his research on the competence and accuracy of intellectual knowledge, aesthetically also investigates the accuracy of affective knowledge, that is, beauty. The beauty inherent in mathematics is very important for mathematicians, and it is called the aesthetics of mathematics. Perspective, ratio, symmetry, order, harmony can be measured in all conditions. Art also has measurable aspects, which include the numbers of nature with mathematically expressed symmetry. These concepts constitute the aesthetics of mathematics. Measurements related to these concepts can be formulated in various areas of expertise in mathematics. The principles of mathematics are used in the examination of perspectives, proportions, shapes and symmetries, which are the basis of art and science. Therefore, the use of mathematical rules is not only useful, but also a necessity (Atalay, 2006).

Music includes a variety of mathematical structures, from the most basic to the most complex. Music and mathematics are two interrelated disciplines in many respects. It is thought that the first academic studies on these two disciplines began in the 6th century BC with the Greek philosopher and mathematician Pythagoras. The systematic structure of the relations between the sounds that Pythagoras put forward with the discovery of various numerical ratios between the frequencies of the sounds constitutes the basis of music theory (Riedweg, 2005). Realizing that the sound depends on the length of the string drawn, Pythagoras established the relationship between harmony and integers in music. Each harmonic composition of the really drawn wires can be shown as the ratio of integers. For example, 16/15 of the length of a wire that produces the do sound gives the sound of 6, while 5/5 la sound, 4/3 left sound, 3/2 fa sound, 8/5 mi sound, 16/9 of them give re sound. This reveals the legitimacy of Leibniz, who says that music is a secret arithmetic exercise (Orhan, 1995).

Until today, many philosophers, mathematics and music people have been researching the relationship between these two disciplines, and the mathematical structure of music has been tried to be understood. Generally, some musical concepts such as diatonic and chromatic sequence, intervals, rhythm, measure, form, melody, chords, sequence, octave equivalence, nativities, timbre, acoustic, equally spaced sound system and alternative methods of accord are mathematically explained (Wright, 2009).

It is known that the shape of many musical instruments is also related to mathematical concepts. For example; The shapes of stringed or wind instruments are similar to the graph of $x \geq 0$ and $y = 2x$ exponential curve. The study of the quality of musical sounds was made by the mathematician J. Fourier in the 19th century. Fourier proved that the musical instrument and all musical sounds emanating from human beings can be defined with mathematical expressions and this can be done with periodic sinus functions (Orhan, 1995).

The piano keys allow visual explanation of the connection between the Fibonacci series (1,1,2,3,5,8,13,21,34,…) and the music created by the Italian mathematician L. Fibonacci. An octave on the keyboard represents the musical interval between two notes, one higher than the other. The frequency of the higher note is twice the lower one. The keyboard is divided into one octave, 5 black and 8 white keys, with a total of 13 keys. Five black keys are divided into two groups, one double and one triple. 2, 3, 5, 8 and 13 are Fibonacci Numbers. Thirteen notes in octave form make up the chromatic sequence, the most popular range in Western music. The chromatic sequence precedes the 5-point pentatonic sequence and the 8-point diatonic sequence. For example, the big six are composed of do and la notes, respectively, they make 264 and 440 vibrations per second, 264/440 = 3/5 is a Fibonacci ratio. A small hexadecimal range consists of the notes mi and do and vibrates 330 and 528 per second 330/528 = 5/8 Fibonacci ratio (Koshy, 2001).

The ratio of two consecutive numbers in the Fibonacci sequence is approximately $\phi = 1.61804$, called the golden ratio. Golden ratio is a classification of art and aesthetics as a measure of harmony and beauty. The golden ratio is a biological fact that exists in nature, without being caused by human design, and it is known to be used in music. Musical instruments are also often made based on the number ϕ. As with the violin design, Fibonacci Numbers and ϕ were used in the design of the high quality vocal cord. In addition, it is assumed that many famous composers (Mozart, Beethoven, Bach, Chopin, Béla Bartók, ...) use Fibonacci Sequence and Golden Ratio in their works and it is tried to be proved. For example, it was proved that Mozart used the golden ratio in the works of No1.K.279, No2.K.280, No7.K.309, No10.K.330, No15.K.545, No16.K.570. In addition, there are composers who use the Fibonacci series consciously and indicate it (Lehmann and Posamentier, 2007).

The feature that distinguishes musical sounds from noise is that musical sounds have the feature of giving a distinctive pitch. The pitch is the parameter of the sound, which shows information about the level of treble. The criterion of the perception of a screen related to a sound is the degree of periodic (term) of that sound. With the ability of human beings to hear and imitate the sound they hear, the music obtained from the melodic and beautiful audio sequences is based on certain basic concepts. These basic concepts can be explained with classical music theory and terminology at the first stage. Just like visually complex forms in music, music is an aesthetic form of auditory perception.

Fractal is defined as a form that repeats itself within a specific mathematical formula. Fractal geometry is to provide a mathematical explanation for the complex forms of the forms that exist in nature. In 2015, Beytekin applied the logic of Fractal Geometry algorithm to the modern jazz theory, analyzed the harmonies without mixing the rhythm phenomenon and created the visual models of the jazz chords. Design processes have established connections between the models created and psychological perception processes (Beytekin, 2015).

Today, there are studies examining the relationship between music and mathematics through geometric modeling, but it is seen that such studies have been carried out on a small scale in our country. Gülsoy, Güney and Özdamar In 2013, Beethoven's "Vierte Symphony, Op. 60" symphony was performed by math coding, and the regression model of the Furink work was a manifold in Minkowski space (Gülsoy et al. 2013).

Ahmet Adnan Saygun (1907-1991), who is one of the important names of the polyphonic music of the Republican Period in our country, is the first composer of modern Turkish music and the first artist to have received the title of State Artist (www.wikipedia.com). Saygun, who was born in İzmir on September 7, 1907, is one of the cornerstones of Turkish music life as a composer, ethnomusicologist and music educator in our country. Forty years have given examples in a wide variety of music forms without interruption and with the same productivity. He also has music studies in folklore and

ethnomusicology, and his book "Folk Music Research in Turkey" with Bela Bartok (www.turkcebilgi.com).

The Op.33 Demet suite for violin and piano composed by Saygun in 1956 is among the most popular works of contemporary Turkish music. The composer's work, which was given during the middle creation period, brings together various folk dances in suite form and evokes the composer approaches of the first creation period. On the other hand, in the 1930s, he moved away from French resonance, which clearly showed himself in Saygun's music. Where he sings, the violin refers to the melody of the composer's stage works. The harmonies and figurative elements heard in piano accompaniment now fall away from the Impressionist attitude and approach the operatic language as in the violin. Bartók-inspired rhythmic and maqam sheer, a language that speaks directly.This form of musical expression is one of the first examples of a classic that has become a classic in contemporary Turkish music and frequently used by other composers in the following years (Aydın, 2018).

Demet Suite, which Saygun dedicated to his friends Henri and Henriette Guilloux during his teaching at the Ankara State Conservatory, consists of four sections, each lasting about four minutes. The work takes its source from Turkish folk music. However, these elements have been processed with a different polyphony understanding and have gained a new identity. Part I is an introductory music, prelude, in a heavy and wide (Lento) tempo. His style evokes a kind of improvisation and a taxis that started the Aydın Ağır Zeybeği with two zurnas. Part 2 Horon

is the development of the input music played with the fiddle before the black sea song is processed in a live (Vivo) tempo. Part 3 is an Aegean Zeybeği at a very slow pace. Part 4 is inspired by Sepetçioğlu, who elegantly reflects the melody and play atmosphere of Kastamonu region. Demet, first voiced by Suna Kan and Ferhunde Erkin, was taped on Ankara Radio on January 12, 1964 (Aktüze, 2003).

Mathematical coding and analysis of musical works, analysis of the works by means of computer-aided software, production of different approaches and providing opportunities for working between the disciplines are considered useful. In this sense, it is seen as an innovative approach to transform the abstract sounds into a concrete by transferring them to a geometric environment, and to perform structural analyzes by considering the height and duration values of the sounds that make up the works in different combinations. The aim of working with this perspective; A. Adnan Saygun's Op.33 Demet suite is the creation of the 3D geometric model of the violin party of the Prelude section through mathematical coding.

METODOLOGY

In this study, regression analysis of the mathematical coding of the note sound heights and sound durations of the violin party of the prelude section of A. Adnan Saygun's Op.33 Demet suite was performed and the most appropriate geometric modeling was performed. Regression analysis is used to explain the relationship between a dependent variable and independent variables that are supposed to have an effect on a dependent variable with a mathematical model. Regression

analysis examines the effect and direction of one or more variables (multiple regression) on another variable. In multiple linear regression analysis, beta values with standardized regression coefficients are used to determine the relative importance of independent variables with different measurement units and variances for the dependent variable. Standardized Beta value refers to the correlation between these variables. F and p values reveal the level of significance of the regression model established (Bayram, 2004).

Multiple regression analysis makes it possible to interpret the total variance explained in the dependent variable by the independent variables, the statistical significance of the explained variance and the direction of the relationship between the independent variable and the dependent variable (Büyüköztürk, 2002).

The data of this study was obtained by coding the note sound heights and note sound values of the determined work. The distribution table of the loudness that constitutes the work is given in Table 1 and the distribution table of the sound duration values of the work is given in Table 2.

Table 1. Distribution of Loudness Values Creating the Work

Loudness Values	Frequency	%
0	6	3,4
1	1	0,6
3	21	11,6
4	19	10,8
6	17	9,7
7	5	2,8
8	6	3,4
10	10	5,7
12	1	0,6
13	3	1,7
15	14	8,0
16	10	5,7
18	15	8,5
19	5	2,8
20	6	3,4
21	2	1,1
22	13	7,4
23	1	0,6
24	2	1,1
25	5	2,8
27	6	2,4
28	5	2,8
30	3	1,7
Toplam	176	100

When Table 1 is examined, the definition range of the work's loudness is [0, 30] and the most used sounds are 3 (11.6%) and 4 (10.8%), while the least used sounds are 1, 12 and 23 (0.6%). It has been observed. In the work, a total of 23 sound combinations were created and 176 notes were used. This distribution is given in Chart 1.
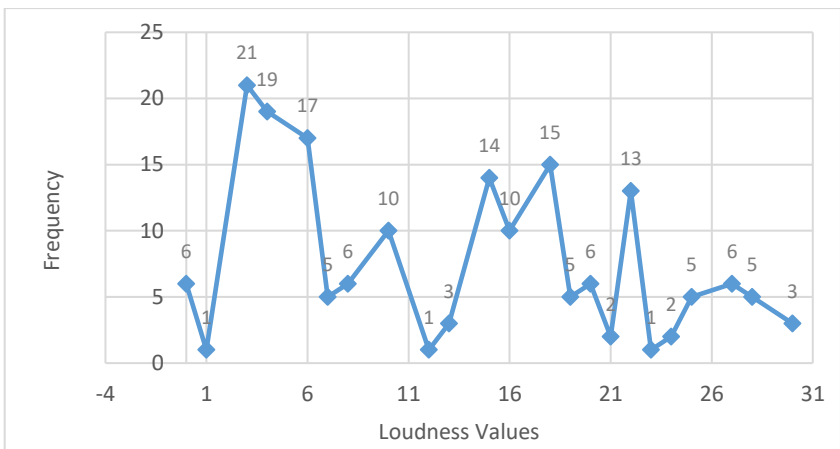
Chart 1. Distribution Graph of Loudness Values Creating the Work

Table 2. Distribution of Sound Duration Values Forming the Work

Sound Duration Values	Frequency	%
1	25	14,2
2	12	6,8
3	3	1,7
4	32	18,2
5	9	5,1
8	54	30,7
12	19	10,8
16	10	5,7
24	4	2,3
32	3	1,7
48	3	1,7
64	2	1,1
Toplam	289	100

When Table 2 is examined, the definition interval of the sound duration of the work [1, 64] and the most used note sound duration values are 8 (30.7%), 4 (18.2%), while the least used sound duration value is 64 (1.1%). With musical expression, eight and sixteenth note values are mostly used in the work. Dotted octal, square, dotted and dotted binary values are also included. This distribution is given in Chart 2.
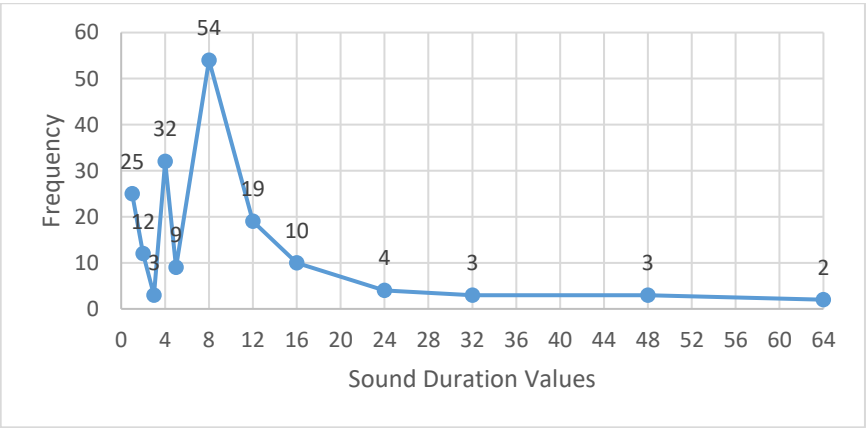
Chart 2. Distribution Chart of Sound Duration Values

FINDINGS

Note loudness (x) and sound duration values (y) of the work given in Tables 1 and 2 are taken as independent variables. In order to relate the cumulative time variable as a dependent variable, multiple regression analysis was performed to find statistical significance with some functions. Regression analysis tables regarding the loudness and note duration values of the work are given below. In order to find out what percentage of the total change in the dependent variable is explained by

the independent variables, R^2 value was examined in Table 3 in the regression analysis.

Table 3. Regression Models

Model	R	R^2	Adjusted R^2	Std. Error of the Estimate
1	0,877	0,769	0,763	217,416
2	0,883	0,780	0,773	212,653
3	0,886	**0,785**	0,777	210,772

As a result of regression analysis, 3 models are created in Table 3. R^2 value of the third model is preferred because it is 0,785. According to this model, it is stated that the dependent variable is explained by the independent variables entering the model at the rate of 78.5%. ANOVA table created according to these data is given in Table 4.

Table 4. Musical Notation Loudness and Musical Notation Values: ANOVA

Source of Variance	df	Sum of Squares	Mean Squares	F	p
Regression	6	26466729,8	44111221,6		
Resudial	163	72413003,0	44425,172	99,283	0,000
Total	169	33708032,8			

The ANOVA table shows that the model of regression established is significant [F / 1,175) = 99,283, p = 0,000 <0.05. Multiple regression analysis to determine whether the selected model predicted is given in Table 5.

Table 5. Multiple Regression Analysis Regarding Prediction of the Model

Model	B	Std. Error	Beta	t	p
Constant	221,120	37,684		5,876	0,000
x	40,375	2,239	0,744	18,057	0,000
sin(6x)	119,203	23,298	0,207	5,116	0,000
sin(10x)	-128,300	28,061	-0,187	-4,572	0,000
tan(2x)	-26,420	5,425	-0,237	-4,870	0,020
cos(7x)	83,033	31,582	0,127	2,629	0,009
sin(4y)	59,922	30,191	0,085	1,985	0,049
R=0,886 R^2=0,785 F=99,283 p=0,000					

When the multiple regression analysis results related to predicting the model in Table 5 are examined, it is understood that there is a significant relationship between the functions of x, sin (6x), sin (10x), tan (2x), cos (7x) and sin (4y). These functions explain approximately 78.5% of the model created. When the t test results regarding the significance of the regression coefficient are examined, it is understood that the functions of x, sin (6x), sin (10x), tan (2x), cos (7x), sin (4y) have an important effect on the model.

As a result of this analysis, the cumulative time dependent variable

$$z(x, y) = 221,120 + 40,375x + 119,203\sin(6x)$$
$$- 128,300\sin(10x) - 26,420\tan(2x)$$
$$+ 83,033\cos(7x) + 59,922\sin(4y)$$

regression equation corresponding to these independent variables such as note loudness = x and note sound values = y was obtained.

For the 3D geometric model of this regression equation, the general purpose mathematical problem solving software was drawn using Maple 13, which is one of the most trusted software in the world as mathematics calculation, programming, and modeling software, and the surface in Graphic 1 was created.
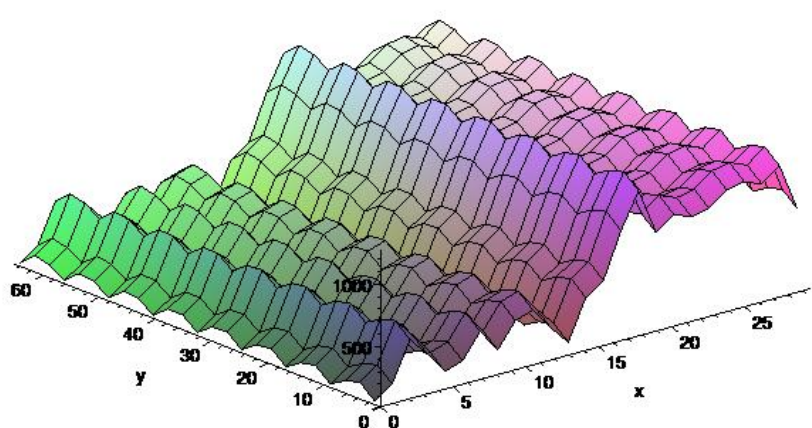
Graphic 1. Geometric models

In Graphic 1, the geometric model, which is drawn depending on the sound pitches and sound values of the work, formed the three-dimensional surface formed by algebraic and trigonometric curves. When the notation of the work is examined, it is seen that the theme starts from the middle register with the first octave re sound, after the thematic structure is processed in this region, the sound limit is expanded by going to the second octave region and a larger volume is reached with the contribution of different rhythmic structures. This shows the harmony of auditory and visual work with the geometric model.

CONCLUSION AND SUGGESTIONS

In this study, the geometric modeling of the violin party of the Op.33 Demet suite prelude section of A. Adnan Saygun, one of the leading names of the polyphonic music of the republican period in our country, was created. Mathematical coding was made according to the volume and duration values of the selected work, and many three-dimensional regression models were obtained by making regression analysis in the SPSS program. Within these regression models, 3D geometrical model equations forming the melodic and rhythmic lines of the music piece are represented by the curves x, sin (6x), sin (10x), tan (2x), cos (7x), sin (4y). This geometric model is a combination of algebraic and trigonometric functions.

The authors made some similar studies and the three-dimensional geometric model in these studies was found to have different equations. When geometrical modeling of Saygun's "İnci" piano piece is made, the equations of the three-dimensional geometric model that form the melodic lines of the piece are based only on the trigonometric function for two-layered right and left hand parties (Demirbatır and et al. 2018). In the geometric modeling of Saygun's Op.31 "Partita" solo cello, the 3D geometric model's equations were found to be algebraic, trigonometric and inverse trigonometric (Demirbatır et al. 2020). In the geometric modeling of the minor two-voice intensity with BWV 784, one of Bach's educational works, the 3D geometric model's equations were observed to consist of a combination of algebraic, trigonometric, inverse trigonometric and exponential functions (Demirbatır et al.

2020). Accordingly, it can be seen that different functions and models can be created for each piece's melody, rhythm, form, texture and processing.

It is thought that further analysis and analysis of musical works through different methods, analysis and modeling through mathematical coding will contribute to the field in terms of both disciplines. The works of composers who write works in different periods and styles of music history can be analyzed through geometric modeling. Approaches of composers' understanding of composing can also be examined in this way. At the same time, different methods and techniques that can be applied in this field, analysis and geometric modeling methods can be developed.

REFERENCES

Alexander, R. (2003), Hugo Riemann and the birth of Modern Musical Thought, Cambridge University Press, Great Britain.

Aktüze, İ. (2003). Müziği Okumak, Cilt-4. İstanbul: Pan Yayıncılık.

Atalay, B. (2006). Matematik ve Mona Lisa. Albatros kitabevi, İstanbul.

Aydın. Y. (2018). http://bso.bilkent.edu.tr/tr/wp- content/uploads/ 180412-program, (Erişim tarihi 06.11.2019).

Bakım, S. (2014). Fibonacci dizisi ve altın oranın müzik kullanımının incelenmesi, Selçuk Üniversitesi Fen Bilimleri Enstitüsü, Yüksek Lisans tezi.

Bayram, N. (2004). Sosyal Bilimlerde SPSS ile Veri Analizi. Ezgi Kitabevi, Bursa.

Beytekin, S. (2015). Cazın Piyano Üzerinden Matematiksel Analiz ile Fraktal Geometri ile İlişkisinin Analizi, İstanbul Teknik Üniversitesi Fen Bilimleri Enstitüsü, Yüksek Lisans tezi.

Bigerelle, M., Iost, A. (2000). Fractal dimension and classification of music. Chaos Solitons & Fractals, 11, 2179 – 2192, .

Bilal A.B., Muhammad A.W., Nusrat, Sidrat U.M.A. (2015). A Study On Relatıonshıp Between Mathematıcs And Musıc, International Journal of Multidisciplinary Research and Modern Education ISSN (Online): 2454-6119.

Büyüköztürk, Ş. (2002). Sosyal Bilimler İçin Veri Analizi El Kitabı. Pegem Akademi Yayıncılık.

Campbell P. (1986). The music of digital computers. Nature 324:523–528.

Carmıne C. (2018). Towards a Music Algebra: Fundamental Harmonic Substitutions in Jazz, International Journal of Advanced Engineering Research and Science, 5(1).

Demirbatır R.E., Yağcı F., Ezentaş R. (2018). Matematiksel Kodlama Yoluyla A. Adnan Saygun'un "İnci" Adlı Piyano Parçasının Geometrik Modellemesi. Uluslararası Necatibey Egitim Ve Sosyal Bilimler Arastırmaları Kongresi, 26-28 Ekim 2018, Balıkesir. 483-492.

Demirbatır R.E., Yağcı F., Ezentaş R. (2020). A. Adnan Saygun'un Op.31'Partita' Adlı Solo Viyolonsel (IV. Bölüm) Eserinin Geometrik Modellemesi. UludağÜniversitesi Fen-Edebiyat Fakültesi Sosyal Bilimler Dergisi, 21(38), 31-50.

Demirbatır R.E., Yağcı F., Ezentaş R. (2020). J.S. Bach'ın Eğitim Amaçlı Eserlerinden BWV 784 La Minör Envansiyonunun Geometrik Modellemesi. UludağÜniversitesi Eğitim Fakültesi Dergisi, 33(2).

Doğangün D. (2015). Ahmed Adnan Saygun'un Op.31 'Viyolonsel İçin Solo Partita'sı Ve Eserin 1955 Türkiye'si Sanat Hayatındaki Yeri, İnönü University Journal of Culture and Art 1(1), 61-69.

Devlin, K. (2000). The math gene: How mathematical thinking evolved and why numbers are like gossip, Basic Books, Great Britain.

Eberhard K. (2008). Euler Transgressıng Lımıts: The Infınıte And Musıc Theory", Quaderns d'Història de l'Enginyeria- volume ix - 9.

Eftekhari A. (2011). Fractal geometry of texts: An initial application to the works of Shakespeare, Journal of Quantitative Linguistics, 13(2-3), 177.

Guerino M. (2002). The Topos of Music: Geometric Logic of Concepts, Theory, and Performance, Birkhauser Verlag, Basel, Boston, Berlin,.

Gülsoy F., Güney İ., Özdamar E. (2013). Mathematical and Statistical Modeling of the Musical Compositions, Balkan Journal Of Mathematıcs, 1, 35-43.

Hsu, K.J., Hsu, A. (1990). Fractal geometry of music. Proceedings of National Academy of Sciences, 87, 938 – 941.

Kıratlı S. D. (2016). Ahmet Adnan Saygun'un 'Viyolonsel İçin Partita' Adlı Eserinin Teknik İncelenmesi Cumhuriyet Üniversitesi Sosyal Bilimler Enstitüsü Müzik Anabilim Dalı Yüksek Lisans Tezi

Koshy, T., (2001). Fibonacci and Lucas Numbers with Applications, Wiley-Interscience Publication, Canada, 6-38.

Köhler, R. (1997). Are there fractal structures in language? Units of measurement and dimensions in linguistics. Journal of Quantitative Linguistics, 4, 1–3.

Lehmann, I., Posamentier, A.S., (2007). The (Fabulous) Fibonacci Numbers, , Prometheus Books, 2007, 271-291.

Mann, A., Newsom. (2000). Music History from Primary Sources, Library of Congress, Washington.

Marcus, D.S. (2004). The Music of the Primes: Why an Unsolved Problem in Mathematics Matters, Harper Perrenial

Marta A.G. (1993). Solfege, Ear Training, Rhythm, Dictation, and Musiz Theory: Comprehensive Course. Front Cover, University of Alabama Press,.

Orhan, C. (1995). Matematik ve Müzik. Matematik Dünyası. 6-7.

Paraşkev H. (1996). Temel Müzik Yeorisi, Ceviri: Atilla Sağlam &Bedri Koçancı, Pan Yayıncılık.

Riedweg C. (2005). Pythagoras: His Life, Teaching and Influence, Cornell University Press, .

Rehding A. (2003). Hugo Riemann and the birth of Modern Musical Thought, Cambridge University Press.

Robert M. (2016). The Handbook of Fourier Analysis and Its Applications,

Schroeder MR. (1987). Is there such a thing as fractal music? Nature 325:765–766.

Stolzenburg, F. (2009). A Periodicity-Based Theory for Harmony Perception and Scales. In Proceedings of the 10th International Society for Music Information Retrieval Conference.

Uçan, A. (1994). Müzik Eğitimi. Temel Kavramlar- İlkeler- Yaklaşımlar. Ankara: Müzik Ansiklopedisi Yayınları.

Voss R.F and Clarke J. (1975). 1/f noise in music and speech. Nature 258:317–318,

Wright, D., (2009). Mathematics and Music, Department of Mathematics, Washington University, St. Louis, 6-13.

www.wikipedia.com, (Erişim tarihi 11.06.2019).

www.turkcebilgi.com, (Erişim tarihi 11.06.2019).

CHAPTER 3

A NOVEL NAGINI ROBOT DESIGNING

Oğuzhan GİRGİN[1], Dr. Yunus DOĞAN[2]

[1] Dokuz Eylül University, Faculty of Engineering, Computer Engineering, Izmir, Turkey, oguzhan.girgin@ceng.deu.edu.tr
[2] Dokuz Eylül University, Faculty of Engineering, Computer Engineering, Izmir, Turkey, yunus@cs.deu.edu.tr

INTRODUCTION

The aim of the project is a robot that could be used as a spy and the robot's name is Nagini. Developers choose this project because one robot can spy only one condition but Nagini can be spying on land and in water. Nagini's cost is low than other spy robots, for example; drones, dog robots. Spy robots can spy on land, on-air and in water. Every spy robot can only use in one condition. But Nagini has some advantages than others because Nagini can move on land, and in water. Nagini has 2 heads; one head is used for moving up and down to head, the second head is used for moving right or left to head. So that Nagini can move in water and on land. Some spy robots are moving on air so that they must have a high power battery. A high power battery is so expensive so that drones are the most expensive robot in the robot world. Nagini has not a high-power battery because its movement looks like a snake's movement. Nagini has 4 dc motor for movement and dc motor's voltage is 5 volts so that Nagini has a low power battery. Nagini's cost is low than the others.

Some spy robots' size is so high or width. So that, these robots cannot spies for a long time. But Nagini has optimal size. Some robots which are moving on land can mud, but Nagini can't mug because it moves like a snake. Nagini project is one of the projects with many applications in the world. Many versions of this project have been produced or developed. One of these projects is Carnegie Mellon' snake robot, this robot has six arms, every arm looks like a snake, but a movement like is a scorpion. Carnegie Mellon's snake robot needs a

high-power battery because it has six snake arms so that it's so expensive. Carnegie Mellon's snake robot has six arms and every arm has four dc motor. So that it's cost so expensive and the size is not optimal. Carnegie Mellon's snake robot's weight is heavy, but it's so useful because the movement is so easy, and it can move on every type of condition on the land. Military service is too expensive to buy and have big spy machines, and these machines are not designed for every condition. The purpose of the Nagini project is to provide users with the convenience of time and energy in many different areas. The Nagini robot was designed to do the spying. This Nagini robot has not a high-power battery so that it is cheap. This robot is the owner's assistant, who acts efficiently to use energy because in addition to the batteries. The developer devoted the progress of the Nagini robot project to specific stages. These stages are divided into hardware and software.

In hardware, layer connection is provided between Arduino, motors, battery, and communication sensor. Arduino Uno is the brain of the hardware; it controls every sensor on a snake. The software layer has one algorithm for movement. The robot can move with a like snake. Firstly, dc motor turns around with torque and attracts the tail of Nagini, and then motors push the Nagini's queue. Thus, Nagini can move.

In the next sections; the literature reviews where the studies supporting our project mention, the requirements containing the electronic components, the design, where contains the plans and

diagrams, the implementation of the robot, the tests with the results and the conclusion are described.

1. LITERATURE REVIEW

In a study, development of a Nagini robot system for combat operations, this robot is for the surveillance of human activities on the battlefield or border areas to reduce infiltration by the enemy. The robot consists of a night vision wireless camera that can transmit videos of the battlefield to prevent any damage and loss in human life (Patoliya and Patel, 2015). Another study containing high-end project Nagini robot can include new developments in the military industry literature. This robot can enter the enemy area silently and send the information to us via a wireless camera. Since human life is always valuable, these robots replace soldiers in war zones. This spy robot is used for star hotels, shopping malls, jewelry showrooms, etc. where threats from intruders or terrorists (Jain, Firke, Kapadnis, Patil and Rode, 2014). Additionally, Some Japanese researchers are working on a robot that can help humans, and are researching techniques that can support this relationship. In this article, the project assumes a remote control mobile spy robot using PIC 16F628A and PIC 16F877. Two different PICs are used together with the wireless system to remotely control and control the Spy robot. CCD camera is used to capture the information surrounding the robot. A 4-bit LCD display is mounted on a remote control to display the user command. To use the spy robot at night in the dark area, it is adjusted by the LED connected with CCD lighting circuits (Khaing, Wai Mo Mo and Kyaw Thiha, 2014).

A group of engineers is running a project similar to our last project. Wireless running spy robots can be extremely useful if they can be remotely controlled over a wider working range. The availability of multiple modes for wireless control operations can further increase their capabilities and application diversity. The remote control application was developed for the Android platform based smartphone. Voice commands use online conversion from speech to text format. Tilt movements controls use the smartphone's accelerometer (Maheshwari, Tushar, 2015).

In another study, the information about the algorithm of the spy robot is given. A small piece of dismissal: This literature provides a monitoring vision for human collaborating robots. It follows the human back and shoulder so that the robot can follow a person. Obviously, if a robot could follow us in the real world, it would be very convenient and comfortable for us (Morioka, Kazuyuki, Yudai Oinaga and Yuichi Nakamura 2012). Usually, an application is designed for specific purposes, such as smartphones and tablets on the Android platform. A study in 2017 describes the design and implementation of an Android-based spy robot process. An Android-based application, the RC Bluetooth controller, is used to control this spy robot. This robot can be controlled by an application of Android phones. The Arduino-based microcontroller is used to process instructions and provide appropriate instructions. Bluetooth technology is used to interface between Arduino and Android. A hand

for collecting and holding objects and a camera for streaming live video is used to observe any object and movement of the robot. This robot can go anywhere in the Bluetooth network range and perform wisely (Hasan, ASM Shamim 2017). It contains information about the spy robot in a research project. A remote controlled spy robot circuit that can be controlled using the wireless remote control. It can receive audio and video information from the environment and can be sent to a remote station via RF signals. The maximum range is 125 meters. It overcomes the limited infrared remote control range. The circuit uses HT 12E, HT 12D encoder and decoder. 433MHz ASK transmitter and receiver are used for remote control. H-bridge circuits are used to drive motors. Two 12V DC / 100RPM gear motors are used as drivers (Rao, T. Krishnarjuna, P. Kalyani and Harikrishna Musinada, 2014).

A study mentions building an RF-based spying robot equipped with a wireless camera that can reduce human victims. This robot sends the signal to the base station using a wireless camera (Patoliya, Jignesh, Haard Mehta and Hitesh Patel, 2015). In another research, many robots were produced for production purposes and can be found in factories around the world. The design of the robot is such that it is controlled by a mobile application Arduino can be interfaced with the Bluetooth module via the UART protocol. Robot motion can be controlled according to the commands received from Android (Singh, Akash, Tanisha Gupta and Manish Korde, 2017).

The research in 2012 is very similar to our project. Security and surveillance cameras play an important role in security and monitoring applications. It is designed for various purposes such as biometric surveillance cameras, Aerial surveillance cameras, and load surveillance cameras. The spy ball can be used as a surveillance device and is therefore made shockproof. This ball also supports personal video streaming application with different options for video capture and recording possibilities. After testing this ball on various platforms, excellent video shooting with stability is achieved (Rasheed, M. and I. Hussain. 2012).

An article presents a project aimed at building a biologically inspired amphibious snake-like robot, so the project is similar to the Nagini robot (Crespi, Alessandro, 2005). Moreover, a project about the snake movement implements an algorithm on the robot in another study in 1998. Our algorithm and this project algorithm are different, but the two algorithms are successful. Snake robot mobility in hilly terrain depends on the robot's ability to rise from a horizontal position to a vertical so that he can climb obstacles. At first glance, removing the N body segments seems to require O (N / sup 2 /) dynamic torque. However, this article describes a practical algorithm that only requires O (1) dynamic torque (Nilsson, Martin, 1998).

In a study in 2009, a useful environment for snake robots to support our project is mentioned. Snake robots have the potential to make significant contributions in areas that may be too narrow or too dangerous to work for personnel such as rescue missions, firefighting

and maintenance. Over the past 10-15 years, published literature on snake robots has increased significantly. The purpose of this article is to investigate the various mathematical models and motion models offered for snake robots. Both completely kinematic models and models, including dynamics, have been studied. In addition, different approaches to biologically inspired motion and artificially produced motion models for snake robots are discussed (Transeth, Aksel Andreas, 2009).

Another article describes the movement of the snake in the water, the Nagini robot should drink and the water should move, so our project is interested in this article. Experiments have been conducted to characterize how movement speed depends on the frequencies, amplitudes and phase delays of fluctuating walks, both in water and on the ground. The results show that the fastest walks are different from one environment to another and have wider optimum zones in the parameter area for the scan gaps. Swimming walks are faster than crawl walks for the same frequencies. The fastest movement for both environments is achieved with less than one total phase delay. These results are compared with data from fish and amphibian snakes (Crespi, Badertscher & Guignard, 2005).

While animals can adapt quickly to injury, existing robots cannot 'think outside the box' to find compensatory behavior when damaged: they can be limited to preset self-perception capabilities, can only diagnose expected failure modes, and a pre-programmed contingency plan and complex robots for any potential damage for practicality.

Thus, if an animal's algorithm comes out on the robot, these robots will be most useful for any condition (Cully and Antoine, 2015).

The proposed algorithm takes into account its communicative mobility to facilitate human-robot interaction. The well-known traditional artificial potential field method (APF) has been expanded by the movement characteristics of pets. The proposed algorithm includes speed and direction information and can be used in unknown dynamic environments. The main contribution of this article is to define an online, local route planning method by adapting animal motion features for human-robot interaction. The algorithm was implemented in an embedded system and evaluated on MOGI-ETHON, a holonomically driven mobile robot (Kovács and Bence, 2016).

2. REQUIREMENTS
2.1. Functional Requirements

Various components are needed to make Nagini Robot such as a servo motor, Hc-05 Bluetooth sensor, Arduino Uno, Nrf24l01, motor driver l298n and battery. The purpose of the 5 * 3.7 Volt lithium batteries is to supply Arduino Uno and other sensors and motors with the necessary power.

2.2. Non-Functional Requirements

The Nagini robot was designed to control only the one user. The user of the robot needs a good software to be able to control by the user, the software part of the robot consists of two stages. The first of these

stages is as moves: The robot interprets the data coming from the owner, then divides them into four sets: go, right, left. After that, the robot commands the two motors that are connected to it with the data that the user owns and moves the robot user with this algorithm. In addition, if the robot is too far behind the owner, the robot sends a signal to the owner via hc-05 wireless module and the user waits for the robot until he reaches a certain range.

3. DESIGN
3.1. Scenarios

The description of the architecture is illustrated using small usage scenarios or scenarios that have become the fifth view. Scenarios define sequences of interactions between objects and between processes. In Figure 1, they are used to identify architectural elements and to demonstrate and verify architectural design. In this section, the user and the robot will show the status of the data when transmitted and if there is a problem in the robot add-ons will be used by the user.
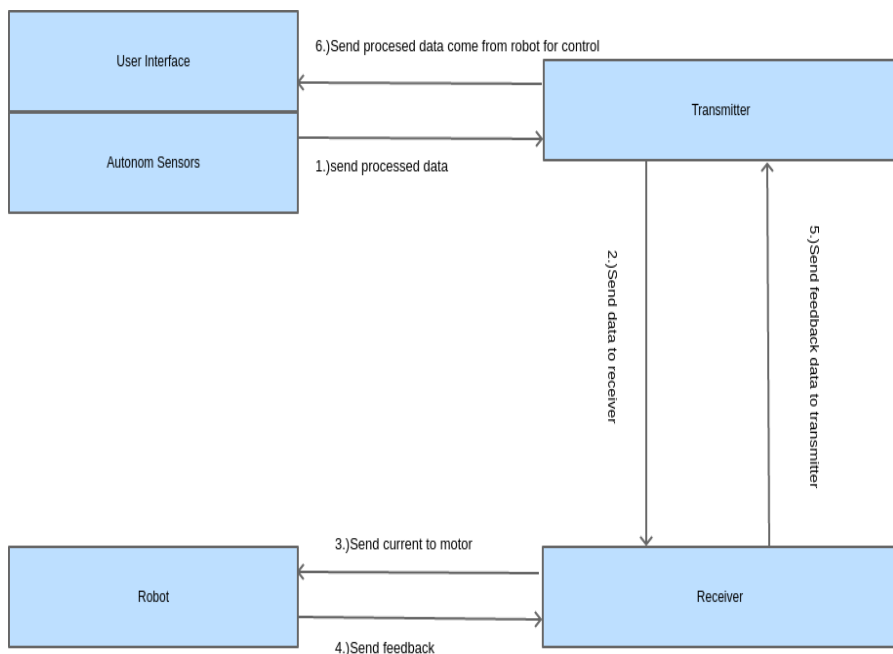
Figure 1: Scenarios

3.2. ER Diagram

In this section, Figure 2 shows the hardware part of the robot is introduced. The robot receives data from the user via Bluetooth in this circuit and uses this data to interpret the data received from the user using the GPS and compass sensor. The data is then controlled using Arduino uno and transistor to control the current to the motors, which means the robot follows the user.
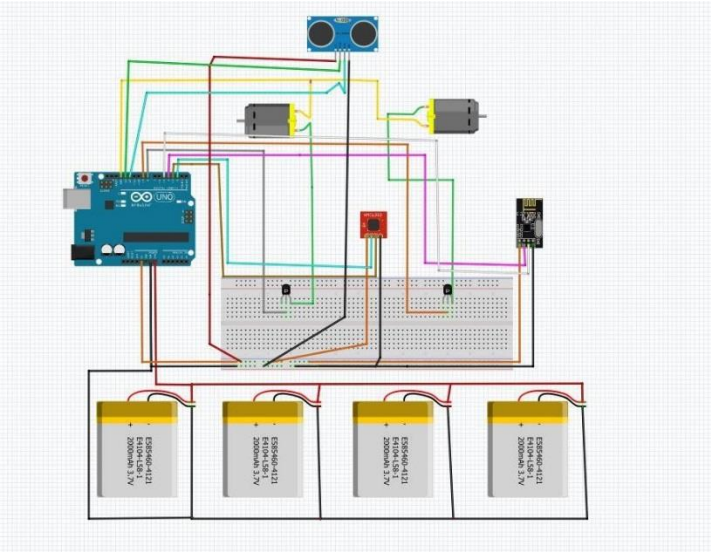
Figure 2: ER Diagram

3.3. UI Design
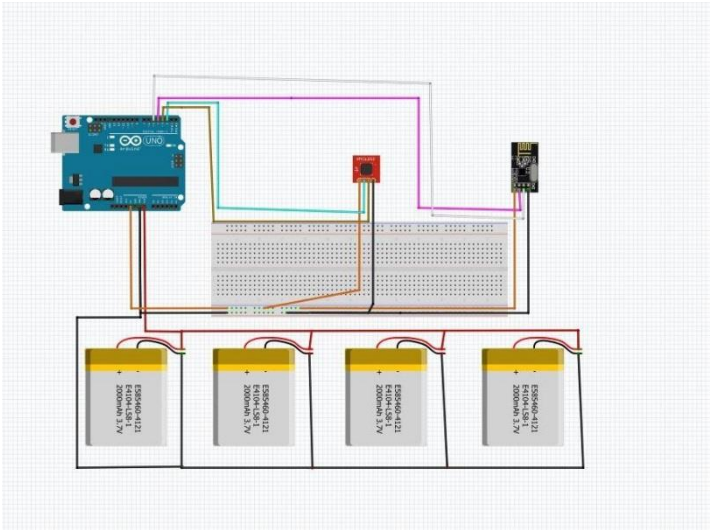
Figure 3: UI Design

In this section, Figure 3 shows a hardware interface is designed for the user to manage the robot and learn the status of the robot. Here, the operator communicates with the Bluetooth and can monitor the status of the robot with the LCD screen and if the robot has anything, it can control the robot.

3.4. Activity Diagram
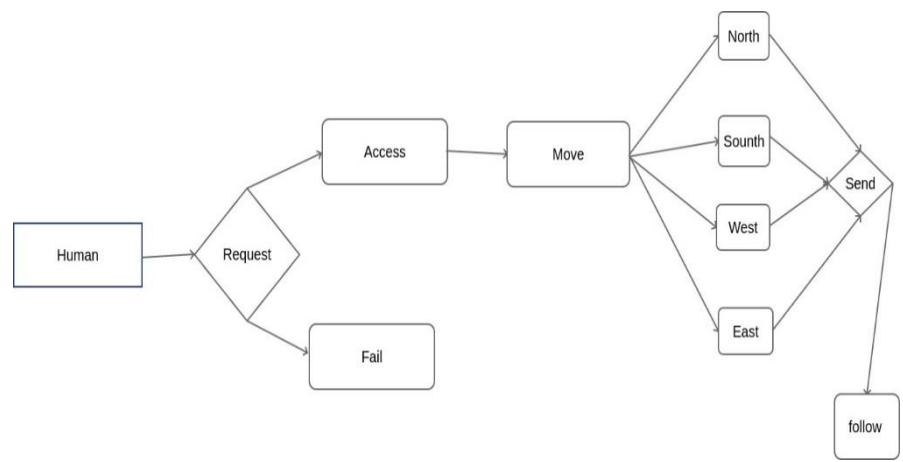
Figure 4: Activity Diagram

The activity diagram is another important diagram in UML to define the dynamic aspects of the system. The activity diagram is basically a flow chart that represents the flow from one activity to another. Effectiveness can be defined as the operation of the system. Figure 4 shows the operations from user to robot. First, an acceptance mechanism is used for the user to agree with the robot. After this stage, the movement types of the user are transmitted to the robot and follows the robot owner.

4. IMPLEMENTATION

In the hardware part of our Nagini robot project, I designed the hardware needs of our robot. Nagini robot movement is look like snake's movement, motor push and attached cylinders, so robot can move like snake. Every cylinder has a one dc motor, and every dc motor apart each other. In head of Nagini has two motors for up, down movement and right, left movement. While Nagini body is in Figure 5, Nagini's head is in Figure 6.

Figure 5: Body of Robot

Figure 6: Head of robot part 2

Nagini Robot has several movement types, so that dc motors must work synchronous each other. One movement is forward, if user want to move the robot forward, robot's motors work reverse each other, for example one motor turns right, another motor turns left, in this way robot can move forward. On Figure 7 robot's motor wear on robot. All motors can provide to several movement, another example is Nagini robot's head and tail can touch each other, this example is on Figure 8.

Figure 7: Robot wears motors

Figure 8: Robot movement type

When camera has an unsuccessful position, user should rotate head of robot, so that developer add a motor which is rotate head of robot. This motor can rotate when user's command sends to interested data. This motor is on Figure 9.
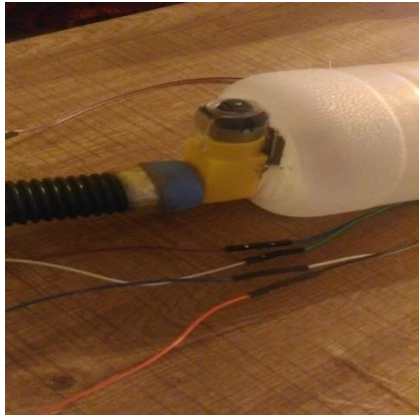
Figure 9: Motor rotate head of robot

Figure 10: Motor' s movement is up.

Head of robot should move up and down for on hard condition lands. If user move up to camera so that robot's head should move up or

another position is down of head. So that developer adds a motor for up movement and down movement. On Figure 10, the motor movement is up, on Figure 11, the motor movement is down.

Figure 11: Motor' s movement is down.

Dc motors can just one direction without change cables +5volt and gnd. If just software changes this motor's direction user should use motor driver. So that developer made motor driver for change motor's direction.
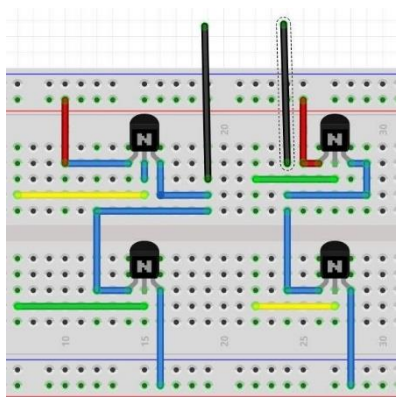
Figure 12: Motordriver's schema.

Figure 12 shows the driver schema. Figure 13 shows the driver which is made by developer. This driver is for 5 motors.
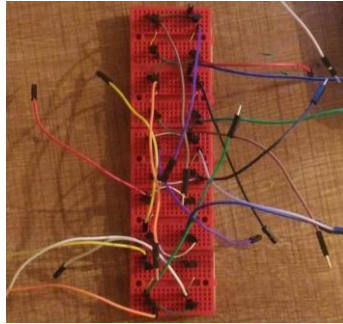
Figure 13: Motor driver.

When coming end of project driver will be in head of Nagini robot. Figure 14 shows the driver in head of robot.
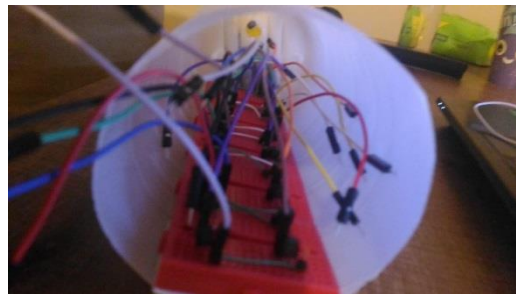
Figure 14: Motor driver is in head of robot.

Motor's cables connect to each other on motor driver. Motor driver is used for forward movement and back movement. After motor's cables connection, cables connect on Arduino which is brain of robot. Figure 15 shows connection of cables.
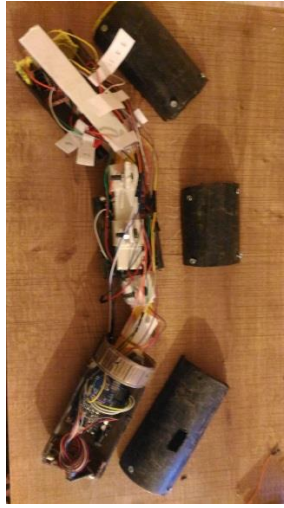
Figure 15: Connection of cables on Robot.

Figure 16 shows the brain of the robot. Arduino is connected drivers and communication sensor. Communication sensor is nrf24L01 which is wireless module.

Figure 16: Brain of the Robot

User should use command device which is send to signal about command to the Nagini robot. Button used for stopping the robot. Other buttons are used forward, right, left and another movement. Figure 17 shows the command user interface.

Figure 17: Command User Interface of Robot

Finally, the robot has been obtained like Figure 18.

Figure 18: End the Body of Robot

The project's hardware part combines with the software part. Transmitter and receiver have a software. Transmitter send data using a canal which is same receiver's canal. After that receiver take data, after use data for robot's movement.

Transmitter Pseudo Code is like the following code;

Define a canal for communication with receiver.
Start communication.
User press the button.
-Button's cable goes to Arduino's port as an input.
-Arduino take the input from button.
-Use this input for a message.
Finally send data.

Receiver Pseudo Code is like the following code;

Define a canal for communication with transmitter.
Start communication.
Catch data from transmitter.
Use this data with if conditions.
Command to move the motors.
After all this time, robot can move.

```
#include <Servo.h>
Servo servoNesnesi;
int pusher=12; void setup()
{Serial.begin(9600); servoNesnesi.attach(5); pinMode(pusher,OUTPUT);}
void loop() { if(Serial.available()>0){
```

int GelenVeri = Serial.read(); Serial.println("Data"); Serial.println(GelenVeri);
if(GelenVeri == 49){digitalWrite(pusher,HIGH); servoNesnesi.write(120);
delay(500);}
elseif(GelenVeri == 50){digitalWrite(pusher,HIGH); servoNesnesi.write(90);
delay(500);}
elseif(GelenVeri == 51){servoNesnesi.write(150); digitalWrite(pusher,HIGH);
delay(500);}
elseif(GelenVeri == 48){servoNesnesi.write(120); digitalWrite(pusher,LOW);
delay(500);}}}

5. TESTS AND RESULTS

In this part, transmitter, receiver and motors was tested.
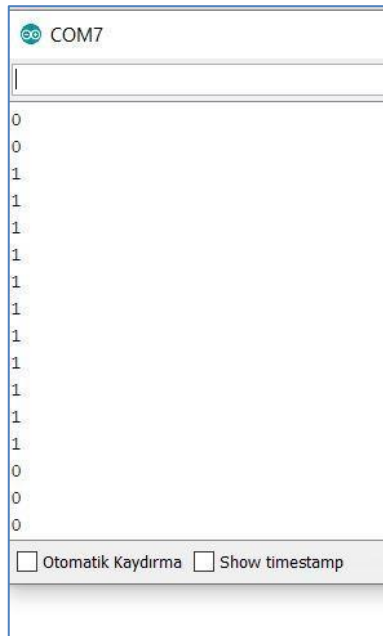
Figure 19: Result of 433 MHz transmitter

Figure 19 shows the 433 MHz transmitter's data transfer and Figure 20 shows the nrf24l01's transmitter's data transfer. So that nrf24l01 is more powerful and useful than 433 MHz. Nrf24l01 is faster than 433 MHz transmitter, because data transfer is good. Nrf 24l01 need less power for transmit the data than 433 MHz.
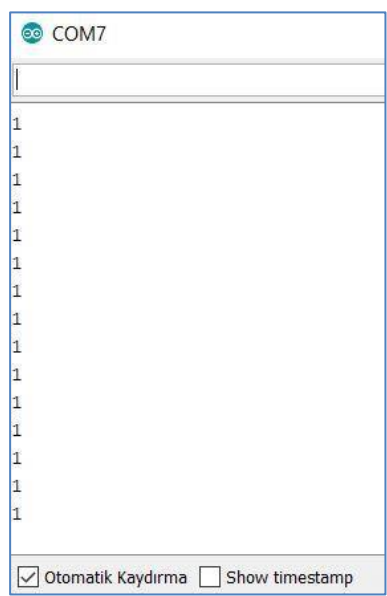
Figure 20: Result of Nrf24l01 transmitter

After that, forward message, right message, left message was tested. Forward message is "1", right message is "2", left message is "3". So that is transmitter send "1" to receiver, robot will move to forward. İf transmitter send "2" to receiver, robot will move to right. If transmitter send "3" to receiver, robot will move to left. Figure 21 shows forward command in receiver, right command in receiver and left command in receiver.
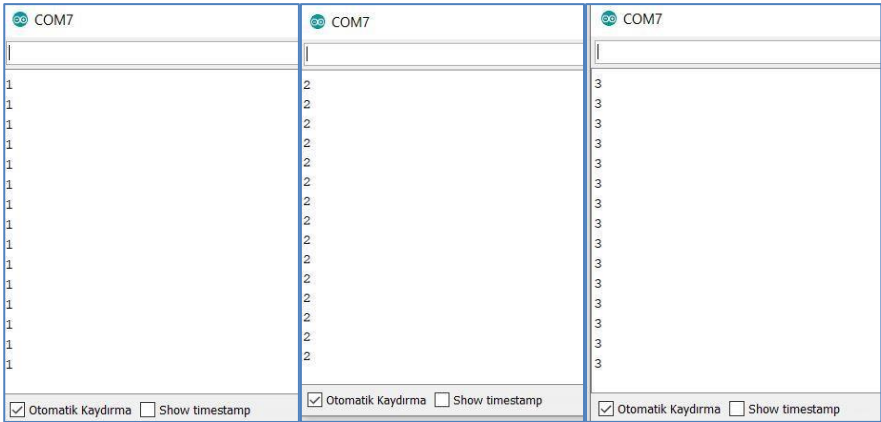
Figure 21: Forward movement data in receiver, right movement's data in receiver and Left movement's data in receiver
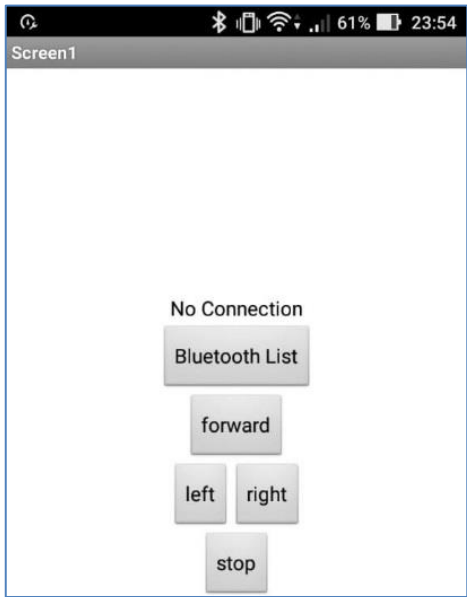
Figure 22: User Interface for Phone

Bluetooth technology is so easy for communication because every person can carry phone. Communication is so fast. Connection is so

easy because user interface allows Bluetooth connection with a one button. Figure 22 shows the user interface. Before connection user should choose robot's Bluetooth device. Figure 23 shows the Bluetooth list. After connection a successful message on screen. On Figure 24 shows the successful message on screen. After all test, 433 MHz, nrf24l01 and Bluetooth hc-05 was compared on table, Table 1 show that.
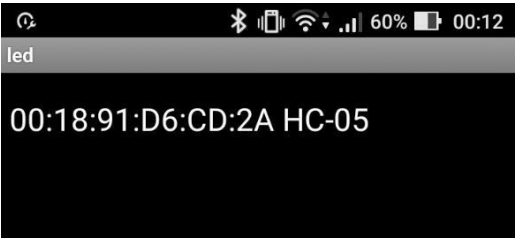
Figure 23: Bluetooth List on Phone Screen
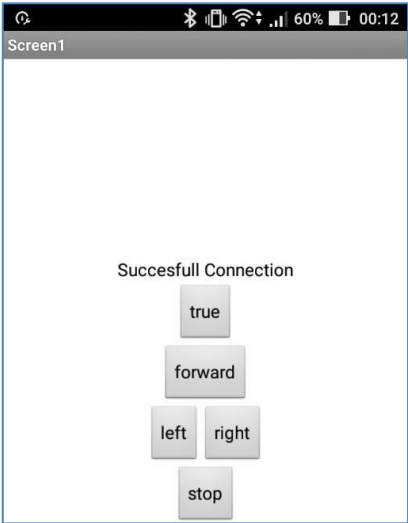
Figure 24: Successful Message on Phone Screen

Table 1: Compare Nrf24l01, 433 MHz and Bluetooth

	Nrf24l01(transmitter)	433mhz(transmitter)	Hc-05 Bluetooth
Data transfer speed	Fast	slow	fast
Power for work	3.3 volt	5 volt	5 volt
Used cables	7 cables	3 cables	4 cables
Network security	Has a special canal	No security	Latest technology

After all process robot is on Figure 25. Robot has 3 parts for the movements. The middle art is the brain of the robot.
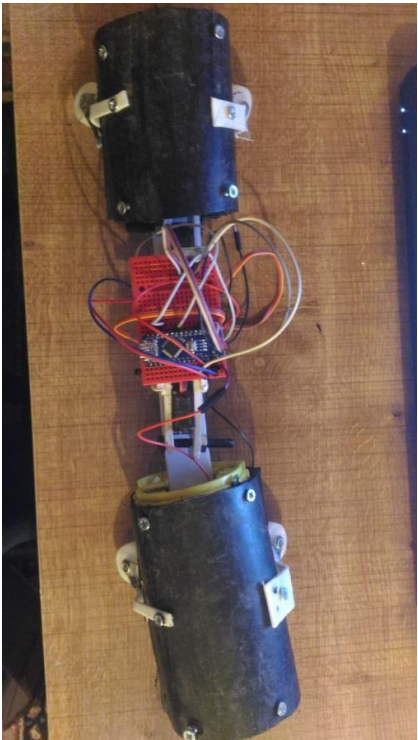
Figure 25: The completed Nagini robot

CONCLUSION

As a result, Nagini robot has movement: forward, right and left. User has a command device. Robot and command device use hc-05 Bluetooth for communication. Users can connect own phone, after that user can control Nagini robot. Nagini robot can move forward, right and left.

The robot can be developed. Maybe camera can be attached to this robot. Maybe powerful wireless module can be attached to Nagini robot. Robot can be made more useful by using other algorithms. Nagini robot can be pioneer for other animal robots. Nowadays more robots can imitate the other animals, for example: dog robot made by Boston Dynamics, dog robot is so fast than cheetah. Another robot is can carry heavy materials. This robot can use in real life. This is very close. Maybe Nagini robot can swim on sea. Figure 6.9 show the primitive of the Nagini robot.

Summary, a robot can move as an animal like snake. Every animal has a movement algorithm, so that all of them is different. Nagini robot can develop by engineers. On Future, most robot use animal's movement algorithm for help the people. Animal's movement algorithm is so hard for coded because movement changes every type of condition every time.

REFERENCES

Ali, H., Tariq, N., Ahmad, S., Rasheed, M., Chattha, T. H., & Hussain, A. (2012). Growth and radiation use efficiency of wheat as affected by different irrigation levels and phosphorus application methods. J. Anim. Plant Sci, 22(4), 1118-1125.

Crespi, A., Badertscher, A., Guignard, A., & Ijspeert, A. J. (2005). AmphiBot I: an amphibious snake-like robot. Robotics and Autonomous Systems, 50(4), 163-175.

Crespi, A., Badertscher, A., Guignard, A., & Ijspeert, A. J. (2005, April). Swimming and crawling with an amphibious snake robot. In Proceedings of the 2005 IEEE international conference on robotics and automation (pp. 3024-3028). IEEE.

Cully, A., Clune, J., Tarapore, D., & Mouret, J. B. (2015). Robots that can adapt like animals. Nature, 521(7553), 503-507.

Hasan, A. S., Jewel, M. K. H., Mostakim, M. N., Bhuiyan, N. H., Rahman, M. K., Hossain, S. D., & Hossain, M. K. (2017). Smartphone Controlled Spy Robot with Video Transmission and Object Collector. International Journal of Engineering and Manufacturing (IJEM), 7(6), 50-58.

Jain, P., Firke, P. N., Kapadnis, K. N., Patil, T. S., & Rode, S. S. (2014). RF based Spy robot. Int. Journal of Engineering Research and Applications, 4(4), 06-09.

Khaing, W. M. M., Thiha, K., & Mandalay, M. (2014). Design and Implementation of Remote Operated Spy Robot Control System. International Journal of Science, Engineering and Technology Research (IJSETR), 3(7).

Kovács, B., Szayer, G., Tajti, F., Burdelis, M., & Korondi, P. (2016). A novel potential field method for path planning of mobile robots by adapting animal motion attributes. Robotics and Autonomous Systems, 82, 24-34.

Maheshwari, T., Kumar, U., Nagpal, C., Ojha, C., & Mittal, V. K. (2015, December). Capturing the spied image-video data using a flexi-controlled spy-robot. In 2015 Third International Conference on Image Information Processing (ICIIP) (pp. 330-335). IEEE.

Morioka, K., Oinaga, Y., & Nakamura, Y. (2012). Control of human-following robot based on cooperative positioning with an intelligent space. Electronics and Communications in Japan, 95(1), 20-30.

Nilsson, M. (1998). Snake robot-free climbing. IEEE Control Systems Magazine, 18(1), 21-26.

Patoliya, J., Mehta, H., & Patel, H. (2015, November). Arduino controlled war field spy robot using night vision wireless camera and Android application. In 2015 5th Nirma University International Conference on Engineering (NUiCONE) (pp. 1-5). IEEE.

Rao, T. K., Kalyani, P., & Musinada, H. (2014). Radio Frequency based Remote operated SPY Robot. International Journal of Ethics in Engineering & Management Education, 1(2).

Singh, A., Gupta, T., & Korde, M. (2017, August). Bluetooth controlled spy robot. In 2017 International Conference on Information, Communication, Instrumentation and Control (ICICIC) (pp. 1-4). IEEE.

Transeth, A. A., Pettersen, K. Y., & Liljebäck, P. (2009). A survey on snake robot modeling and locomotion. Robotica, 27(7), 999-1015.

CHAPTER 4

AFFORDANCE AND RESTORATIVE DIMENSIONS OF THE BUILT ENVIRONMENT AS SOURCES OF ENVIRONMENTAL STRESSOR

Asst. Prof. Dr. Bülent ÜNAL[1], Asst. Prof. Dr. İpek MEMİKOĞLU[2], Asst. Prof. Dr. Elif GÜNEŞ[3]

[1] Atılım University, School of Fine Arts, Design and Architecture, Department of Industrial Design, Ankara, Turkey. bulent.unal@atilim.edu.tr

[2] Atılım University, School of Fine Arts, Design and Architecture, Department of Interior Architecture and Environmental Design, Ankara, Turkey. ipek.memikoglu@atilim.edu.tr

[3] Atılım University, School of Fine Arts, Design and Architecture, Department of Interior Architecture and Environmental Design, Ankara, Turkey. elif.gunes@atilim.edu.tr

INTRODUCTION

The relationship between human behavior and the built environment presumes two basic forms: our behavior affects environmental quality and the quality of our environment affects our mental and physical health. When individuals are exposed to suboptimal environments; in other words, when environmental requirements go beyond personal coping limits, stress occurs. Stress is defined broadly as any situation in which the environmental demands exceed the individual's ability to respond (Evans, 1982). It is a process in which environmental events or forces, called stressors, threaten individual's existence and well-being and by which the individual responds to this threat. Both physical and psychosocial characteristics of the built environment can be stressors that can generate stress by creating fear, anxiety and anger. Thus, environmental conditions may directly engender negative effects on individual behavior and health.

This study aims to investigate the impact of interior design elements classified by Evans and McCoy (1998) under the affordance and restorative dimensions of environment as potential environmental stressors. With respect to the interior design concepts, ambiguity, sudden perceptual changes, perceptual cue conflict and feedback form affordance; on the other hand, minimal distraction, stimulus shelter, fascination and solitude form the restorative dimension.

AFFORDANCES

The theory of affordance was first asserted by the perceptual psychologist James J. Gibson (Gibson, 1979). He coined the word "affordance" as follows:

> *"The affordances of the environment are what it offers the animal, what it provides or furnishes, either for good or ill. The verb to afford is found in the dictionary, but the noun affordance is not. I have made it up. I mean by it something that refers to both the environment and the animal in a way that no existing term does. It implies the complementarity of the animal and the environment."* (127).

To understand how users build close relationships with objects and how these relationships can be controlled by developers / designers necessitates the development of useful and desirable products. This approach points out the importance of the concept of affordances as an instrument for understanding the relationships between technical functions and user tasks (Galvao and Sato, 2005). Thus, affordances describe action possibilities with respect to a specific agent (Raubal and Moratz, 2008).

In figure 1, there is an example for affordance of an object in the built environment (Cantada, 2010). In this example, the goal is to turn on/off the light bulb. For achieving this goal, the affordances are push-able, flip-able and rotate-able, while the objects are buttons, switches and knobs. The actions are pushing the button, flipping the switch and

rotating the knob. The light from the light bulb is considered as feedback that tells the user whether the action is successful or not. The crucial case in this example is this electrical system will teach the user about itself even if he had no prior experience with push buttons, switches and knobs.
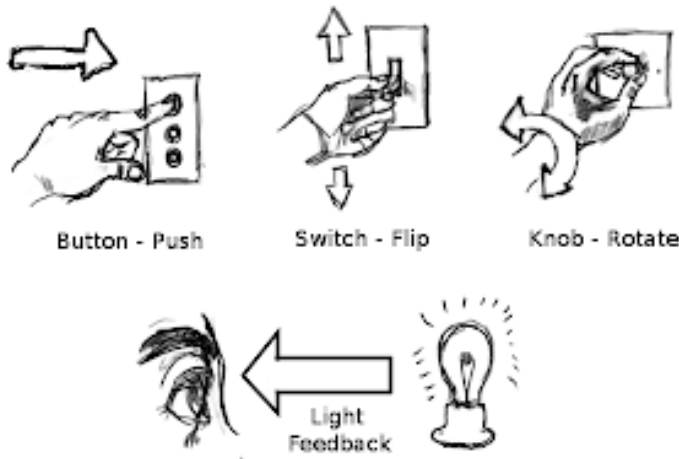
Figure 1. An example of affordance of an electrical system

Therefore, it is clear with the above example that the physical characteristics of an object affect its function and use. The form of an object makes it better suited not only for some functions than other but also for some interactions than others. The objects performs efficiently and intuitive to use if the affordances are good (Universal Design Principles, 2019, prg.1). Merely, when affordances are bad, it will have a potential to generate stress, since the object will not be operated by the user. Thus, it is worth to say that as affordances are perceived directly, designers should be able to identify and manipulate affordances easily. They should utilize common tools that are

predetermining design requirements, doing thought experiments, experimenting with prototypes, and using computer assisted design systems for modern design engineering (Maier and Fadel, 2007).

With respect to the interior design concepts, ambiguity, sudden perceptual changes, perceptual cue conflict and feedback forms affordance dimension.

Ambiguities and complex information about the practical meaning of interior elements can cause stress. Weak affordance may happen when conflicting contradictory information is present and when rapid changes in visual access generated by movement across a sharp vertical or horizontal boundaries (Evans and McCoy, 1998). The design of the staircases in Zhongshuge Bookstore in China creates a complex environment for the users, thus it can be an example for ambiguity in indoor space (see Figure 2). It is possible that this environment may create frustration and annoyance as the user cannot see how or what something in this environment occur.
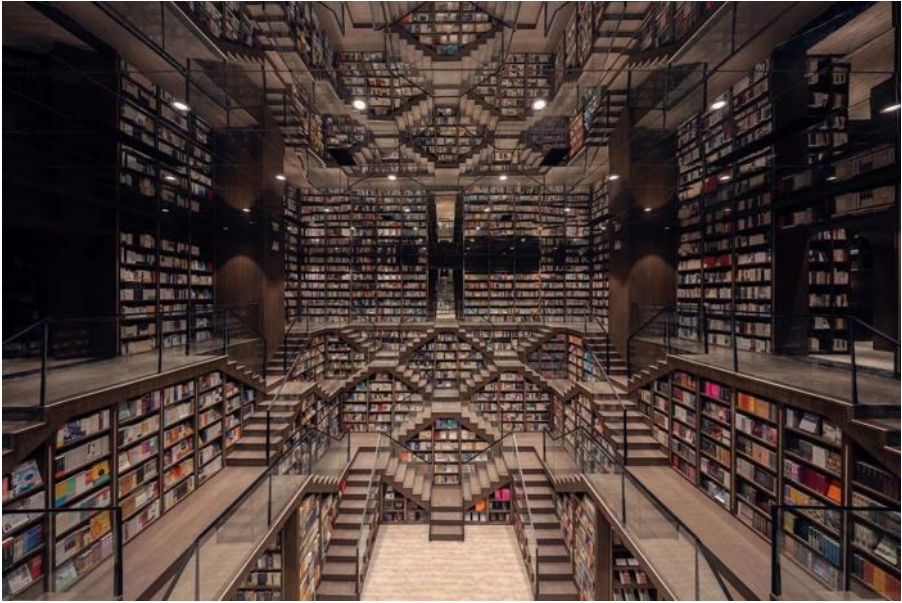
Figure 2. Zhongshuge Bookstore in China
(Retrieved April 6, 2020 from https://www.awesomeinventions.com/zhongshuge-bookstore-china-illusion/)

RESTORATIVE

The interaction with the built environment plays a significant role in the social, physical and psychological well-being of the individual. In everyday experience, people face mental fatigue and various sources of stress. Stress, which is an interrelation between the individual and the built environment, occurs when the individual evaluates his or her resources as insufficient to meet the demands of the built environment (Evans, 1982; Lazarus and Folkman, 1984). The resources become depleted as the individual mentally works over a week or after intense engagement in a project (Hartig, 2004). For the individual to recover from mental fatigue and reduce the stress level by means of relaxation, restorative environments are necessary (Kaplan and Talbot, 1983;

Korpela, De Bloom and Kinnunen, 2015). Restoration is defined as the renewal or recovery of psychological, physiological and social resources that have become diminished or depleted in meeting everyday demands (Hartig, 2004).

Restorativeness occurs as a result of dynamic interactions between the individual and the built environment, in which place-specific processes occur (Scopelliti and Giuliani, 2006). Restorative environments, which possess various attributes that facilitate recovery from mental fatigue and permit restoration, can be understood by the theoretical framework of attention restoration theory (ART) (Kaplan 1995; Kaplan and Kaplan, 1989). According to ART people can mitigate fatigue by entering built environments characterized by four restorative qualities: being-away, fascination, extent and compatibility (Kaplan 1995; Kaplan and Kaplan, 1989). Being-away implies being physically and/or mentally removed from daily routines and/or demanding activities. A new environment becomes restorative if it promotes a change in the individual's thoughts and allows the individual to escape from the pressures and obligations of everyday life. Fascination refers to the capability of the environment to involuntarily catch one's attention and presents an experience with aesthetically pleasing stimuli, in other words, being engaged without effort. Extent refers to the degree of coherence and order in the environment that can engage the mind and promote involvement and exploration. Compatibility refers to the degree to which the characteristics of the environment support the individual's activities,

purposes and inclinations. It is concerned with the match between what the individual wants to do, can do and must do (Kaplan 1995; Kaplan and Kaplan, 1989)

The combination of these qualities encourages involuntary attention and enables voluntary or focused attention to recover and restore (Kaplan, 1995; Staats, 2012). ART proposes that the more an environment is compatible, fascinating, extensive and allows being away, the more it will have a restorative potential (Scopelliti and Giuliani, 2006). Although certain types of settings (such as religious buildings) and activities (such as sleep) provide restorative opportunities, ART argues that exposure to nature and natural elements and view of nature have an aesthetic advantage and provide restoration (Kaplan and Kaplan, 1989). Research has demonstrated that natural environments are experienced and perceived as more restorative than urban environments (Berto, 2007; Hartig and Staats, 2003; Herzog, Black, Fountaine and Knotts, 2010; Kaplan and Berman 2010; Kaplan and Kaplan, 1989; Ohly et al., 2016).

Restorative qualities are represented by design elements that draw the attention effortlessly, reduce mental fatigue caused by focused, voluntary attention and minimize stress (Evans and McCoy, 1998). The restorative design elements that function as a coping resource can be changed by the balance between environmental demands and personal resources. These elements include retreat, fascination and exposure to nature (Evans and McCoy, 1998). Stimulus shelters and privacy nooks provide solitude and retreat, in other words, they allow

the individual to escape from prolonged or high levels of environmental demands of everyday life (see Figure 3). Fascination, which is being engaged by features of the environment or exploration of the environment and is aesthetically pleasing, can be created by window views, burning fireplaces and displays such as aquariums (Evans and McCoy, 1998). Window views to natural elements help to attenuate the negative impact of job stress on intentions to resign (Korpela et al., 2015).

Figure 3. Cozy window seat as stimulus shelter
(Retrieved April 8, 2020 from https://www.architectureartdesigns.com/30-inspirational-ideas-for-cozy-window-seat/)

CONCLUSION

In our interaction with the built environment, the quality of the built environment plays a significant role in our social, physical and psychological well-being. In some cases, built environments do not support the individual's activities that result in mental fatigue or stress. Stress is a crucial field of research for various disciplines and to minimize the risk of its occurrence in built environments, architects, interior architects and designers should carefully consider the design of affordable and restorative built environments.

REFERENCES

Berto, R. (2007). Assessing the restorative value of the environment: A study on the elderly in comparison with young and adolescents. *International Journal of Psychology*, 42(5), 331-341.

Cantada, R. (2010). Affordance and educational games. Retrieved March 8, 2020 from https://paaralan.blogspot.com/2010/09/affordance-and-educational-games.html

Evans, G. W. (1982). *Environmental stress.* Cambridge University Press: New York.

Evans, J. and McCoy, J. (1998). When buildings don't work: The role of architecture in human health. *Journal of Environmental Psychology*, 18, 85-94.

Galvao, A. B. and Sato, K. (2005). Affordances in product architecture: Linking technical functions and users' tasks. ASME 2005 International Design Engineering Technical Conferences and Computers and Information in Engineering Conference, 24-28 August, Long Beach, California, USA.

Gibson, J. J. (1979). The theory of affordances. In *The ecological approach to visual perception*, Boston: Houghton Mifflin, Lawrence Erlbaum Associates.

Hartig, T. (2004). Restorative environments. In C. Spielberger (Ed.), Encyclopedia *of Applied Psychology*, vol.3, (pp. 273-279). San Diego, CA: Academic Press.

Hartig, T. and Staats, H. (2003). Guest editors' introduction: Restorative environments. *Journal of Environmental Psychology*, 23, 103-107.

Herzog, T. R., Black, A. M., Fountaine, K. A. and Knotts, D. J. (1997). Reflection and attentional recovery as distinctive benefits of restorative environments. Journal of Environmental Psychology 17, 165-70.

Kaplan, S. (1995). The restorative benefit of nature: Toward an integrative framework. *Journal of Environmental Psychology*, 15, 169-182.

Kaplan, S., and Berman, M. G. (2010). Directed attention as a common resource for executive functioning and self-regulation. *Perspectives on Psychological Science*, 5, 43-57.

Kaplan, R. and Kaplan, S. (1989). *The Experience of Nature: A Psychological Perspective*. Cambridge: Cambridge University Press.

Kaplan, S. and Talbot, J. F. (1983). Psychological benefits of a wilderness experience. In I. Altman and J. Wohlwill (Eds.), *Behavior and the natural environment*. (pp. 163-203). Boston: Springer

Korpela, K., De Bloom, J. and Kinnunen, U. (2015). From restorative environments to restoration in work. *Intelligent Buildings International*, 7(4), 215-223.

Lazarus, R. S. and Folkman, S. (1984). *Stress, appraisal, and coping*. New York, NY: Springer.

Maier, J. R. A. and Fadel, G. M. (2007). Identifying affordances. International Conference on Engineering Design, ICED'07, 28-31 August, Cite Des Sciences Et De L'industrie, Paris, France.

Ohly, H., White, M. P., Wheeler, B. W., Bethel, A., Ukoumunne, O. C. Nikolaou, V. and Garside, R. (2016). Attention restoration theory: A systematic review of the attention restoration potential of exposure to natural environments. *Journal of Toxicology and Environmental Health, Part B*, 19(7), 305-343.

Raubal, M. and Moratz, R. (2008). A functional model for affordance-based agents. In E. Rome et al. (Eds.), *Affordance-based robot control.* (pp. 91-105). Berlin Heidelberg: Springer-Verlag.

Scopelliti, M. and Giuliani, M.V. (2006). Restorative environments in later life: An approach to well-being from the perspective of environmental psychology. *Journal of Housing for the Elderly*, 19(3-4), 203-226.

Staats, H. (2012). Restorative environments. In S. Clayton (Ed.), *The Oxford handbook of environmental and conservation psychology*. (pp. 445-58). New York, NY: Oxford University Press.

The Zhongshuge Bookstore in China. Retrieved April 6, 2020 from https://www.awesomeinventions.com/zhongshuge-bookstore-china-illusion/

Universal Design Principles. (2019). Retrieved February 02, 2019 from http://universalprinciplesofdesign.com/examples/

https://www.architectureartdesigns.com/30-inspirational-ideas-for-cozy-window-seat/

CHAPTER 5

γ-Al$_2$O$_3$-SUPPORTED MATERIALS FOR CATALYZING THE HYDROLYTIC DEHYDROGENATION OF AMMONIA BORANE

Assoc. Prof. Dr. Mehmet Sait İZGİ[1],
Assoc. Prof. Dr. Orhan BAYTAR[2],
Lecturer Müge YAYLA[3], Assoc. Prof. Dr. Hilal ÇELİK KAZICI[4],
Prof. Dr. Ömer ŞAHİN[5]

[1] Siirt University, Chemical Engineering, saitizgi@gmail.com
[2] Siirt University, Chemical Engineering, baytarorhan@gmail.com
[3] Van Yuzuncu Yil University, Chemical Engineering, muge.yayla23@gmail.com
[4] Van Yuzuncu Yil University, Chemical Engineering, hilalkazici@yyu.edu.tr
[5] Siirt University, Chemical Engineering, sahinomer2011@gmail.com

INTRODUCTION

The most important phenomenon human beings are in need of in the world to satisfy their primary and secondary needs is energy. The need for energy in the world increases rapidly with the increase in population and industrialization. Current sources do not satisfy the need. For this reason, the necessity of new energy sources emerges [1]. Alternative energy sources have remained on the agenda of scientists for a long time. Especially possessing minimum harm to the environment, being renewable and low-cost are the major qualifications that an alternative energy source should have. H_2 energy, that is H_2-based energy, is the first of these alternatives [2]. H_2 is the most abundant element in the universe and the most suitable element for the environment and it is seen very common in the nature in compound form [3] also considered as a promising alternative fuel for the future which can be produced from clean and renewable energy sources such as special semiconductor material solar light and water [4]. Consequently, It is quite significant to improve a procedure for high release of H_2 for safe storage under temperate conditions [5].

Ammonia borane (AB), commonly used for chemical hydrogen storage materials, has high theoretically H_2 content (19.6 wt%), longtime constancy in solutions and non-toxic advantages [6-9]. As a result of various researches, certain methods were determined for H_2 production from AB. These are; thermal dehydrogenation in high temperatures (thermolysis), catalytic hydrolysis, methanolysis [10-12]. From the methods, H_2 production was provided by using hydrolysis.

In hydrolysis, usually, the reaction of AB and water is provided with an appropriate catalyst [13].

$$NH_3BH_3 + 2H_2O \rightarrow NH_4^+ + BO_2^- + 3H_2 \qquad (1)$$
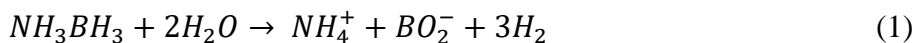
In the hydrolytic dehydrogenation method of AB, many catalyst types have experimented [6,14-22]. The development of non-noble metal catalyst for the hydrolysis of the AB is extremely important, considering that the noble metals are very expensive [23-30]. Multimetallic catalyst systems may offer a solution that addresses heterogeneous catalysts considered in the effective hydrogen release of the AB in terms of activity and cost [31].

In this work, we reports the synthesis, characterization and application of H_2 release of multimetallic-based CoCuB catalyst supported in γ-Al_2O_3. By using support material, it has been tried to provide high surface area, low agglomeration and stability. Co and Cu were selected because they are highly reactive metals in the hydrolysis of boron-based metal hydrides and B was coupled with $NaBH_4$ reduction method during synthesis which showed superior catalytic performance with a high rate of maximum hydrogen production rate (14000 mLg^{-1}min^{-1}).

H_2 PRODUCTION IN THE BATCH REACTOR

The CoCuB catalyst was produced by chemical reduction method for H_2 release from AB solutions. In the chemical reduction technique, the specified amounts of $CuCl_2$ and $CoCl_2.6H_2O$ were prepared in C_2H_5OH solution. The metal-containing solution was then added into

5, 10, 20 to 0.1 g by weight of γ-Al₂0₃. The solution was stirred at 25 °C during 12 hours. As a result, a 50 mL NaBH₄ aqueous solution was added dropwise under constant stirring at 5 °C to the solution containing the metal and support material. The resulting catalysts were then washed sequentially with pure water and ethyl alcohol. The obtained catalyst was dried in a vacuum oven at 80 °C during 5 hours under nitrogen gas. The prepared Co-Cu-B / γ-Al₂O₃ supported catalyst was used to determine the variation of H_2 production rate over time using the burette method. The H_2 production specific rates (r_{H_2}) were determined using data from the initial reaction rate and stabilization steps (70 mL of hydrogen was produced) with respect to following reaction (2):

$$r_{H_2} = \frac{70 \, mL}{t_{70}(min) w_C(g)} \tag{2}$$

Here, r_{H_2} indicates the H_2 production specific rate, t_{70} is the time for 70 mL of H_2 production, and w_c symbolizes the weight of elemental Co, Cu and B in the catalyst.

X-ray diffraction (XRD) results were obtained on D8 Bruker using Cu Kα (λ =0.15405 nm, 40 kV, 40 mA). Scanning electron microscopy (SEM-EDX) samples were analysed using Zeiss EVO Model. X-ray photoelectron spectroscopy (XPS) measurement was performed with ESCALAB 250Xi spectrophotometer. The pore morphology of the catalysts were carried out on a surface area analyzer (Quantachrome Corporation, USA) via N_2 adsorption/desorption at -196 ºC. The specific surface areas of the catalysts were measured from Brunauere

EmmetteTeller (BET) equation which using the N_2 adsorption/desorption isotherms.

CATALYST CHARACTERIZATIONS

To investigate the morphological features of Co-Cu-B/ γ-Al$_2$O$_3$, scanning electron microscopy (SEM) measurements were applied. SEM pictures of Co-Cu-B unsupported and Co-Cu-B catalysts supported with γ-Al$_2$O$_3$ are shown in Fig 1. The SEM (Fig. 1) images of Co-Cu-B/ γ-Al$_2$O$_3$ show that discrete Co-Cu-B nanoparticles are homogeneously dispersed on γ-Al$_2$O$_3$ surface.

Unsupported Co-Cu-B

Co-Cu-B/Al$_2$O$_3$
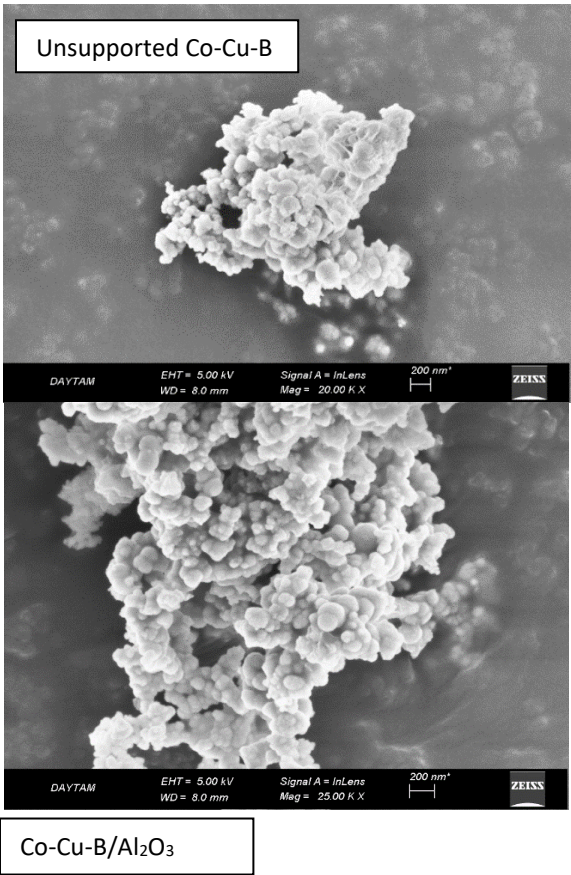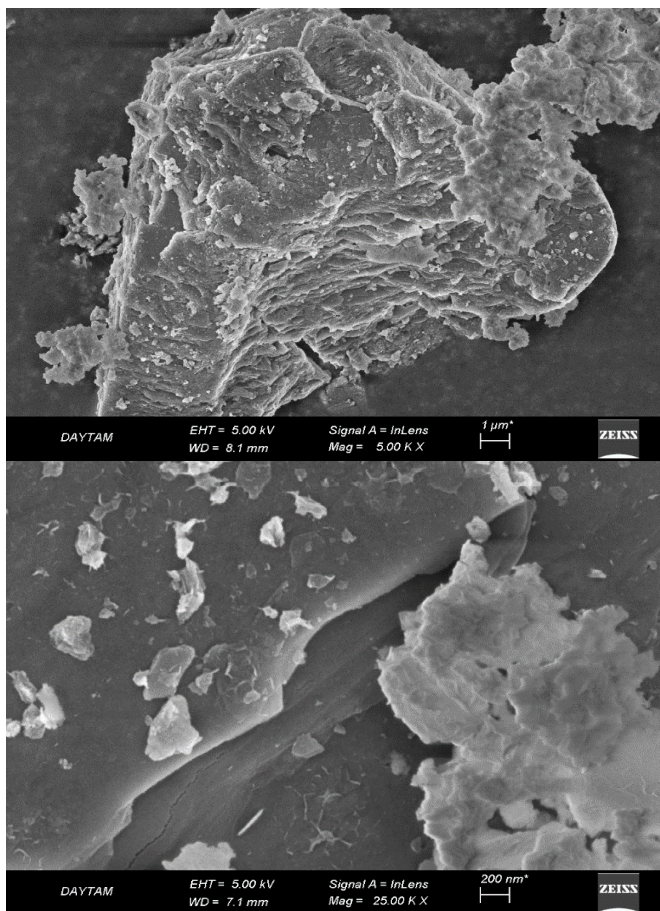
Figure 1. SEM images of catalysts

The chemical compounds of the unsupported Co-Cu-B, and supported Co-Cu-B catalysts were determined using EDX (Fig. 2). The unsupported Co-Cu-B catalyst contains 74.61% of Co and 18.86 % of Cu; the supported Co-Cu-B catalyst contains 8.99 % of Co, 48 % of γ-Al_2O_3. EDX analysis confirms the presence of elemental Co, Cu and γ-Al_2O_3, which are homogeneously distributed within catalysts.
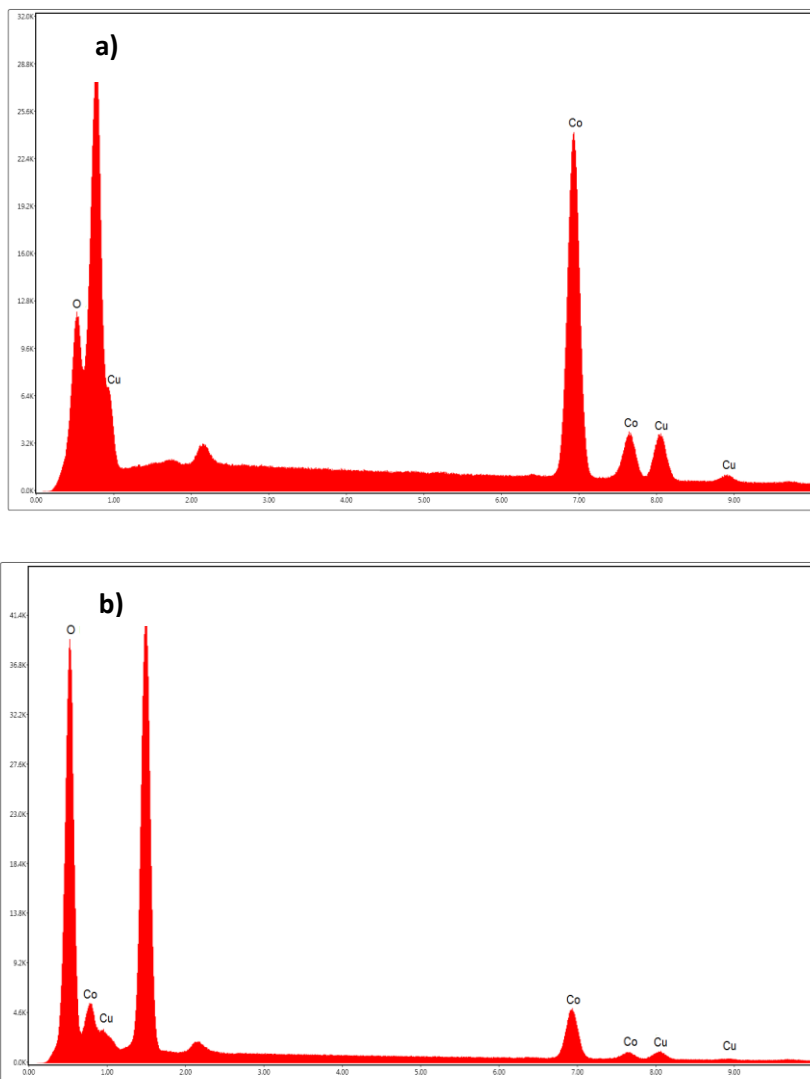
Figure 2. EDX spectra of **a)** unsupported catalyst **b)** γ-Al_2O_3 supported catalyst

Fig. 3. indicates XPS spectra for the supported and unsupported Co-Cu-B catalyst. On both graphs one peak clear, for all the catalyst composition, corresponding to the $Co2p3=2$ level at the binding

energies (BE) in a range of 770 - 781:8 eV. Thus, it is stated that the element Co is in both oxidized and elementary states. For Cu, only one peak is seen corresponding to a metallic state at binding energy of about 930 eV. Co-Cu-B catalyst supported on γ-Al$_2$O$_3$ is shifted by 10 and 30 eV toward higher values which might be assigned to both the quantum size impact.
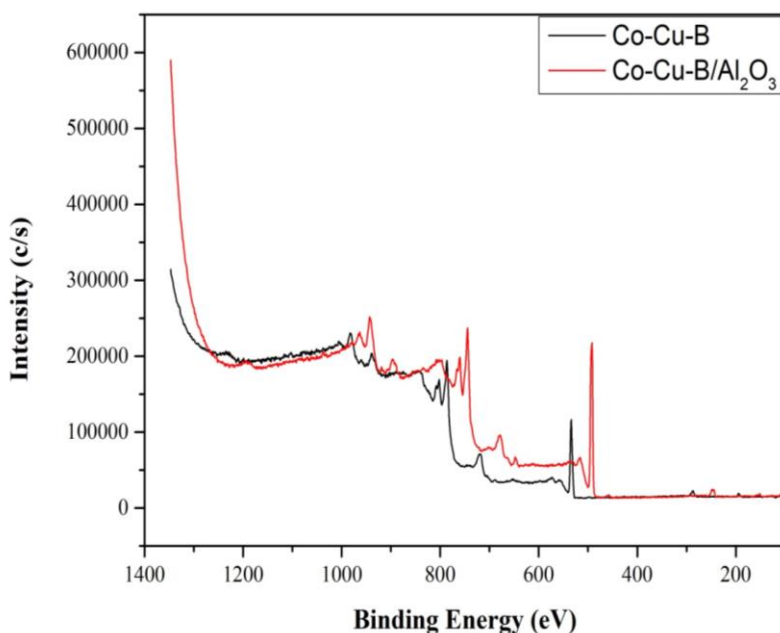
Figure 3. XPS spectra of catalysts

X-ray diffraction (XRD) models of unsupported and γ-Al$_2$O$_3$ supported Co-Cu-B catalyst are shown in Figure 4. XRD patterns both of them Co-Cu-B based alloy powders indicate a peak at $2\theta = 45$ º, which is attributed to the amorphous situation of Co-B alloy. Other peaks at around 38º assigned to exist of Cu metal, are also followed up for Co-Cu-B catalyst powders. The peaks at around 46° and 66°

indicated to γ-Al$_2$O$_3$ support. At the same time for γ-Al$_2$O$_3$ supported/Co-Cu-B catalyst, the increase expressed in the base diffraction pattern density at around $2\theta = 36°$ demonstrates a decent crystal formation.
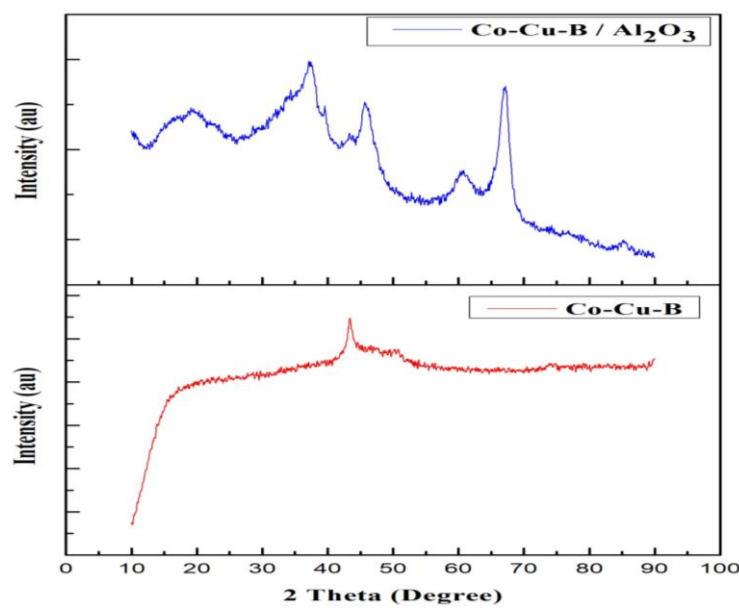
Figure 4. XRD pattern of catalysts

The BET surface area analyzed for on γ-Al$_2$O$_3$ and Co-Cu-B catalysts unsupported on supported- Co-Cu-B. As seen Table 1, the surface areas of the catalysts increase as the concentration of the support material increases.

Table 1. BET analysis of catalysts

BET Surface Area: 19.3600 m^2/g	**BET Surface Area:** 116.4129 m^2/g
Unsupported Co-Cu-B	Co-Cu-B/ γ-Al$_2$O$_3$

MEASUREMENT OF ACTIVITY

Firstly, the effect of the percentage of the support material γ-Al$_2$O$_3$ nanoparticles on H$_2$ production rate was studied (Figure 5). To this end, catalysts were synthesized to be 5-10-20% (wt.) respectively, in three different percentages of the support.
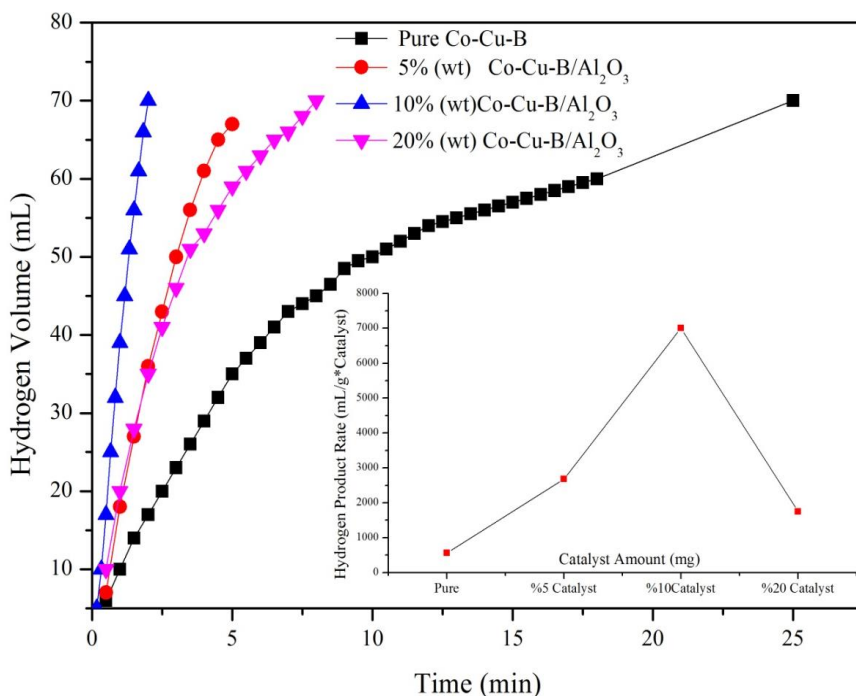
Figure 5. The effect of the percentage amount of γ-Al$_2$O$_3$.

According to Figure 5, we can clearly see that the increase in the percentage of support is not necessarily positive to improve H_2 production rate, but it is more effective to achieve a synergistic percentage in the catalyst. In subsequent experiments, the γ-Al_2O_3 support rate was synthesized as 10% by weight (weight).

The effect of the amount of CoCuB/ γ-Al_2O_3 on the hydrolysis reaction of AB

H_2 production rate from AB was examined by changing 25 to 100 mg of the CoCuB/ γ-Al_2O_3 catalyst as shown in Fig. 6. The H_2 production rate firstly increased sharply when 50 mg (7000 mLg^{-1}min^{-1}) of catalyst was reacted and then slowed down (3500 mLg^{-1}min^{-1} for 100 mg) with increasing catalyst amount. These results showed that the amount of catalyst influences the H_2 release rate as well as the amount of AB per catalyst unit. Therefore, to achieve high catalytic efficiency catalyst was used as little as possible in 50 mg catalysts subsequent experiments.
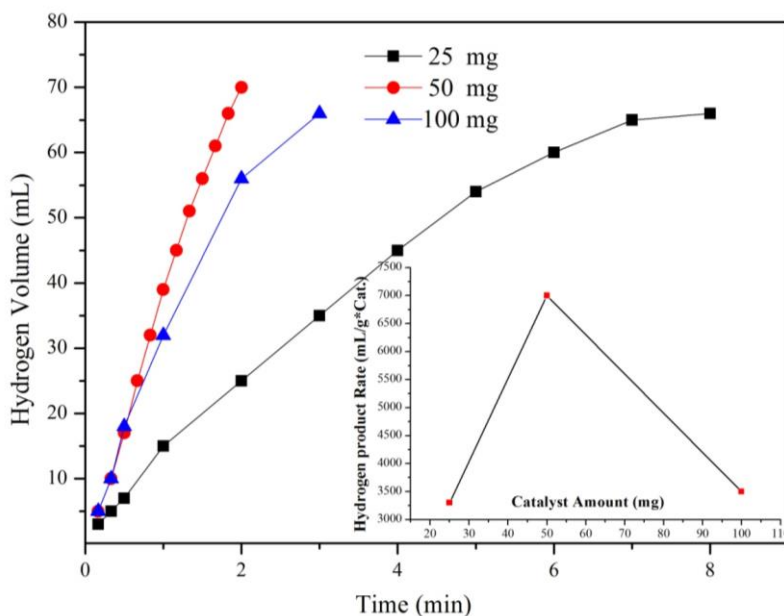
Figure 6. Effect of different catalyst amounts on the hydrolysis of AB

The effect of AB concentration on the hydrolysis reaction

Figure 7 shows the effect of different AB concentrations on hydrogen production. H_2 production rate increased when AB concentration increased from 0.5 to 2 mmol. As the concentration in the solution increases, the energy density increases due to viscosity. This causes limitation in transporting the AB from the solution to the catalyst surface. 1 mmol AB was determined to be suitable concentration for the study.
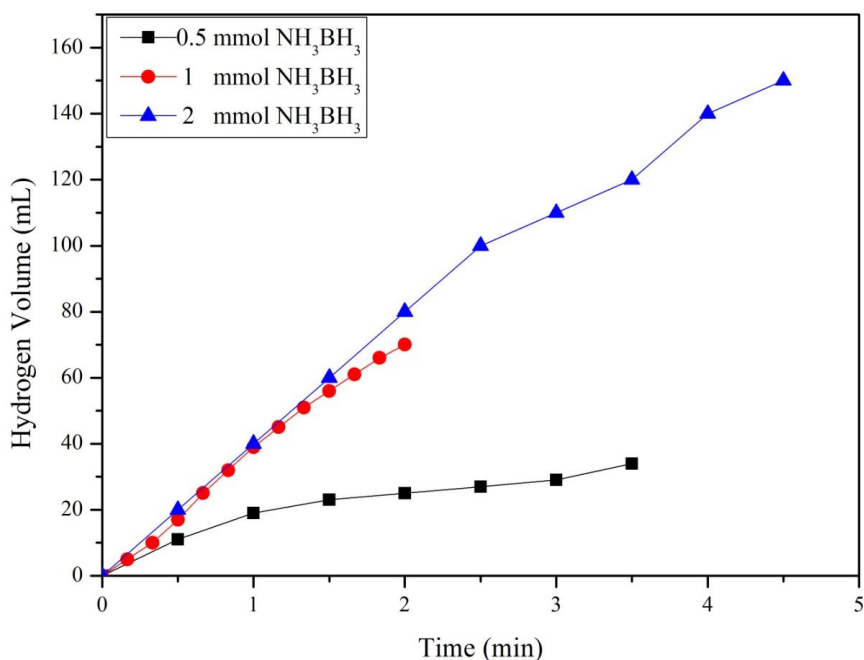
Figure 7. The effect of different AB concentration on the hydrogen production

The effect of concentration of NaOH

The effect of synthesized CoCuB / γ-Al$_2$0$_3$ catalyst on AB hydrogen release was examined by changing NaOH concentrations. It has been observed that the presence of NaOH affects the release of hydrogen from the AB to a certain extent (Figure 8). In Figure 8, it is clear that the catalyst produces 70 mL of H$_2$ in about 2 minutes using 1% NaOH by weight, and H$_2$ produces 65 mL in about 6 minutes using 5% (by weight) NaOH. In this case, the most effective NaOH concentration was determined to be 1% by weight on AB hydrolysis.
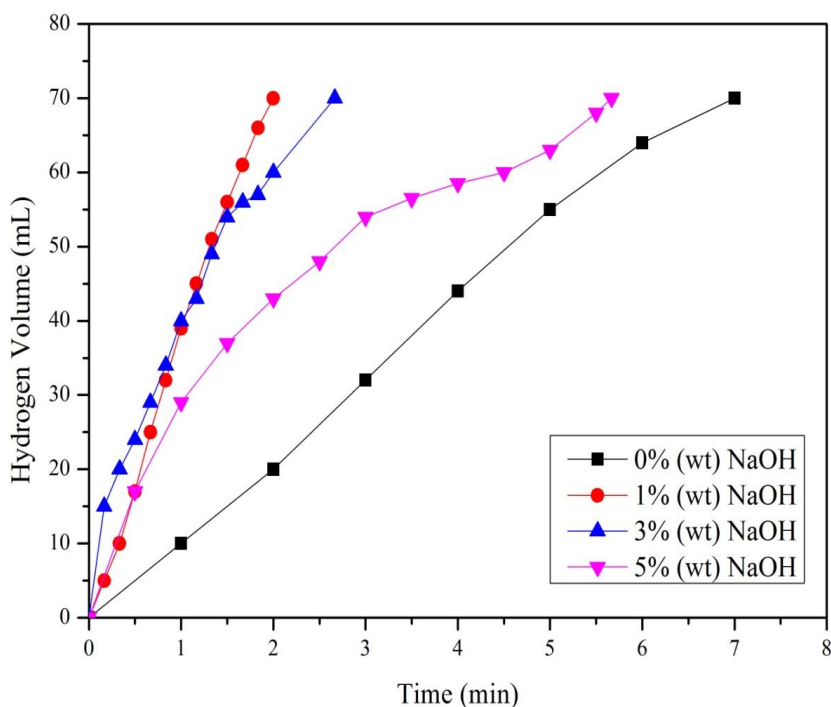
Figure 8. The effect of NaOH amounts on the hydrogen production from AB

The effect of temperature and evolution of Ea on the hydrogenetion of AB

It is very general and clear information that temperature greatly affects the catalytic activity of various reactions. Results exhibit that the H_2 generation reaction rate increases with the solution temperature increases as assumed. Activation energy, initial and Arrhenius form of H_2 production rate were obtained for CoCuB/ γ-Al_2O_3 catalysts by using Eq. (2), at the different temperatures (30-60 ºC) [32].

$$r = k_o e^{-Ea/RT} \hspace{3cm} (2)$$

wherein the symbols are explained in order; r is the ratio of H_2

production ($mLmin^{-1}g^{-1}$), k_0 is the reaction constant ($mLmin^{-1}g^{-1}$), Ea; activation energy of AB hydrolysis ($Jmol^{-1}$), R and T are gas constants (8.314 $Jmol^{-1}K^{-1}$) and reaction temperature (K), respectively. As a result, the slope of the linear graph showed activation energy of 6.74 $kJmol^{-1}$. This result is lower than the of most Co and Cu-based and other catalysts presented in the literature (Table 2), showing the excellent catalytic activity of the as-prepared CoCuB/ γ-Al_2O_3. Based on Ea, a comparison between both supported and unsupported catalysts and the rate of hydrogen production which is the catalytic activity parameter is presented in Table 2.
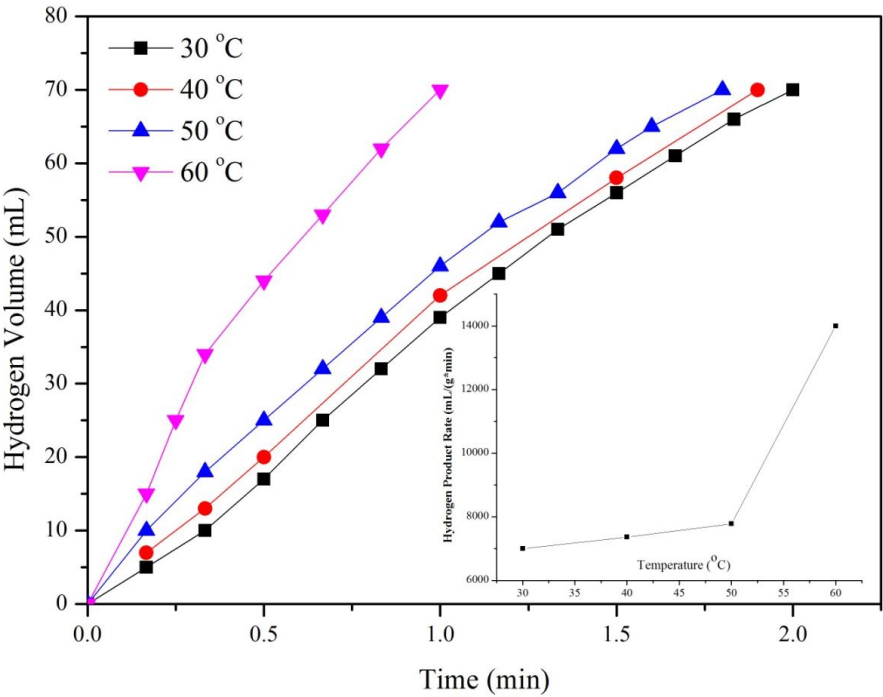
Figure 9. Plots of time versus volume of produced H_2 from the AB solution catalyzed by CoCuB/ γ-Al_2O_3 catalyst at various temperatures

1/T

-1,95

0,00295   0,003   0,00305   0,0031   0,00315   0,0032   0,00325   0,0033   0,00335

-2

ln(k)   -2,05

-2,1

y = -811,1x + 0,442
R² = 0,9697

-2,15

-2,2

-2,25
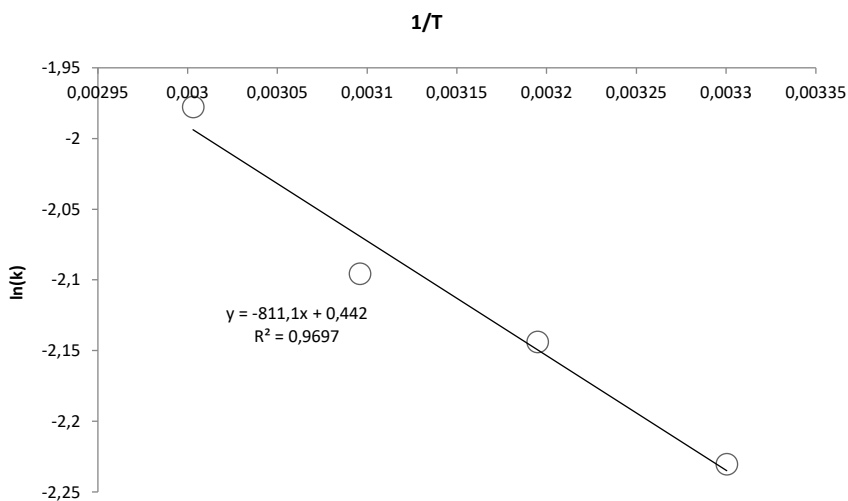
Figure 10. Arrhenius plot for calculating the activation energies of supported multimetallic catalysts on the γ-Al$_2$O$_3$. Data were obtained from Fig. 9

Table 2. A comparison for the efficient of the catalysts in H$_2$ production.

Catalyst	Temperature °C	H$_2$ production rate (mLmin^{-1}gcat^{-1})	Ea (kJmol^{-1})	Ref.
Co–P/ Ni foam	RT	1350	48	[33]
Co/Ni foam	RT	2650	59	[34]
Co–W–B/foam sponge	RT	3327.7	32.2	[35]
Co–Ni–P/Pd–TiO$_2$	RT	170	54	[36]
Cu$_{0.3}$@Fe$_{0.1}$Co$_{0.6}$	RT	6674	38.7	[37]
Cu(0)/ Hydrogel	30	242	52	[38]
Cu/Co$_3$O$_4$	RT	1411	-	[39]
Co–Mo–B NPs/Cu foil	RT	5818	55.2	[40]
Co@g-C$_3$N$_4$-rGO	RT	3560	35.4	[41]
Co@CoOx@CG	30	5560	40	[42]
Co@Pt	30	5869	-	[43]
Co-Cr-B/γ-AlO$_3$	30	3260	56.06	[22]
Co–Fe–P	30	2858	25	[44]
Cu$_{0.4}$Co$_{0.6}$/boron nitride nanofibers	25	3387	21.8	[45]
Co-Cu-B/(10 wt%) γ-Al$_2$O$_3$	30 / 60	7000 / 14000	6.74	This work

RT: Room temperature

CoCuB nanoparticles which interacted with γ-Al_2O_3 had been investigated by a simple preparation method. The optimal (10%) γ-Al_2O_3 catalyst of Co-Cu-B showed a superior catalytic performance in the AB hydrolytic reaction and its H_2 release rate achieves 14000 mL min^{-1}·g^{-1}, and the Ea of 6.74 kJ mol^{-1} is even smaller than that of noble metal catalysts. The high catalytic activity was attributed to good distributed Co-Cu-B/(10 wt%) γ-Al_2O_3, regular catalyst distribution, favourable metal-to-metal synergy and favoured metal-to-support interaction. The main purpose of these studies is to develop catalysts that will increase the potential of chemical hydrogen storage materials for portable fuel cells.

However, there are still difficulties for practical applications such as cost, activation, control of by-product and reaction kinetics. Further development of these hydrolytic dehydrogenation materials can make significant contributions to the future of sustainable energy.

REFERENCES

1. Manoharan Y, Hosseini SE, Butler B, Alzhahrani H, Fou BT, Ashuri T, Krohn J (2019) Hydrogen Fuel Cell Vehicles; Current Status and Future Prospect. Applied Sciences-Basel 9 (11). doi:10.3390/app9112296

2. Sherif SA, Barbir F, Veziroglu TN (2003) Principles of hydrogen energy production, storage and utilization. Journal of Scientific & Industrial Research 62 (1-2):46-63

3. Zuttel A (2004) Hydrogen storage methods. Naturwissenschaften 91 (4):157-172. doi:10.1007/s00114-004-0516-x

4. Bowker M (2012) Photocatalytic Hydrogen Production and Oxygenate Photoreforming. Catalysis Letters 142 (8):923-929. doi:10.1007/s10562-012-0875-4

5. Hou CC, Li Q, Wang CJ, Peng CY, Chen QQ, Ye HF, Fu WF, Che CM, Lopez N, Chen Y (2017) Ternary Ni-Co-P nanoparticles as noble-metal-free catalysts to boost the hydrolytic dehydrogenation of ammonia-borane. Energy & Environmental Science 10 (8):1770-1776. doi:10.1039/c7ee01553d

6. Wang S, Zhang D, Ma YY, Zhang H, Gao J, Nie YT, Sun XH (2014) Aqueous Solution Synthesis of Pt-M (M = Fe, Co, Ni) Bimetallic Nanoparticles and Their Catalysis for the Hydrolytic Dehydrogenation of Ammonia Borane. Acs Applied Materials & Interfaces 6 (15):12429-12435. doi:10.1021/am502335j

7. Basu S, Brockman A, Gagare P, Zheng Y, Ramachandran PV, Delgass WN, Gore JP (2009) Chemical kinetics of Ru-catalyzed ammonia borane hydrolysis. Journal of Power Sources 188 (1):238-243. doi:10.1016/j.jpowsour.2008.11.085

8. Kazici HC, Yildiz F, Izgi MS, Ulas B, Kivrak H (2019) Novel activated carbon supported trimetallic PdCoAg nanoparticles as efficient catalysts for the

hydrolytic dehydrogenation of ammonia borane. International Journal of Hydrogen Energy 44 (21):10561-10572. doi:10.1016/j.ijhydene.2019.02.198

9. Stephens FH, Pons V, Baker RT (2007) Ammonia - borane: the hydrogen source par excellence? Dalton Transactions (25):2613-2626. doi:10.1039/b703053c

10. Rakap M, Ozkar S (2010) Hydrogen generation from the hydrolysis of ammonia-borane using intrazeolite cobalt(0) nanoclusters catalyst. International Journal of Hydrogen Energy 35 (8):3341-3346. doi:10.1016/j.ijhydene.2010.01.138

11. Kazici HC, Yilmaz S, Sahan T, Yildiz F, Er OF, Kivrak H A comprehensive study of hydrogen production from ammonia borane via PdCoAg/AC nanoparticles and anodic current in alkaline medium: experimental design with response surface methodology. Frontiers in Energy. doi:10.1007/s11708-020-0808-7

12. Kazici HC, Salman F, Izgi MS, Sahin O (2020) Synthesis of Metal-Oxide-Supported Triple Nano Catalysts and Application to H-2 Production and H2O2 Oxidation. Journal of Electronic Materials 49 (6):3634-3644. doi:10.1007/s11664-020-08061-6

13. Meng XY, Yang L, Cao N, Du C, Hu K, Su J, Luo W, Cheng GZ (2014) Graphene-Supported Trimetallic Core-Shell Cu@CoNi Nanoparticles for Catalytic Hydrolysis of Amine Borane. Chempluschem 79 (2):325-332. doi:10.1002/cplu.201300336

14. Jiang HL, Umegaki T, Akita T, Zhang XB, Haruta M, Xu Q (2010) Bimetallic Au-Ni Nanoparticles Embedded in SiO2 Nanospheres: Synergetic Catalysis in Hydrolytic Dehydrogenation of Ammonia Borane. Chemistry-a European Journal 16 (10):3132-3137. doi:10.1002/chem.200902829

15. Zhou X, Meng XF, Wang JM, Shang NZ, Feng T, Gao ZY, Zhang HX, Ding XL, Gao ST, Feng C, Wang C (2019) Boron nitride supported NiCoP

nanoparticles as noble metal-free catalyst for highly efficient hydrogen generation from ammonia borane. International Journal of Hydrogen Energy 44 (10):4764-4770. doi:10.1016/j.ijhydene.2019.01.026

16. Shan XL, Du J, Cheng FY, Liang J, Tao ZL, Chen J (2014) Carbon-supported Ni3B nanoparticles as catalysts for hydrogen generation from hydrolysis of ammonia borane. International Journal of Hydrogen Energy 39 (13):6987-6994. doi:10.1016/j.ijhydene.2014.02.122

17. Sun DH, Mazumder V, Metin O, Sun SH (2011) Catalytic Hydrolysis of Ammonia Borane via Cobalt Palladium Nanoparticles. Acs Nano 5 (8):6458-6464. doi:10.1021/nn2016666

18. Akbayrak S, Tonbul Y, Ozkar S (2016) Ceria supported rhodium nanoparticles: Superb catalytic activity in hydrogen generation from the hydrolysis of ammonia borane. Applied Catalysis B-Environmental 198:162-170. doi:10.1016/j.apcatb.2016.05.061

19. Demirci UB, Miele P (2014) Cobalt-based catalysts for the hydrolysis of NaBH4 and NH3BH3. Physical Chemistry Chemical Physics 16 (15):6872-6885. doi:10.1039/c4cp00250d

20. Fernandes R, Patel N, Miotello A, Jaiswal R, Kothari DC (2012) Dehydrogenation of Ammonia Borane with transition metal-doped Co-B alloy catalysts. International Journal of Hydrogen Energy 37 (3):2397-2406. doi:10.1016/j.ijhydene.2011.10.119

21. Yang L, Cao N, Du C, Dai HM, Hu K, Luo W, Cheng GZ (2014) Graphene Supported cobalt(0) nanoparticles for hydrolysis of ammonia borane. Materials Letters 115:113-116. doi:10.1016/j.matlet.2013.10.039

22. Izgi MS, Sahin O, Saka C gamma-Al2O3 supported/Co-Cr-B catalyst for hydrogen evolution via NH3BH3 hydrolysis. Materials and Manufacturing

Processes:7. doi:10.1080/10426914.2019.1594280

23. Xu Q, Chandra M (2006) Catalytic activities of non-noble metals for hydrogen generation from aqueous ammonia-borane at room temperature. Journal of Power Sources 163 (1):364-370. doi:10.1016/j.jpowsour.2006.09.043

24. Kazici HC, Yayla M, Ulas B, Aktas N, Kivrak H (2019) Development of Nonenzymatic Benzoic Acid Detection on PdSn/GCE/Vulcan XC-72R Prepared via Polyol Method. Electroanalysis 31 (6):1118-1124. doi:10.1002/elan.201900088

25. Kazici HC, Caglar A, Aydogmus T, Aktas N, Kivrak H (2018) Microstructured prealloyed Titanium-Nickel powder as a novel nonenzymatic hydrogen peroxide sensor. Journal of Colloid and Interface Science 530:353-360. doi:10.1016/j.jcis.2018.06.079

26. Kazici HC, Yayla M (2019) An electrocatalyst for detection of glucose in human blood: synergy in Pd-AuNPs/GOx/C surfaces. Chemical Engineering Communications 206 (12):1731-1742. doi:10.1080/00986445.2019.1576645

27. Kazici HC, Salman F, Kivrak HD (2017) Synthesis of Pd-Ni/C bimetallic materials and their application in non-enzymatic hydrogen peroxide detection. Materials Science-Poland 35 (3):660-666. doi:10.1515/msp-2017-0072

28. Kazici HC, Salman F, Caglar A, Kivrak H, Aktas N (2018) Synthesis, characterization, and voltammetric hydrogen peroxide sensing on novel monometallic (Ag, Co/MWCNT) and bimetallic (AgCo/MWCNT) alloy nanoparticles. Fullerenes Nanotubes and Carbon Nanostructures 26 (3):145-151. doi:10.1080/1536383x.2017.1420061

29. Duzenli D, Sahin O, Kazici HC, Aktas N, Kivrak H (2018) Synthesis and characterization of novel Ti doped hexagonal mesoporous silica catalyst for

nonenzymatic hydrogen peroxide oxidation. Microporous and Mesoporous Materials 257:92-98. doi:10.1016/j.micromeso.2017.08.030

30. Avci C, Cicek F, Kazici HC, Kivrak A, Kivrak H (2018) A novel study on the stepwise electrodeposition approach for the synthesis of Pd based nanoparticles, characterization and their enhanced electrooxidation activities. International Journal of Nano Dimension 9 (1):15-23

31. Rachiero GP, Demirci UB, Miele P (2011) Bimetallic RuCo and RuCu catalysts supported on gamma-Al2O3. A comparative study of their activity in hydrolysis of ammonia-borane. International Journal of Hydrogen Energy 36 (12):7051-7065. doi:10.1016/j.ijhydene.2011.03.009

32. Baytar O, Izgi MS, Horoz S, Sahin O, Nar S (2019) Al2O3 SUPPORTED Co-Cu-B (Co-Cu-B/Al2O3) CATALYST FOR HYDROGEN GENERATION BY HYDROLYSIS OF AQUEOUS SODIUM BOROHYDRIDE (NaBH4) SOLUTIONS. Digest Journal of Nanomaterials and Biostructures 14 (3):673-681

33. Eom K, Kim M, Kim R, Nam D, Kwon H (2010) Characterization of hydrogen generation for fuel cells via borane hydrolysis using an electroless-deposited Co-P/Ni foam catalyst. Journal of Power Sources 195 (9):2830-2834. doi:10.1016/j.jpowsour.2009.11.084

34. Paladini M, Arzac GM, Godinho V, De Haro MCJ, Fernandez A (2014) Supported Co catalysts prepared as thin films by magnetron sputtering for sodium borohydride and ammonia borane hydrolysis. Applied Catalysis B-Environmental 158:400-409. doi:10.1016/j.apcatb.2014.04.047

35. Li C, Wang D, Wang Y, Li GD, Hu GJ, Wu SW, Cao ZQ, Zhang K (2018) Enhanced catalytic activity of the nanostructured Co-W-B film catalysts for hydrogen evolution from the hydrolysis of ammonia borane. Journal of Colloid and Interface Science 524:25-31. doi:10.1016/j.jcis.2018.03.085

36. Rakap M, Kalu EE, Ozkar S (2011) Polymer-immobilized palladium supported on TiO2 (Pd-PVB-TiO2) as highly active and reusable catalyst for hydrogen generation from the hydrolysis of unstirred ammonia-borane solution. International Journal of Hydrogen Energy 36 (2):1448-1455. doi:10.1016/j.ijhydene.2010.10.097

37. Qiu FY, Dai YL, Li L, Xu CC, Huang YN, Chen CC, Wang YJ, Jiao LF, Yuan HT (2014) Synthesis of Cu@FeCo core-shell nanoparticles for the catalytic hydrolysis of ammonia borane. International Journal of Hydrogen Energy 39 (1):436-441. doi:10.1016/j.ijhydene.2013.10.080

38. Ozay O, Inger E, Aktas N, Sahiner N (2011) Hydrogen production from ammonia borane via hydrogel template synthesized Cu, Ni, Co composites. International Journal of Hydrogen Energy 36 (14):8209-8216. doi:10.1016/j.ijhydene.2011.04.140

39. Yamada Y, Yano K, Xu QA, Fukuzumi S (2010) Cu/Co3O4 Nanoparticles as Catalysts for Hydrogen Evolution from Ammonia Borane by Hydrolysis. Journal of Physical Chemistry C 114 (39):16456-16462. doi:10.1021/jp104291s

40. Wang Y, Meng W, Wang D, Wang ZR, Zou KL, Cao ZQ, Zhang K, Wu SW, Li GD (2019) Ultrafine cobalt-molybdenum-boron nanocatalyst for enhanced hydrogen generation property from the hydrolysis of ammonia borane. International Journal of Hydrogen Energy 44 (41):23267-23276. doi:10.1016/j.ijhydene.2019.07.068

41. Duan SS, Han GS, Su YH, Zhang XY, Liu YY, Wu XL, Li BJ (2016) Magnetic Co@g-C3N4 Core-Shells on rGO Sheets for Momentum Transfer with Catalytic Activity toward Continuous-Flow Hydrogen Generation. Langmuir 32 (25):6272-6281. doi:10.1021/acs.langmuir.6b01248

42. Xing CC, Liu YY, Su YH, Chen YH, Hao S, Wu XL, Wang XY, Cao HQ, Li BJ

(2016) Structural Evolution of Co-Based Metal Organic Frameworks in Pyrolysis for Synthesis of Core-Shells on Nanosheets: Co@CoOx@Carbon-rGO Composites for Enhanced Hydrogen Generation Activity. Acs Applied Materials & Interfaces 8 (24):15430-15438. doi:10.1021/acsami.6b04058

43. Yan JM, Zhang XB, Akita T, Haruta M, Xu Q (2010) One-Step Seeding Growth of Magnetically Recyclable Au@Co Core-Shell Nanoparticles: Highly Efficient Catalyst for Hydrolytic Dehydrogenation of Ammonia Borane. Journal of the American Chemical Society 132 (15):5326-+. doi:10.1021/ja910513h

44. Oh S, Song D, Kim H, Sohn D, Hong K, Lee M, Son S, Cho E, Kwon H (2019) Cobalt-iron-phosphorus catalysts for efficient hydrogen generation from hydrolysis of ammonia borane solution. Journal of Alloys and Compounds 806:643-649. doi:10.1016/j.jallcom.2019.07.190

45. Yang X, Li QL, Li LL, Lin J, Yang XJ, Yu C, Liu ZY, Fang Y, Huang Y, Tang CC (2019) CuCo binary metal nanoparticles supported on boron nitride nanofibers as highly efficient catalysts for hydrogen generation from hydrolysis of ammonia borane. Journal of Power Sources 431:135-143. doi:10.1016/j.jpowsour.2019.05.038

CHAPTER 6

NEW GENERATION CHEMICAL MATERIALS: SYNTHESIS AND PROPERTIES FOR ENERGY APPLICATIONS

Asst. Prof. Dr. Ebru YABAŞ[1], Prof. Dr. Pınar BAŞER[2],
Prof. Dr. Mehmet KUL[3]

[1] Sivas Cumhuriyet University, Advanced Technology Research and Application Center, Sivas, Turkey. eyabas@cumhuriyet.edu.tr
[2] Sivas Cumhuriyet University, Science Faculty, Department of Physics, Sivas, Turkey. pbaser34@gmail.com
[3] Sivas Science and Technology University, Aviation and Space Sciences Faculty, Department of Aircraft Engineering, Sivas, Turkey. kulmeh@gmail.com

INTRODUCTION

Phthalocyanines have the potential to be used in many areas of technology due to their stable π-conjugated system and chemical properties. Phthalocyanines, which are a synthetic analogue of porphyrin macrocycle, are organic semiconductor compounds. Phthalocyanines have an intense blue-green color and attract attention in many applications due to their strong absorption at high wavelengths such as 600-750 nm [Lenzoff and Lever 1989; Lenzoff and Lever 1993; Lenzoff and Lever 1996; Zhang et al. 2010; Nyokong 2007]. Due to their physical, chemical, optical and electronic properties, phthalocyanines have applications in fields such as organic solar cells, photovoltaic applications, optical recording medium, nonlinear optical application, light absorption, electrical conduction, photoconduction, energy conversion, electrodes, chemical sensors and catalyst. The solubility of phthalocyanines is very poor, which limits use in many areas of application. The solubility of the phthalocyanine ring can be increased as desired by means of substituted groups and metal ions attached to the center [Atilla et al. 2009; Jiang 2010; Lenzoff, Lever 1993].

On the other hand, pyrimidine is a highly π-deficient aromatic heterocycle and it can therefore be used as electron withdrawing part in push-pull structures for ICT. Also the protonation, hydrogen bond formation and chelation ability of the pyrimidine ring are of great importance in the usability in many applications [Petroz 2006; Chien 2004].

A synthesized new generation compound will be obtained by combining these two important groups of compounds.

It is desired that organic compounds to be used in optoelectronic and energy applications do not exhibit aggregation behavior, have high fluorescence quantum efficiency, have high wavelength absorption and have appropriate trajectory levels to allow electron transfer [Zhang et al. 2010; Babudri et al. 2007; Torre et al. 2010].

Photoluminescence is an analytical spectroscopic method that does not damage the material to investigate semiconductor properties through optical radiation. By using this method, it is possible to know about the Fermi level of the p-type doped materials, the band structure, the optical properties of the semiconductors and the low-level shallow impurities in the epitaxial layers [Olego, D., Cardona 1980]. It is known that the properties of the photoluminescent properties are related to the growth conditions (or methods), impurity properties, additive concentration and temperature [Kim et al. 1993].

Photoluminescence (PL) is the natural diffusion of light from a material under optical excitation. When the semiconductor is stimulated by a laser that emits a photon that has a higher value than its own band gap, it is stimulated to the energy levels of the transmission band by absorption of an electron and photons in the valence band and form electron-discrete pairs. Electron-rupture pairs formed by optical stimulation in semiconductor materials emit this energy that they lose while returning to their basic energy states. In order to characterize the optical properties of our samples to be used in this study, UNIRAM

brand Wide Spectrum (200-2200 nm) High Resolution Photoluminescence Spectrometer measurement system was used in Sivas Cumhuriyet University Advanced Technology Application and Research Center (CÜTAM).

1. EXPERIMENTAL

1.1. General

Reactions were carried out under nitrogen atmosphere. All solvents were dried by molecular sieves or proper methods [Armarego, Chai, 2003]. The pyrimidine substituted phthalonitrile derivative as starting material was prepared according to the literature [Yabaş 2017]. IR spectra were recorded on a PerkinElmer Spectrum100 FT-IR Spectrometer using ATR. UV-vis spectrum was recorded on a Shimadzu UV-1800 UV-vis spectrophotometer. ^{1}H-NMR spectra were obtained by using JEOL Resonance ECZ400S 400 MHz spectrometer. Fluoresans spectrum of compound was conducted with Shimadzu RF 5301fluo-rescence spectrophotometer. The surface morphology of thin films of organic materials were examined with a TESCAN® MIRA3 XMU (Brno, Czechia) brand scanning electron microscope. Electrothermal 9100 digital melting point apparatus was used to determine the melting point.

1.2. Synthesis

Synthesis of pyrimidine derivative tetrasubstituted titanium phthalocyanine

The solution in DMSO:Pentanole (3:1) mixture of pyrimidine substituted phthalonitrile and titanium(IV) butoxide ($Ti(OC_4H_9)_4$) was heated at 180^oC at the presence of DBU (1,8-diazabicyclo[5.4.0]undec-7-ene) for 18h. After cooling, the green mixture was precipitated by n-hexane:ether (1:1) and filtered off. The green oily solid was washed with MeOH, H_2O and acetone respectively. It also was dried. The product was purified by column chromatography with silicagel (THF/methanol (10/1)). The green solid was soluble in THF, DMF and DMSO. Yield: 31%. Mp: >300^oC. ^1H NMR (400 MHz, DMSO-d_6, 25 ^oC): δ= 8.9-8.0 (br m, Pc Ar-H, bipyridine-H); 5.2 (s, -OH). UV-Vis (DMSO) λ_{max}/nm; 667, 602, 343. IR (ATR) υ (cm^{-1}) 3184-2929;1770; 1724; 1643; 1582; 1489; 1443; 1205; 1063; 1022; 767.

1.3. PL measurement

Thin films of the compound were prepared on the glass surface by drop-casting method. These thin films were used in PL measurements. UNIRAM brand Wide Spectrum (200-2200 nm) High Resolution Photoluminescence Spectrometer measurement system was used for PL. Samples are loaded in a closed-circuit cooler so that measurements can be taken in the 10-300 K temperature range. Laser used to stimulate the sample in photoluminescence measurements is a Single Mode diode laser with a wavelength of 732 nm. This laser is dropped onto the sample. It focuses on the input of the spectrometer with the help of luminescence lenses and mirrors released from the sample after stimulation of the semiconductor. The energy resolution of the photoluminescence system used is good and it can distinguish sharp and

close peaks that can be seen in the spectrum. In this arrangement, the CCD camera and spectrometer are completely controlled by a computer by software. This optical signal obtained with the help of the detector is converted into electrical signal. The corresponding wavelength (or intensity-energy) graph of this signal, which corresponds to the luminescence radiation of the material, is drawn and the photoluminescence spectrum is obtained.

In this study, PL measurements were evaluated in the temperature range of 50 to 300K. Low temperature photoluminescence measurements were performed by a 785 nm single-mode diode laser with 100 mW optical output power. The signal was detected by the Andor Solis CCD detector with a backlit pixel format of 2000x256 pixels.

1.4. Preparation of organic thin films

Thin films of pyrimidine derivative tetrasubstituted titanium phthalocyanine compound were prepared by the drop-casting method. While preparing thin films, solutions of the pyrimidine derivative tetrasubstituted titanium phthalocyanine compound in tetrahydrofuran (THF) were prepared. The organic solution were dropped on the glass surface and left to dry at room temperature [Yabaş et al. 2020].

2. RESULTS AND DISCUSSION

Pyrimidine derivative tetrasubstituted titanium phthalocyanine compound was synthesized as a result of tetramerization reaction of pyrimidine derivative substituted phthalonitrile with titanium(IV)

butoxide (Ti(OC$_4$H$_9$)$_4$) (Scheme 1). The synthesized product was purified by solubility differences and column chromatography. The new purified product was characterized by ^{1}H-NMR, UV-Vis, IR. In order to determine the potential for use in energy applications of the compound, photoluminescence, fluorescence properties, aggregation behaviors with UV-vis spectrophotometer, and surface properties with SEM were examined.
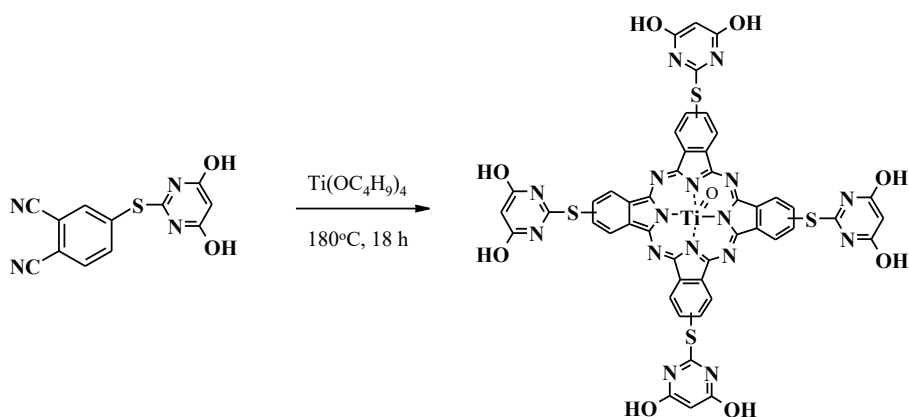
Scheme 1. Synthesis of Pyrimidine Derivative Tetrasubstituted Titanium Phthalocyanine Compound.

The formation of the phthalocyanine structure is usually observed with the formation of characteristic Q-band. The characteristic Q-band being a single band confirms that the resulting phthalocyanine is metallophthalocyanine [Nyokong 2007]. The single Q-band (667 nm) observed in the UV-Vis spectrum of pyrimidine derivative tetrasubstituted titanium phthalocyanine compound, confirms the formation of titanium phthalocyanine.

The IR spectrum of pyrimidine derivative substituted phthalonitrile compound shows a sharp peak at 2235 cm^{-1} of the C≡N group in the phthalonitrile [Yabaş 2017]. This peak was observed to disappear after pyrimidine derivative tetrasubstituted titanium phthalocyanine compound was formed. This change confirms the formation of the phthalocyanine by performing the tetramerization reaction (Figure 1).
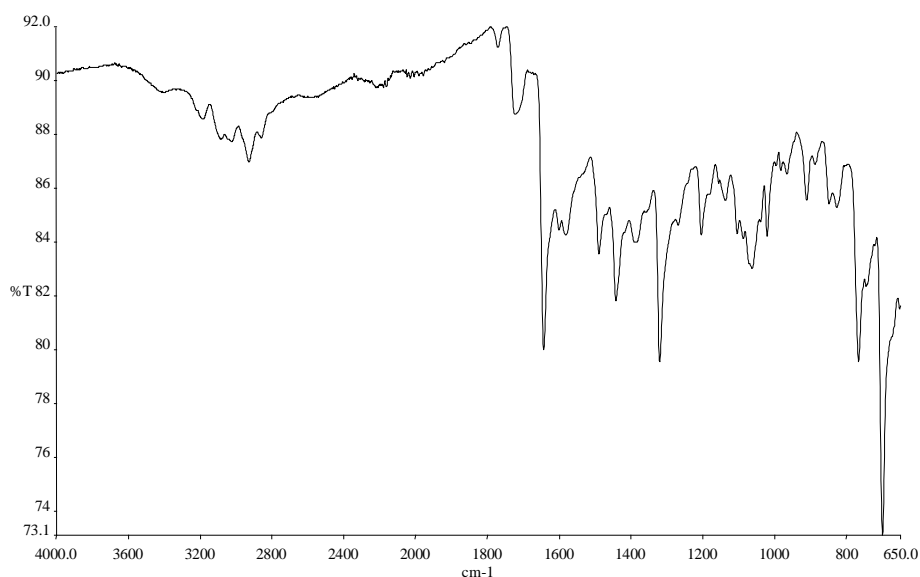
Figure 1. IR Spectrum of Pyrimidine Derivative Tetrasubstituted Titanium Phthalocyanine Compound.

In the ^{1}H-NMR spectra of pyrimidine derivative tetrasubstituted titanium phthalocyanine compound the peaks and the integral ratios of the peaks are consistent with the desired structure.

The emission spectrum of pyrimidine derivative tetrasubstituted titanium phthalocyanine compound was measured and the fluorescence quantum yield was calculated. Fluorescence quantum yield was calculated according to the following equation (Equation 1). Unsubstituted ZnPc was used as standard reference ($\Phi_F = 0.18$ in DMSO) [Durmuş, Nyokong 2008; Ogunsipe, Nyokong 2004; Jacques 1981].

$$\Phi_F = \Phi_F(\text{Std}) \frac{F A_{\text{Std}} \eta^2}{F_{\text{Std}} A \eta_{\text{Std}}^2} \qquad (1)$$

The parameters in Equation 1 are described below [Durmuş, Nyokong 2008; Ogunsipe, Nyokong 2004; Jacques 1981].

F and F_{Std} ; the areas under the fluorescence emission curves of the compound and the standard, respectively. A and A_{Std} ; the absorbance of the samples and standard at the excitation wavelength, respectively. η and η_{Std} ; the refractive indexes of solutions used for compound and standard, respectively. $\Phi_F(\text{Std})$; fluorescence quantum yield of unsubstituted ZnPc. According to the data obtained, the fluorescence quantum yield for compound was calculated as 0.36. This value is similar to that of typical metallophthalocyanines [Durmuş, Nyokong, 2007; Yabaş et al. 2020]. The fluorescence quantum yield for compound is higher than the fluorescence quantum yield of unsubstituted ZnPc.

Aggregation behaviors of pyrimidine derivative tetrasubstituted titanium phthalocyanine compound were also investigated. Aggregation behaviors of pyrimidine derivative tetrasubstituted titanium phthalocyanine compound was investigated by UV-Vis spectra measured in different solvents and different concentrations in DMSO (Figure 2). The compound not showed to significant aggregation behavior.
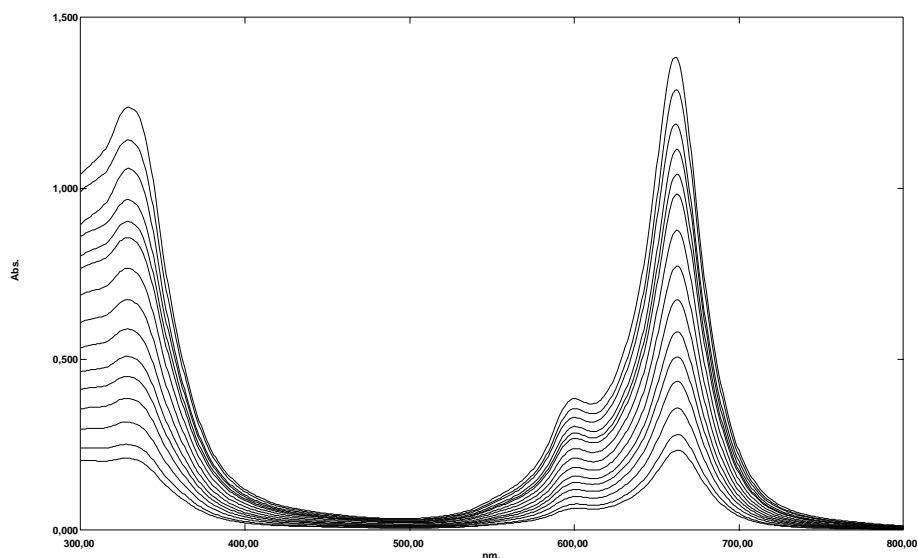
Figure 2. UV-Vis Spectrum Different Concentrations in DMSO of Pyrimidine Derivative Tetrasubstituted Titanium Phthalocyanine Compound.

PL measurements of pyrimidine derivative tetrasubstituted titanium phthalocyanine compound were evaluated in the temperature range of 50 to 300K. Photoluminescence spectra have an important role because they give information about the optical properties, likes Eg, excitons, traps and levels of energy. The relaxation process of the excited states

in the PL materials has been discussed by the exciton migration and the following capture of the exciton at the radiative and the nonradiative sites (traps) [Blasse et al. 1989; Popovic et al. 1979; Sakakibara et al. 2001].

Figure 3 and Figure 4 represents PL spectra for pyrimidine derivative tetrasubstituted titanium phthalocyanine compound film at various temperature.
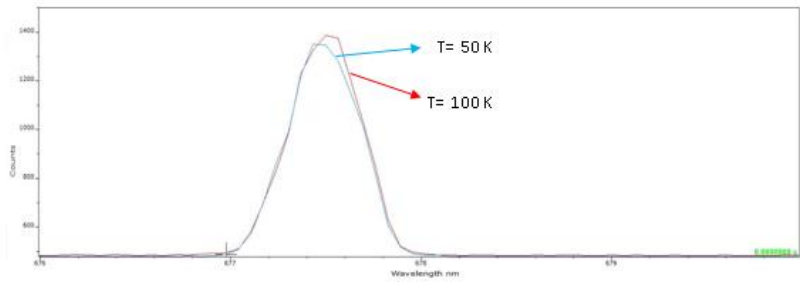
Figure 3. Photoluminescence Spectra for Pyrimidine Derivative Tetrasubstituted Titanium Phthalocyanine Compound Film at 50 K and 100 K Using Excitation Wavelength 732 nm.
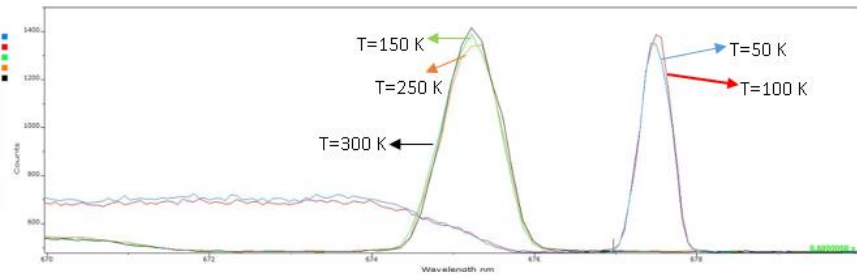
Figure 4. Photoluminescence Spectra for Pyrimidine Derivative Tetrasubstituted Titanium Phthalocyanine Compound Film at 50 K and 300K Using Excitation Wavelength 732 nm.

From the graphic interpretation of Figure 3 and Figure 4, we can say that the PL peak wavelength decreases to 677.4, 677.4, 657.5, 657.6 and 657.5 nm, respectively, as the temperature is increased to 50, 150, 250 and 300K. Also, as can be clearly seen from the graphs, the wavelength of the radiation wavelength is constant in the temperature range of 150 K-300 K, but it is observed that the wavelength increases when the temperature is reduced to 50-100 K. In other words, as the temperature decreases, energy gap decreases.

The absorption edges of the thin films of the synthesized compound are largely red-shifted from the monomer bands, suggesting that the lowest-lying exciton is allowed. At low temperatures, the emission bands moved slightly to red corresponding to the red movement of the absorption edge due to the thermochromism. From these observed features, we can say that it supports the luminescence is emitted from the lowest-lying allowed exciton state. [Blasse et al. 1989; Popovic et al. 1979; Sakakibara et al. 2001].

Pyrimidine derivative tetrasubstituted titanium phthalocyanine compound thin films were prepared by the drop-casting method. Thin film morphologies of organic compound were examined with SEM. In addition, SEM analyzes of powder forms were performed to observe the structural properties of organic compounds before forming films. The formation of coating in pure composition in SEM was tried to be examined. The figure 5 and figure 6 below show SEM photographs of the pyrimidine derivative tetrasubstituted titanium phthalocyanine at different magnifications.

As can be seen from the SEM images of the compound, although there are plate formations in the structure, it is generally porous and nucleation and growth morphology prevails (Figure 5).

A

B
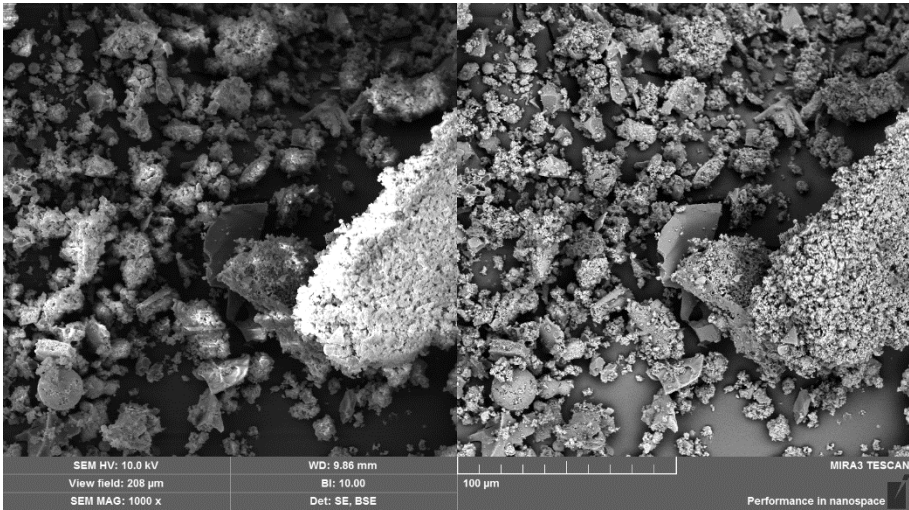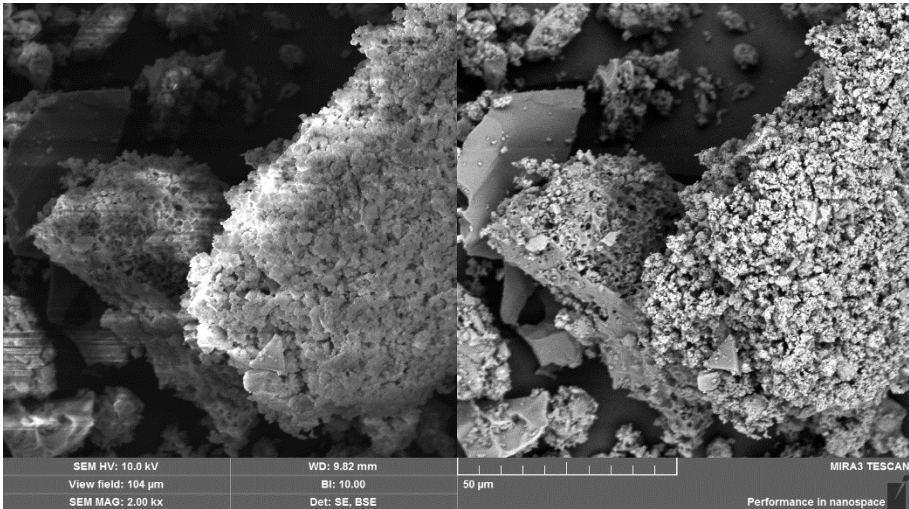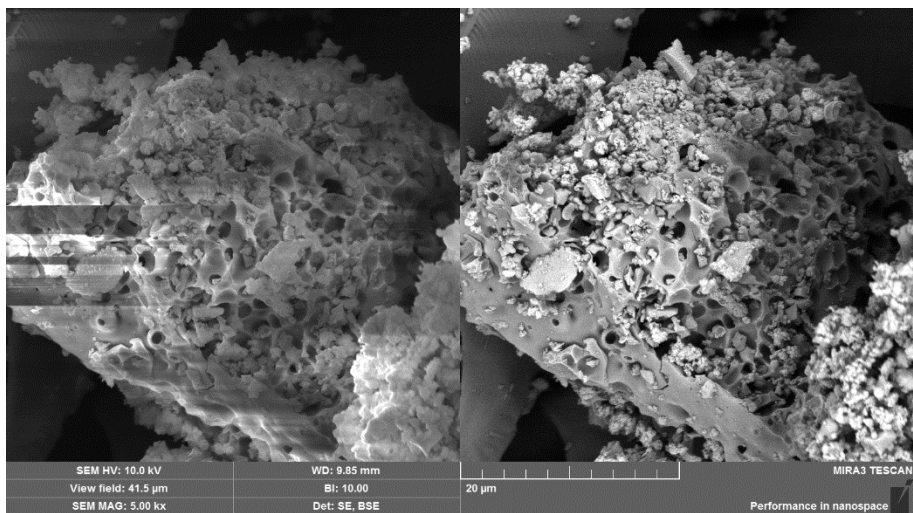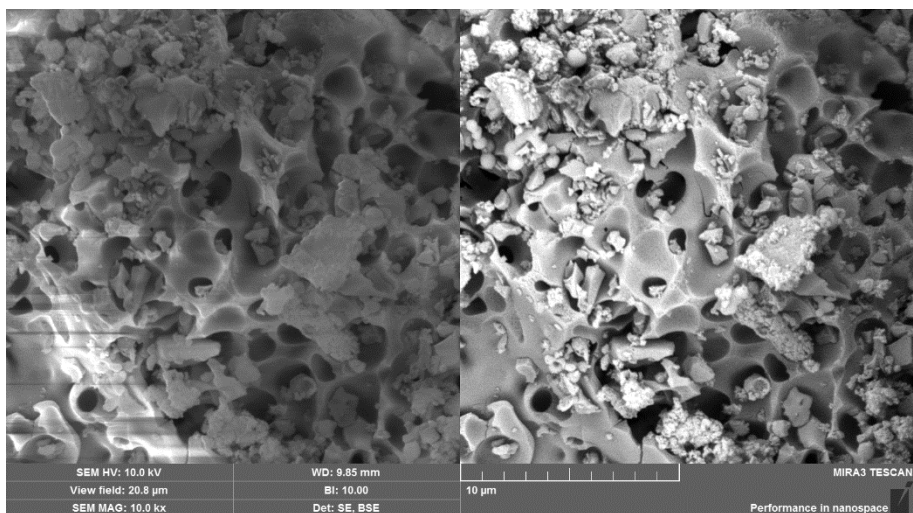
Figure 5. SEM Images of Pyrimidine Derivative Tetrasubstituted Titanium Phthalocyanine Compound in Different Magnifications in Powder Form (A-D).

SEM images of thin films of the prepared pyrimidine derivative tetrasubstituted titanium phthalocyanine compound at different magnifications are as follows (Figure 6).
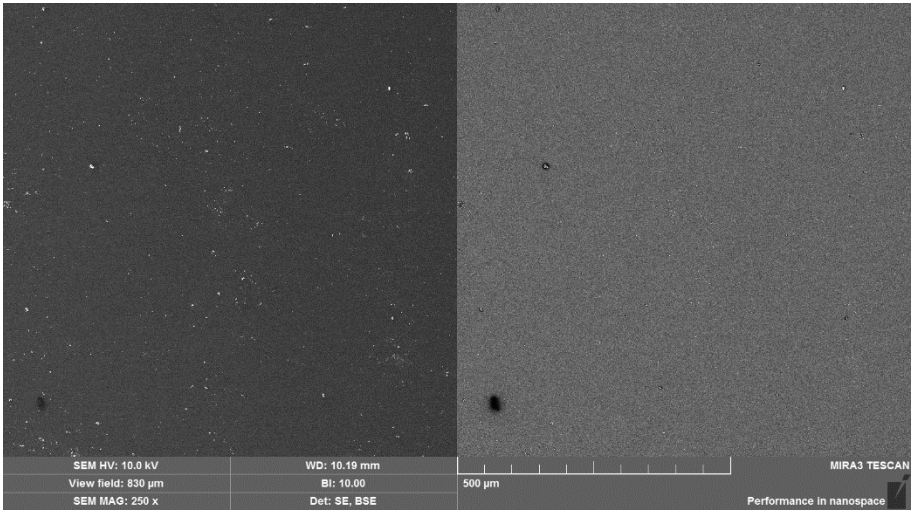
A
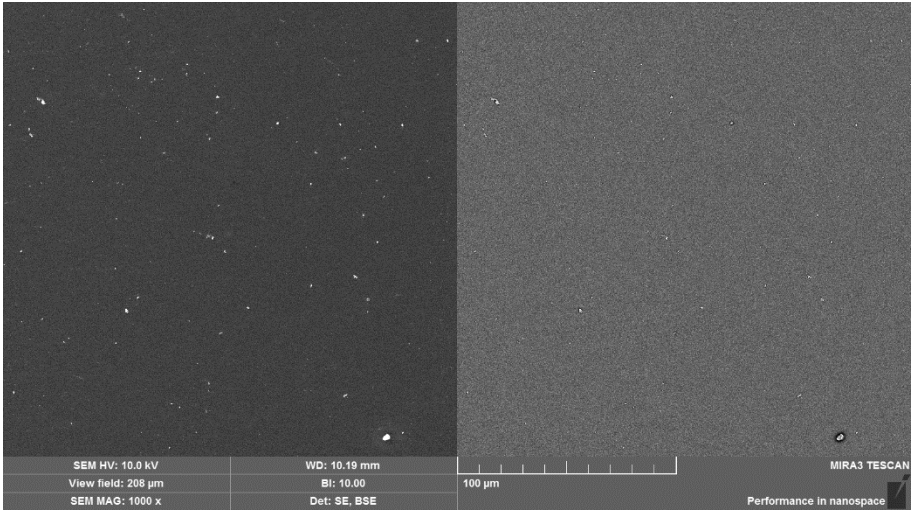
B
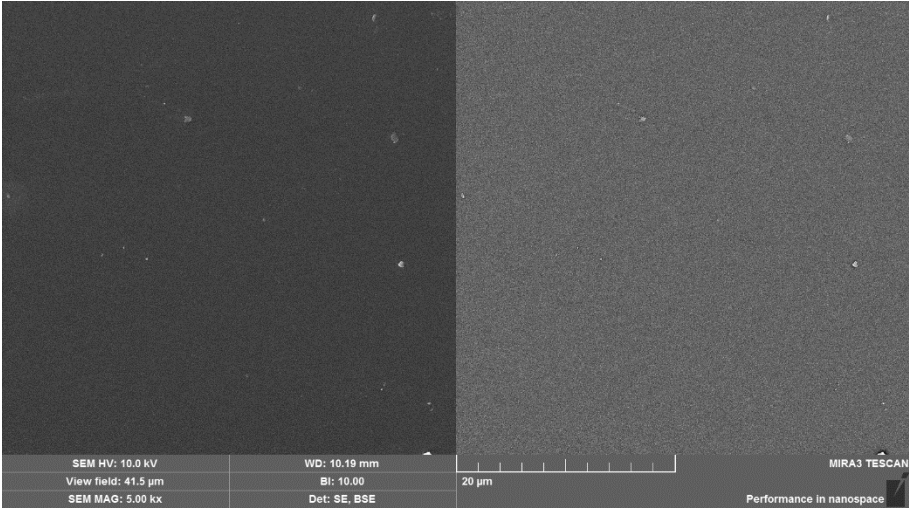
C
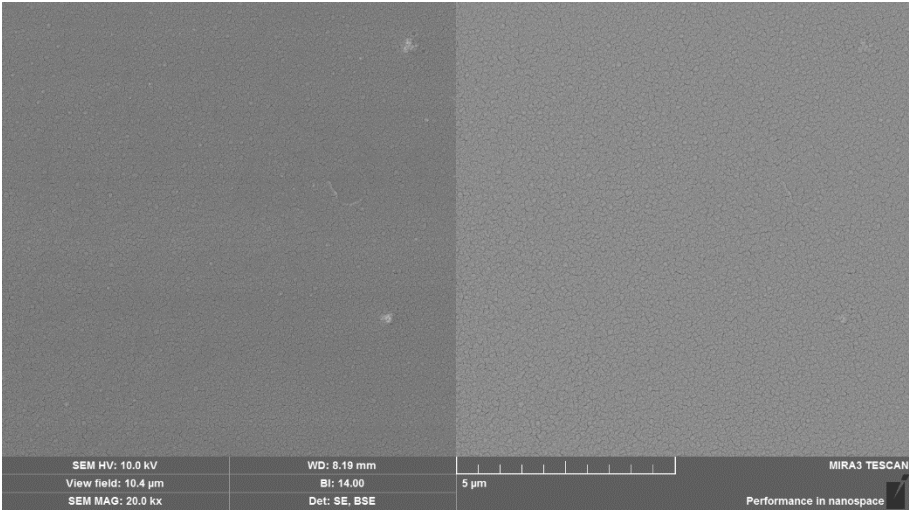
D
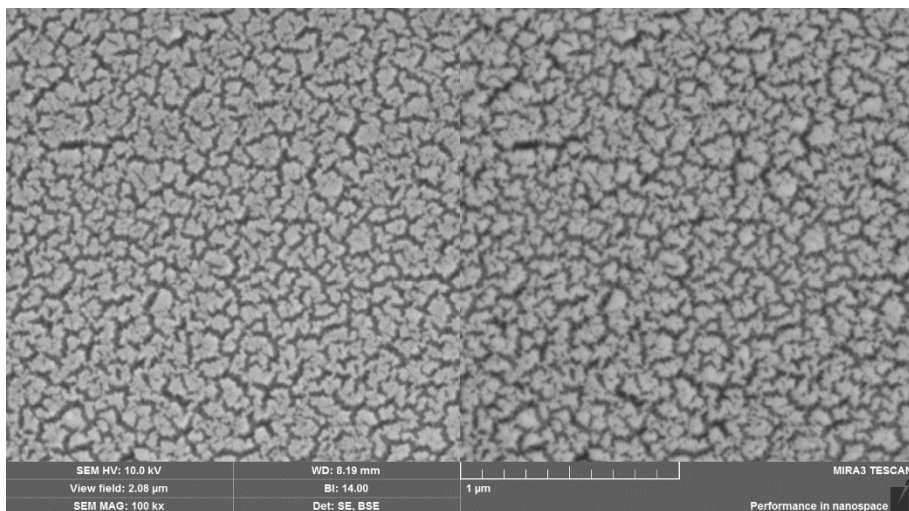
E

Figure 6. SEM images of Pyrimidine Derivative Tetrasubstituted Titanium
Phthalocyanine Compound Thin Film in Different Magnifications (A-E).

The pyrimidine derivative tetrasubstituted titanium phthalocyanine compound appears to have a very smooth surface in the prepared thin film SEM images. In the thin film of the pyrimidine derivative tetrasubstituted titanium phthalocyanine compound, even in small magnifications, smooth surface formation and increased magnification causes surface cracks caused by drying. Accordingly, it can be said that the compound has the potential to be used in thin surface and layered surface formations. On the other hand, the thin films of the compound, which are prepared with a very easy and cost-effective method, are very smooth and increase their usability in many applications.

CONCLUSION

The new pyrimidine derivative tetrasubstituted titanium phthalocyanine compound synthesized and characterized. The aggregation properties of the synthesized new compound were examined in different solvents and different concentrations. No significant aggregation was observed. This feature of the molecule provides an advantage in photovoltaic and optical applications. Fluorescence spectra in the solution phase of the material were examined and fluorescence quantum yield was calculated. The compound was observed to have a very high fluorescent quantum yield. Thin film of the compound was prepared on the glass surface by the drop casting method. The photoluminescence properties of the thin film of the material were examined at different temperatures. On the other hand, thin film surface morphology of the material was examined with SEM and it was observed that the compound has the capacity to form a smooth film. All measurement results showed that the synthesized new material has high potential for energy, photovoltaic and optical applications.

Acknowledgements

REFERENCES

Armarego, W.L.F., Chai, C.L.L. (2003). Purificaiton of Laboratory Chemicals. fifth ed., Butterworth/Heinemann, Tokyo.

Atilla, D., Kılınç, N., Yüksel, F., Gürek, A. G., Öztürk, Z. Z., Ahsen, V. (2009). Synth. Met., 159,13.

Babudri, F., Farinola, G. M., Naso, F., Ragni, R. (2007). Chem. Commun., 10.

Blasse, G., Dirksen, G. J., Meijerink, A., van der Pol, J. F., Neeleman, E., Drenth, W. (1989). Chem. Phys. Lett. 154, 420.

Chien, C. W., Liu, K. T., Lai, C. K. (2004). Heterocyclic columnar pyrimidines: synthesis, characterization and mesomorphic properties, Liquid Crystals. 31, 1007-1017.

Durmuş, M., Nyokong, T. (2007). Synthesis and solvent effects on the electronic absorption and fluorescence spectral properties of substituted zinc phthalocyanines. *Polyhedron, 26*, 2767-277.

Durmuş, M., Nyokong, T. (2008). Photophysicochemical and fluorescence quenching studies of benzyloxyphenoxy-substituted zinc phthalocyanines. Spectrochimica Acta Part *A, 69*, 1170-1177.

Jacques, P., Braun, A.M. (1981). Laser Flash Photolysis of Phthalocyanines in Solution and Microemulsion. Helvetica Chimica Acta, 64, 1800-1806.

Jıang J. (Editor) (2010). Structure and Bonding, Springer-Verlag Berlin Heidelberg, ISBN 978-3-642-04751-0, 135, 1

Kim, S. I., Kim, Y., Lee, M. S., Kim, M. S., Min S. K., Lee, C. (1993). Solid State Commun. 88, 743.

Lenzoff, C. C., Lever, A. B. P. (1989). Phthalocyanines Properties and Applications, Cilt 1, VCH publishers.

Lenzoff, C. C., Lever, A. B. P. (1993). Phthalocyanines Properties and Applications, Cilt 2, VCH publishers.

Lenzoff, C. C., Lever, A. B. P. (1993). Phthalocyanines Properties and Applications, Cilt 3, VCH publishers.

Lenzoff, C. C., Lever, A. B. P. (1996). Phthalocyanines Properties and Applications, Cilt 4, VCH publishers.

Nyokong, T. (2007). Coord. Chem. Rev., 251, 1707.

Nyokong, T. (2007). Effects of substituents on the photochemical and photophysical properties of main group metal phthalocyanines. Coordination Chemistry Review, 251, 1707.

Ogunsipe, A., Nyokong, T. (2004). Effects of substituents and solvents on the photochemical properties of zinc phthalocyanine complexes and their protonated derivatives. Journal of Molecular Structure, 689, 89-97.

Olego, D., Cardona, M. (1980). Phys. Rev. B22, 886.

Petrov, V. P. (2006). Pyrimidine as a Structural Fragment in Calamitic Liquid CrystalsMol. Cryst. Liq. Cryst. 457, 121-149.

Popovic, Z. D., Menzel, E. R. J. (1979). Chem. Phys. 71, 509.

Sakakibara, Y., Bera, R. N., Mizutani, T., Ishida, K., Tokumoto, M., Tani, T. (2001). J. Phys. Chem. B 105, 1547-1553

Torre, G., Bottari, G., Hahn, U., Torres, T. (2010). Struct. Bond, 135, 1.

Yabaş, E., (2017). Synthesis and Investigation of Properties of the New Zinc(II) Phthalocyanine Compound, *6th National Inorganic Chemistry Congress with International Participation, P-30,* Sayfa 98, Burdur-Turkey.

Yabaş, E., Başer, P., Kul, M. (2020). Photoluminescence Properties of Tetra- and Octa-Substituted Double Decker Lu(III) Phthalocyanines, Journal of Materials and Electronic Devices 2, 13-16.

Zhang, Y., Cai, X., Bian, Y., Jiang, J. (2010). Struct. Bond., 135, 275.

CHAPTER 7

EFFECT OF SOME MORDAN/BORİC ACİD IMPREGNATİON (DİFFUSİON/VACUUM) ON RETENTİON / DENSİTY ON WOOD

Prof. Dr. Hüseyin PEKER[1], Dr. Lecturer Hatice ULUSOY[2]

[1] Artvin Çoruh Unıversity, Forest Faculty, Forest Industrıal Engineering Department Artvin, Turkey. peker100@artvin.edu.tr

[2] Muğla Sıtkı Koçman Unıversity, Köyceğiz Vocational School, Forest Department, Muğla, Turkey. haticeulusoy@mu.edu.tr

INTRODUCTION

Forests are shown as a natural and renewable resource for producing goods and meeting community demands. Forest products are divided under the title of primary and secondary forest products. Wood raw material, which is a forest product, meets the need for firewood in trees that are over the administrative age. Wood raw material is the raw material used in industry and has a great use in the world. Industrial wood production by the General Directorate of Forestry in the last 20 years has been around 50-55%. 65% of the wood raw material need is met by the General Directorate of Forestry. In this way, 90% of the revenue source of the General Directorate of Forestry is supplied. Wood raw material production in the world is 3.5 billion m³ (Ünver ve ark., 2005).

Uysal and Özçifçi (2000) investigated the burning properties of 3-layer laminated wood material LVL (Laminated Veneer Lumber) produced from lime wood (Tilia argentea.). Small leaf linden (Tilia argentea) in the outer layers of wood material; white mulberry tree (Morus alba L.) and Uludag fir (Agabeyes bornmulleriana Mattf.) were used in the middle of wood material. The combustion values of LAM samples produced by adhering with PVAc glue according to ASTM E-69 standards were determined. Most; mass loss CO_2 (6.76%) and CO (3754.12ppm) amount in the middle layer oak wood, O_2 (19.53) in the middle layer akdut wood, temperature value in the middle layer Scotch pine and fir samples, the amount of unburned parts and ash 3 layer lime They revealed that they had wood (20%) . Örs and Keskin (2001)

reported that impregnation materials are generally preferred with organic solvent (tributyltin naphthenate, copper naphthenate, pentochlorphenol), oily (creosote) and water-soluble salts (copper, chromium, boron, etc.). Acarkan (2002); boron is a substance used in a wide range from boron cleaning agents to space technology. As well as a large portion thereof is of great importance in terms of boron reserves located in Turkey. It is stated that the use of boron is increasing in industrial areas requiring high technology and that its value is further increased by using it as raw material.

Baysal et al. (2003) in their work titled 'Mechanical Properties of Beech Wood Treated with Different Impregnations'; reported that they achieved the highest bending resistance in the mechanical properties of beech wood with an isocyanate treatment applied on a mixture of borax and boric acid in their impregnation process using boron compounds and water repellents as commercial impregnants.

Çolakoğlu et al. (2003) treated laminated boards made of beech wood, firstly impregnating with boric acid, they reported that the impregnation process caused a modulus of elasticity in bending and a small decrease in bending strength, by investigating the different mechanical properties of the impregnated sheets and but not statistically significant.

The level of use in various areas has been tried to investigate by determining the amount of adhesion in wood by bringing various mordants to the water-based varnish.

MATERIAL AND METHOD

Wood Material and Chemicals

Scotch pine (*Pinus sylvestris L.*) wood, which is grown in our country and preferred in the wood/construction industry, was prefered as part of the study. Processes were carried out in accordance with the principles of TS 2470; wood was used by cutting in the radial direction (TS 2470 ,1976; Ayata, 2014). Boric acid, sodium chloride (NaCl) and aluminum sulphate (Al_2SO_4) 3 are used in impregnation and mordan; 1% concentration was used in application.

METHOD

Sample Preparation for Experiment

While preparing the samples smoothness of the fiber structure of wood, crack of wood, knot of wood, tulle formation and wood without any color distortion were made ready for (TS 2470). Samples were prepared as 10x5x3cm dimensions for the determination of the % retention feature. Specific gravity samples were prepared at 20x20x30 mm dimensions (TS 2470, 1976; Bozkurt ve ark.,1993).

Impregnation Process

The impregnation process was applied in accordance with the conditions in "ASTM-D 1413-76". Experimental samples were applied for 20 minute-vacuum and 20,40,60 minute-diffusion times. In order to prevent the impregnation agent from being affected by wood moisture, test samples have been made completely dry (ASTM 1413, 1976).

% Retention (Net Dry Matter Amount)

After impregnation, the amount of substance remainined (tkoao-% retention) compared to dry wood was calculated from the specified formula.

$$R (\%) = \frac{\text{Moes-Moeö}}{\text{Moeö}} \times 100 \qquad (1)$$

Moes = Sample full dry weight after impregnation (g)
Moeö = Sample full dry weight before impregnation (g)

Air / Full Dry Specific Gravity

Moisture amounts of the test samples were carried out according to TS 2471 and specific weights were carried out according to TS 2472. At the temperature of 20 ± 2 °C and relative humidity as 65 ± 5 %, all the weighing and measurements were performed. Calculations were made with below formula.

$D12 = M12 / V12$
(D12): Air Dry specific gravity (g/cm³) $\qquad (2)$
(M12): Air dry weight of test sample (g)
(V12): Air dry volume (cm³)

Test samples at 12 % relative humidity as normal were used to determine the full dry density. Here, TS 2472 was applied and 0 % value was obtained at 103 ± 2 °C. In order to avoid moisture intake, it was cooled in $CaCl_2$ desiccator and necessary weighing/measurements were made. According to the specified formula (TS 2471, 1976; TS 2472, 1976).

$D0 = Wo / Vo \ g/cm^3$
In Formula;
Do: Full dry density (g/cm³)   (3)
Wo: Full dry weight (g)
Vo: Full dry volume (cm³)

RESULTS AND DISCUSSION

Properties of Solution

Boric acid, sodium chloride ($NaCl_2$) and aluminum sulphate (Al_2SO_4) were used as mordant in the impregnation process. The solutions were prepared at a 1% concentration. Solution properties are given in Table 1.

Table 1. Solution Properties

Impregnation Materıal	Temper. /Solvent (ºC)	pH		Density (g/ml)	
		BI	AI	BI	AI
Boric Acid	22 ºC / DS	4.72	4,73	1,020	1.020
Aluminum Sulphate	22ºC /DS	3.71	3,71	1,065	1.065
Sodium Chloride	22 ºC/ DS	7.20	7,22	1.070	1.070

*__BI__: Before Impregnate *__AI__: After Impregnate __DS__: Distilled water

No remarkable changes in solution pH and densities occurred. This should be taken into account, as the change in acidic and basic values will cause hydrolysis in wood. It has been reported in the literature that acidic structure will affect the physical and mechanical properties of wood.

% Retention

The retention amount is determined in 20 minute-vacuum and various diffusions (20,40,60 minutes) and given in Table 2.

Table 2. % Retention (Vacuum for 25 Min) and Duncan Test Results

İmpregnation Material	Diffusion Time (Min)	Retention (%)	Stnd. Dev.	HG
Boric Acid	20	1.66	1.72	G
	40	2.82	1.86	F
	60	1.98	1.07	H
Aluminum Sulphate	20	3.53	2.29	D
	40	4.24	2.48	C
	60	6.12	2.34	D
Sodium Chloride	20	2.97	2.39	D
	40	4.53	3.77	B
	60	5.48	6.94	**A**

HG: Homogeneity group

The highest value in sodium chloride (6.94%) and lowest in boric acid (1.72%) was determined in 60 minute-diffusion and 20 minute-vacuum time. The highest value in aluminum sulphate (9.90%) and the lowest in sodium chloride (2.43%) was determined in 40 minute-vacuum and 20 minute-diffusion time. We can conclude that these values differ from each other due to the anatomical structure of wood, impregnation time and chemical structure of spruce wood.

No significant difference was observed in the densities and pH values of the solutions measured before and after impregnation. This may be due to working with the new solution in each impregnation variation. It is reported that the concentrations of boric acid, aluminum sulfate and

sodium chloride, which are among the used impregnation materials, are close to the acidic structure, negatively affect the polysaccharides in the wood and increase the probability of hydrolysis (Özçifçi , 2001).

In the researched of Alkan (2016), impregnation was applied to yellow pine (*Pinus sylvestris L.*) wood with a solution obtained from mixtures of boron compounds and natural impregnation materials. it determined that the retention amount in the pine, which is one of the natural impregnating materials, was lower than that of kebraco, and the total retention amount increased as the solution concentration increased.. The highest retention values were observed in impregnated samples with solutions of 1% concentration. It is indicated that retention rate varies due to reasons such as the properties of the solutions and the anatomical structure .

Air Dry / Full Dry Density Amount

Air dry specific gravity values for specific gravity changes 20 minute-vacuum time are given in Table 1 and Figure 1.

Table 3. Air / Full Dry Specific Gravity Change (20 Min Vacuum)

İmpregnation Material	Diffusion Time (min)	Full Dry after impregnation (g/cm³)	Air dry after impregnation (g/cm³)
Control	-	0.43	0.46
Boric Acid	20	0.44	0.46
	40	0.49	0.51
	60	0.46	0.49
Aluminum Sulphate	20	0.46	0.47
	40	0.43	0.44
	60	0.43	0.45
Sodium Chloride	20	0.45	0.47
	40	0.45	0.49
	60	0.42	0.43
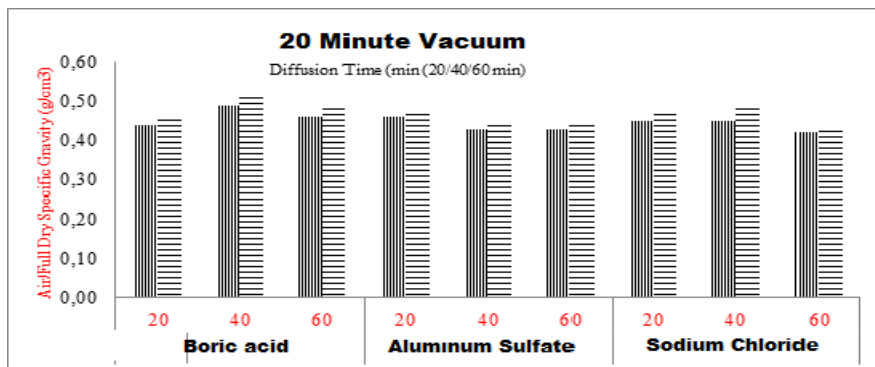
Figure 1. Air/Full Dry Specific Gravity Values

For Air Dry, it was detected that the highest value was (0.51 g / cm^3) at boric acid in 20 minute-vacuum and 40 minute-diffusion and 20 minute-vacuum, the lowest value was (0.43 g/cm^3) at sodium chloride at 60 minute-diffusion; the highest full dry specific gravity was (0.49 g/cm^3) at boric acid in 20 minute-vacuum and 40 minute-diffusion at, the lowest value was (0.43 g/cm^3) at sodium chloride in 20 minute-vacuum and 60 minute-diffusion.

Kaçamer (2010) impregnated uludağ fir and eastern beech wood with Imersol Aqua, Tanalith-E. the density and retention rate of the impregnated air samples in air dry were determined. According to the results of the experiment, it is reported that the highest air dry density value in beech wood as (0.67 g/cm3), which it impregnated with Imersol Aqua, and the highest retention rate as (1.53%) in fir wood, which it impregnated with Imersol Aqua .

Kara (2015) subjected the experimental samples obtained from Larix trees to impregnation with boric acid, borax and prit. the impregnation retention rates, full dry densities and air dry densities of the samples were determined. According to the results of the experiment, the highest impregnation retention rate (124.6 Kg/m³) in the larex wood material, where it has impregnated with borax and the highest full dry density value with prit + Ba (0.61 g/cm^3) and air dry density value with prit + Ba (0.64 g/cm^3) in the larex tree .

In this study, Atılgan et al. (2013) determined the total retention and % retention of the wood material that was impregnated with the tea plant. As a result of their treatment, it is reported that the lowest retention rate in iroco wood (1.58%), and the highest retention rate in beech wood (6.75%). It is resulted that the lowest total retention iroko (31.27 kg/m^3) had the highest total retention value in beech wood (100.65 kg/m^3). According to the retention results; it is stated that the organics obtained from tea plant extract can be used as impregnation agent in wood material.

İn the study of Çiçek (2015), spruce (*Picea orientalis L.*) wood was impregnated according to ASTM 1413-76 standard with three different concentrations of solution (1, 3, 5) prepared from boron compounds and barite; and examined the effects of some physical-mechanical properties. As a result of research, the air dry specific gravity value was reported as the most Barite+Ba (0.80 g/cm^3) .

RESULTS

As environmental pollution increases in our country and in the world, the measures taken in return have been increased. Efforts are being performed to ensure that the chemicals used in wood do not cause environmental pollution. However, the applied methods have emerged with high costs. Therefore, many features of wood are improved with a single application in wood modification. Another method used to ensure the longevity of the wood material is the impregnation process. Although durable, long-lived tree species have been preferred, the tree species with low natural strength must be impregnated to increase the lifetime. Many chemicals are applied in the impregnation process of wood material. One of these chemicals is boron compounds. Today, boron compounds used as impregnations are one of the reliable chemicals. Its use is increasing day by day as the harm to human and environment is at a minimum level.

In the results of working; It seems possible that the use of aluminum sulfate, sodium chloride, boric acid substances as impregnating agents from our country's resources. The use of water-based varnish with the used impregnating materials or the impregnation without varnish shows its ability to be used especially in the furniture industry (park, garden, urban furniture, construction industry, etc.) Positive results in physical-mechanical properties indicate that this is as feasible and additional studies are necessary. It is possible to investigate the availability of other water-based impregnations that do not harm human health, and to obtain healthier positive structures. It is necessary to use these

materials, which appear to be possible for use in parks, gardens, pergolas, benches or flower beds in all outdoor areas, with top surface treatments and to conduct experiments (gloss, surface adhesion, color, surface hardness, etc.). Additionally, the duration of material strength should be determined with its effect on human health.

REFERENCES

Acarkan, N.(2002). Bor ürün Çeşitleri ve Kullanım Alanları", I. Uluslar arası Bor Sempozyumu, Kütahya, 1-5.

Alkan,E., Selim Şen,S., Fidan,S., Yaşar,Ş. (2018). Tara ve Farklı Borlu Bileşikler ile Emprenye Edilen Sarıçam (Pinus sylvestris L.) Odununun Vida Tutma Direncinin Belirlenmesi , Sayı 2,525-531.

ASTM 1413 -76 (1976) Standartd Methods of Testing Wood Preservatives by Laboratory Soilblock Cultures", Annual Book of American Standarts, USA.

Atilgan, A., Ersen, N., ve Peker, H., (2013). Different Types Of Wood Treated With Tea Plant Extract Retention Values. Kastamonu University Journal Of Forestry Faculty, 13(2), 278-286.

Ayata, U. (2014).Isıl İşlem Görmüş (Thermowood) Bazı Ağaç Türlerinde Kullanılan Su-Bazlı Vernik Katmanlarının Hızlandırılmış Uv Yaşlandırma Etkisine Karşı Direncinin Belirlenmesi'', Yüksek Lisans Tezi, Düzce Üniversitesi Fen Bilimleri Enstitüsü, Düzce.

Baysal, E. (2003) .Borlu Bileşikler Ve Doğal Sepi Maddeleriyle Emprenye Edilen Sarıçam Odununun Yanma Özellikleri, Erciyes Üniversitesi Fen Bilimleri Enstitüsü Dergisi, Kayseri, 19 (1-2): 59-69.

Bozkurt A.Y., Göker Y., Erdin N. (1993) ."Emprenye Tekniği", İstanbul Üniversitesi, Orman Fakültesi Yayınları, İstanbul.

Çiçek,S. (2015) .Barit ve Bor Bileşiklerinin Ladin Odununda Tutunabilme Özelliği Ve Dış Mekan Mobilyalarında Kullanılabilme Olanakları, Artvin Çoruh Üniversitesi, Fen Bilimleri Enstitüsü, Yüksek Lisans Tezi, Artvin.

Çolakoğlu, G., Çolak, S., Aydın, İ., Yıldız, Ü.C., Yıldız, S. (2013) Effect of Boric Acid Treatment on Mechanical Properties of Laminated Beech Veneer Lumber, Silva Fennica, 37 (4): 505-510.

Kaçamer, S. (2010) .İmersol Aqua ve Tanalith-E İle Emprenye Edilmiş Isıl İşlemli Ağaç Malzemelerin Yapışma ve Yanma Dirençlerinin Belirlenmesi", Yüksek Lisans Tezi, Karabük Üniversitesi Fen Bilimleri Enstitüsü, Karabük.

Kara, F. (2015) .Prit (FeS$_2$) Maddesinin Odunda Emprenye Edilebilme Özelliği Ve Bazı Teknolojik Özelliklerine Etkileri'' Yüksek Lisans Tezi,   Artvin Çoruh Üniversitesi, Artvin Çoruh Üniversitesi Fen Bilimleri Enstitüsü, Artvin.

Örs, Y., Atar, M., Keskin, H.(2004) .Bonding Strength Of Some Adhesives İn Wood Materials İmpregnated With Imersol-Aqua, International Journal of Adhesion & Adhesives, 24 (1): 287–294.

TS 2470 (1976). Odunda Fiziksel ve Mekaniksel Deneyler İçin Numune Alma Metotları ve Genel Özellikleri, Ankara.

TS 2471 (1976) Odunda, Fiziksel ve Mekaniksel Deneyler İçin Rutubet Miktarı Tayini, Ankara.

TS 2472 (1976). Odunda, Fiziksel Ve Mekaniksel Deneyler Için Birim Hacim Ağırlığı Tayini, Ankara.

Özçifçi, A. (2001). "Emprenye edilmiş lamine ağaç malzemelerin teknolojik özellikleri", Doktora Tezi, Gazi üniversitesi Fen Bilimleri Enstitüsü, Ankara, 89-96,2001.

Uysal, B., Özçifci, A. (2000) .Ihlamur (*Morus Alba L.*) Odunundan PVAc Tutkalı İle Üretilen Lamine Ağaç Malzemenin Yanma Özellikleri, Gazi Üniversitesi Fen Bilimleri Enstitüsü Dergisi, Ankara, 13 (4): 1023-1035.

Ünver, S., Acar,H (2005). Odun Hammaddesi Üretim Çalışmalarının Odun Kalite Sınıfları Üzerine Olan Etkileri'' , Kafkas Üniversitesi, Artvin Orman Fakültesi Dergisi, 6 (1-2).

Note: HORA 2019, Environmental Friendly Boron Compounds in Wood / Mordan Usage and Holding Level, International Congress on Human- Computer Interaction, Optimization and Robotic Applications July 5-7, 4 (5): 20- 23, 2019, Urgüp, Nevşehir, Turkey. (Some of the results are presented at the symposium) The study has been expanded.

CHAPTER 8

IMPREGNATİON (STONE WATER) ON WOOD AND VARİOUS PHYSİCAL PROPERTİES AT SOME VACUUM/DİFFUSİON TİMES

Prof. Dr. Hüseyin PEKER[1], Dr. Lecturer Hatice ULUSOY[2]

---

[1] Artvin Çoruh Unıversity, Forest Faculty, Forest Industrıal Engineering Department Artvin, Turkey. peker100@artvin.edu.tr
[2] Muğla Sıtkı Koçman Unıversity, Köyceğiz Vocational School, Forest Department, Muğla, Turkey. haticeulusoy@mu.edu.tr

INTRODUCTION

Turkey in recent days while battling with fires, Bioversal called "miracle" in fire fighting, is coming to Turkey. Bioversal which was developed in 1992 by the German company and launched fro use in 2002, have been used in 35 countries from the USA to Japan. Bioversal is also taken by the Ministry of Environment in some countries. Bioversal, which has environmental cleaning feature, extinguishes fires instantly and fulfills its cooling task. Especially after the recent increase in fire events and the disappearance of thousands of hectares of forests, alternative firefighting models have been started to be discussed. Bioversal which is mainly used by firefighters to extinguish major fires in 35 countries, have been.brought to Turkey. Bioversal Turkey Distributor (Burak Sirma) stated that Bioversal was purchased by the Ministry of Environment in Italy and Spain, which is also used in 35 countries in the USA, Belgium, Netherlands, Luxembourg, Spain, Brazil, France, England, Germany, Italy and Japan. Additonally, it is mentioned about Bioversal, which was developed in 1992, was used in 2002, when Bioversal was an important invention, and its experiments were carried out for nearly 10 years, and it achieved great success in all fires. It was pointed out that Bioversal is a biological fire extinguisher made from plants, while extinguishing the fire "Bioversal, which prevents the fire from reburning, also disappears by turning into carbon dioxide and water with all harmful substances in its location within 14 days, it has the ability to not create back combustion with its high cooling ability when it is applied correctly once. It has been reported that it does not only extinguish the fire in the fires caused by tanker

accidents over seas, it cuts its contact with the burning area where it prevents leakage when it is applied over the leakage that spreads to the sea, and it prevents degradation of the living life by degrading the fuel (URL 1, 2019). The use of broad-spectrum biocides has been limited, the structural condition of heavy metals has threatened the environment in recent years and the importance level of boron/boron-derived materials have increased. Boron impregnation has a high (toxic) effect against biotic/abiotic effects in both wood and its various derivatives. For this reason, the boron structure has a high level of protection especially in various fields, and its chemical structure is defined as strong in the literature (Kartal ve ark., 2004).

Örs et al. (2005) in their study, it was concluded that wood products, which are the raw materials of the forest products and furniture and decoration sector, can be sufficient to meet the increasing need for wood raw materials with appropriate use and protection methods.

In the study on hygroscopicity levels of wood material, whose impregnation is made with boron compounds, the 1%, 2%, 3%, 4%, 5%, 6% aqueous solutions of boric acid (Ba), borax (Bx) and boric acid/borax mixture of boron compounds were used. According to the results obtained in the study, the lowest hygroscopicity value was obtained in the samples of yellow pine wood which was impregnated with 1% aqueous solution of boric acid borax mixture. It was determined that 6% aqueous solution of the boric acid/borax mixture was the substance that increases the hygroscopicity most (Baysal,2003).

The study in which the effect of vacuum/diffusion times on the adhesion (% retention) properties of eastern spruce (*Picea orientalis (L.) Link*.) wood in the impregnation process, in accordance with the results obtained from "Stone water" (Firetex) used as impregnating agent, the rate of usability in the indoor / outdoor furniture industry has been determined.

MATERIAL AND METHOD

Wood Material

Spruce wood (*Picea orientalis (L.) Link*.) which is grown mainly in Turkey and its eastern spruce wood was obtained from Artvin was used. The samples of alive wood cut radially were made on the basis of TS 2470 (1976).

Stone water

Firetex liquid, which was manufactured by the water of the stone in Balıkesir-Edremit by Kale Group and adds non-flammability to the place where it is applied, is approved by the Fire Brigade of Greece. 1 liter of stone water sample was analyzed by ICP-AES in 2004 by Balıkesir University and the following results were found (URL 2, 2019).

Cellulosic Varnish

It consists of layers, solvent and thinners. The solvents in them are volatile and dry quickly at room temperature without the need for reaction during film formation. Therefore, they form recycled and

structurally stable layers. When the layers are applied one after another, the layers merge and integrate. The flexible building and film cellulosic varnish film is heat resistant, does not soften easily and has high melting degree. The film's brightness increases with friction and its stiffness increases over time. Only 25-35% of the layers are stratified in application (URL 3,2019).

METHOD

Sample Preparation for Experiment

While preparing the samples, smoothness of the fiber structure of wood, crack of wood, knot of wood, tulle formation and wood without any color distortion were made ready for (TS 2470). Samples were prepared as 10x5x3cm dimensions for the determination of the% retention feature (TS 2470, 1976; Bozkurt ve ark., 1993).

Impregnation Process

The impregnation process was applied in accordance with the conditions in "ASTM-D 1413-76". Experimental samples were prepared in 13x5x3 cm dimensions and the test samples were made completely dry so that the impregnation agent was not affected by wood moisture (ASTM 1413, 1976).

Varnishing and Sanding Process

Varnishing was carried out according to the application principles of the manufacturer company. In order to obtain a smooth and perfect surface, sanding should be done at least twice on the wood material

surface. The first sanding process on the wood material surface is done to eliminate the defects caused by machine operations and preliminary preparations. Another sanding process is; It is applied after the first or interfacial processes for coloring and filling purposes. Protuberances resulted from colorants in surface treatment materials at this stage, eliminate defects such as dust etc. on varnished surfaces with layer thickness differences until dry. For this purpose, for both adhesion and cohesion connection (ASTM-D 1666-87), all samples were first treated with sandpaper numbered 120; after the first layer of varnish was removed, the last process was performed with sandpaper numbered 180 (Söğütlü, 2005). Sanding process was applied on the samples that were subjected to 20 minute diffusion with sandpaper numbered 130, samples for 30 minute-diffusion with sandpaper numbered 150, and samples for 40 minute-diffusion with sandpaper numbered 180 (ASTM D 1666 ,1999).

% Retention (Net Dry Matter Amount)

After impregnation, the amount of substance remainined (tkoao-% retention) compared to dry wood was calculated from the specified formula.

$$R (\%) = \frac{Moes-Moeö}{Moeö} \times 100 \qquad (1)$$

Moes = Sample full dry weight after impregnation (g)
Moeö = Sample full dry weight before impregnation (g)

Air / Full Dry Specific Gravity

Moisture amounts of the test samples were carried out according to TS 2471 and specific weights were carried out according to TS 2472. At the temperature of 20 ± 2 °C and relative humidity as 65 ± 5 %, all the weighing and measurements were performed. Calculations were made with below formula.

D12 = M12 / V12
(D12): Air Dry specific gravity (g/cm³)   (2)
(M12): Air dry weight of test sample (g)
(V12): Air dry volume (cm³)

Test samples at 12 % relative humidity as normal were used to determine the full dry density. Here, TS 2472 was applied and 0 % value was obtained at 103 ± 2 °C. In order to avoid moisture intake, it was cooled in $CaCl_2$ desiccator and necessary weighing/measurements were made. According to the specified formula (TS 2471, 1976; TS 2472, 1976).

D0 = Wo / Vo g/cm^3
In Formula;
Do: Full dry density (g/cm³)   (3)
Wo: Full dry weight (g)
Vo: Full dry volume (cm³)

RESULTS AND DISCUSSION

Properties of Solution

The feature of stone water used in the impregnation process is shown in Table 1.

Table 1. Solution Properties

*BI: Before Impregnate *AI: After Impregnate

Impregnation Materıal	Temperature (ºC)	pH		Density (g/ml)	
		BI	AI	BI	AI
Stone water	22	1.65	1.65	1.215	1.215

The solution was used as 100% ready and pH/density was determined. Acidic structure appears, It is supposed that it may cause negativities in the anatomical technological structure of wood.

% Retention

Retention amounts were determined in time (25 minutes for vacuum) and various diffusions and given in Table 2 .

Table 2. % Retention (Vacuum for 25 Min) and Duncan Test Results

Impregnation material	Varnish	Sanding No	Diffusion Time (Min)	Retention (%)	HG
Stone water	Unvarnished	No Sanding	20	16.72	K
			30	26.35	F
			40	28.24	D
	Cellulosic Varnish	130	20	20.15	I
			30	27.85	E
			40	32.81	A
		150	20	18.59	J
			30	24.12	G
			40	30.29	C
		180	20	16.66	K
			30	22.81	H
			40	31.70	B

HG: Homogeneity group

The highest value (32.81%) was determined in 25 minute-vacuum and 40 minute-diffusion time and the lowest (6.66%) was determined in 25 minute-vacuum and 20 minute-diffusion. We can state that these values differ from each other due to the anatomy structure, impregnation time and chemical structure of spruce wood.

According to all the mechanical results that have been sanded, it is stated that the treatments with ACQ in general are not statistically significant in the effect of the mechanical properties of the wood. Various impregnations are applied today to increase the usage time in wood materials. However, since the chemicals have different characteristics, they were not found suitable for various uses. In this application, the effect of some mechanical and physical properties of wood material in the treatment with ACQ was investigated and it was found to have a positive effect. In addition, treatment with ACQ is important in terms of maintaining sufficient adhesion and compatibility with nature with its rapid penetration, in order to preserve environmental-forest values. it has been determined that sufficient adherence has been achieved for various applications in the 72-hour dipping treatment (Bal 2006). It is observed that the solution used during the treatment process, did not change enough to affect the result of measured intensities and pH values in pre-treatment and post-treatment. For this reason, It can be shown that new solutions have been prepared for the impregnations (Özçifçi ve ark., 2009).

From the results of the variance analysis that has been done; The effect of impregnation method and tree type on the mechanical properties of the sample was statistically significant as '$\alpha = 0.05$'. In the Duncan test application results, in retention, the highest value of the samples treated with pressure-vacuum method in scotch pine as 37, 3 kg/m^3 and the lowest value of samples treated with dip method in beech as 3.71 kg/m^3 were obtained. The highest retention value was obtained as "6.42%" in samples treated with pressure-vacuum method in scotch pine, and the lowest retention value as "0.30 %" in samples treated with dip method in beech.

Air Dry / Full Dry Density Amount

Changes on air dry and full dry specific gravity are given in Table 3.

Table 3. Air / Full Dry Specific Gravity Change (25 Min Vacuum)

Varnish	Sanding	Diffusion Time (min)	Full Dry after impregnation (g/cm³)	Air dry after impregnation (g/cm³)
Control	-	-	0.35	0.37
Unvarnished	No sanding	20	**0.39**	**0.43**
		30	0.46	0.51
		40	**0.50**	**0.53**
Cellulosic Varnish	130	20	0.43	0.44
		30	0.49	0.51
		40	0.49	0.52
	150	20	0.42	0.45
		30	0.45	0.47
		40	0.49	0.51
Cellulosic Varnish	180	20	0.43	0.45
		30	0.47	0.51
		40	0.48	0.52

In control samples, the average value of air dryness before impregnation was determined as (0.37 g/cm^3). The highest value of dry full after impregnation was determined as (0.50 g/cm^3) in 25 minute-vacuum and 40 minute-diffusion time, while the lowest value was (0.39 g/cm^3) in 25 minute-vacuum and 20 minute-diffusion time. The highest value of impregnated air dryness was determined as (0.53 g/cm^3) in 25 minute-vacuum and 40 minute diffusion and the lowest value as (0.43 g/cm^3) in 25 minute-vacuum and 20 minute-diffusion time. It was observed that stone water caused a serious increase in all specific gravity value. Esen (2009) subjected the test samples obtained from beech, pine and sapelli trees to impregnation with boric acid, borax, tanalith-e and imersol aqua. The impregnation retention rates, full dry densities and air dry densities of the samples were determined. As a result; the highest impregnation retention rate (6.83) in sapelli wood material impregnated with boric acid; the highest full dry density value (0,66 g/cm^3), air dry density value (0,72 g/cm^3) in beech tree.

Gear (2018) measured the highest air dry specific gravity value as (0.56 g/cm^3) with Aluminum Sulphate and the highest full dry specific gravity value as (0.54 g/cm^3) with Aluminum Sulphate after impregnation. The lowest air dry specific gravity value was measured with Boric Acid (0.43 g/cm^3) and the lowest full dry specific gravity value with boric acid (0.41 g/cm^3) after impregnation. It is concluded that this may arise from the vacuum and diffusion times applied in the impregnation process in wood material and the reaction of the anatomical structure of wood material on the solution.

RESULTS

In a summary, it is possible to use the stone water obtained from our country's own resources as impregnation agent. The use of cellulosic varnish with the used impregnating agent or the impregnation without varnish indicates its ability to be used especially in the furniture industry (park, garden, urban furniture, construction industry, etc.). Getting positive results in physical and mechanical properties shows this to be feasible and makes it necessary to carry out additional studies together. Stone water is produced as an anti-fire material and due to the large amount of Ba, Ni, Mg substances in stone water; combustion results can also be determined by applying a burning test with stone water on various types of wood raw materials. It has a positive structure on both wood adhesion and specific gravity.

REFERENCES

ASTM 1413 -76 (1976) Standartd Methods of Testing Wood Preservatives by Laboratory Soilblock Cultures", Annual Book of Astm Standarts, USA.

ASTM D 1667–87 (1999) Standard Methods for Conducting Machining Tests of Wood and Wood–Base Materials", ASTM Standards, USA.

Bal, B.C. (2006) "Amonyaklı Bakır Quat (Acq) Emprenye Tuzu İle Emprenye Edilen Sarıçam (Pinus Sylvestris L.) Odununun Bazı Fiziksel Ve Mekanik Özelliklerinin Araştırılması Amonyaklı Bakır Quat (Acq) Emprenye Tuzu ile Emprenye Edilen Sarıçam (Pinus Sylvestris L.) Odununun Bazı Fiziksel Ve Mekanik Özelliklerinin Araştırılması'' Yüksek Lisans Tezi, Kahramanmaraş Sütçü İmam Üniversitesi, Fen Bilimleri Enstitüsü, Kahramanmaraş.

Baysal, E. (2003) Borlu Bileşikler ve Doğal Sepi Maddeleriyle Emprenye Edilen Sarıçam Odununun Yanma Özellikleri, Erciyes Üniversitesi Fen Bilimleri Enstitüsü Dergisi, Kayseri, 19 (1-2): 59-69.

Bozkurt A.Y., Göker Y., Erdin N. (1993). Emprenye Tekniği", İstanbul Üniversitesi, Orman Fakültesi Yayınları, İstanbul.

Dişli, B. (2018). "Bazı mordan ve verniklerin sarıçam (*Pinus sylvestris L.*) odununun teknolojik özellikleri", Artvin Çoruh Üniversitesi, Fen Bilimleri enstitüsü, Yüksek Lisans Tezi, Artvin.

Esen, R., (2009). "Emprenye Yapılmış Ağaç Malzeme Üzerine Uygulanan Üstyüzey İşlemlerinin Yanma Direncine Etkilerinin Belirlenmesi" Yüksek Lisans Tezi, Karabük Üniversitesi Fen Bilimleri Enstitüsü, Karabük.

Kartal, S., N. ve Unamura, Y. (2004). Borlu Bileşiklerin Emprenye Maddesi Olarak Ağaç Malzeme ve Kompozitlerde Kullanılması" Uluslararası Bor Sempozyumu (23-25 Eylül), S. 334 Eskisehir.

Örs, Y., Atar, M., ve Demirci, Z. (2005). Effects of impregnation with boron compounds on wood finishing and combustible properties", TUBITAK-The

Scientific and Technological Research Council of Turkey. Project code: MISAG-237.

Özçifçi A., Batan, İ. (2009). Bor Yağının Ağaç Malzemenin Bazı Mekanik Özelliklerine Etkisi, Politeknik Dergisi, Cilt 12, Sayı 4.

TS 2470 (1976). Odunda Fiziksel ve Mekaniksel Deneyler İçin Numune Alma Metotları ve Genel Özellikleri, Ankara.

TS 2471 (1976). Odunda, Fiziksel ve Mekaniksel Deneyler İçin Rutubet Miktarı Tayini, Ankara.

TS 2472 (1976). Odunda, Fiziksel ve Mekaniksel Deneyler İçin Birim Hacim Ağırlığı Tayini, Ankara.

URL1.http://www.agaclar.net/forum/orman-ormancılık-orman-yanginlari-ağaçlan dirma/9750.htm/2019.

URL2.http://www.agaclar.net/forum/orman-ormancilik-orman-yanginlari-agaclan dirma/9750/2019.

URL3.http://dekra-mobilya.blogspot.com.tr/2008/01/üst-yüzey-işlemleri.html./2019.

Note: HORA 2019, Biotechnological Product (Stone Water) and Impregnation in Wood, International Congress on Human- Computer Interaction, Optimization and Robotic Applications July 5-7, 4 (5): 24- 27, 2019, Urgup, Nevşehir, Turkey. (Some of the results are presented at the symposium) The study has been expanded.

CHAPTER 9

THE IMPORTANCE OF DEVELOPING HYDROGEN PEROXIDE SENSOR AND DETERMINATION OF CANDIDATE SENSOR WITH VARIOUS MULTI-METALLIC SUPPORTED CATALYSTS

Assoc. Prof. Dr. Mehmet Sait İZGİ[1], Lecturer Fırat SALMAN[2],
Assoc. Prof. Dr. Hilal ÇELİK KAZICI[3]

[1] Siirt University, Chemical Engineering, saitizgi@gmail.com
[2] Van Yuzuncu Yil University, Chemical Engineering, frtsalman.che@gmail.com
[3] Van Yuzuncu Yil University, Chemical Engineering, hilalkazici@yyu.edu.tr

INTRODUCTION

Hydrogen peroxide (H_2O_2) is widely used in pharmaceuticals and industrial processes such as paper whitening, disinfection and sterilization, and food processing [1]. H_2O_2 is one of the main components of reactive oxygen types and is an indicator of oxidative stress, which is significant for the progression of Alzheimer's, Parkinson's, and other neurological diseases [2]. H_2O_2 is also a by-product of many oxidase enzymes, such as glucose oxidase, xanthine oxidase, and lactate oxidase [1]. Therefore, accurate, fast, reliable, cheap, and practical determination of H_2O_2 in many areas such as clinical control, food industry, environmental monitoring is significant [3]. Analytical techniques such as chromatography, spectrophotometry, chemiluminescence, electrochemistry, titrimetry, fluorescence are used for H_2O_2 determination[4] [5]. Among these techniques, **electrochemical techniques** come into prominence due to their high sensitivity, simplicity, quick response, ease of use, and not requiring expert personnel, being suitable for immediate and on-site measurement, selectivity, and low cost. Electrochemical techniques are widely used in the development of H_2O_2 sensors and biosensors due to these properties [6] [7] [8] [9]. Electrochemical H_2O_2 sensors can be examined in two groups as enzymatic and non-enzymatic. Enzymatic H_2O_2 sensors possess advantages such as low observability limit, high sensitivity, and good selectivity. However, enzyme sensors have disadvantages such as the enzyme immobilization methods, the high cost of enzymes, the enzyme activity being dependent on environmental conditions, and the shortening of sensor life due to a

decrease in enzyme activity. Enzyme-free H_2O_2 biosensors possess advantages such as simplicity, low cost, high stability, and fast response [10, 11]. The determination of H_2O_2 by the electrochemical method can be performed on the basis of oxidation or reduction of the substance on the electrode surface [12] [10, 13].

ELECTROCHEMISTRY

Electrochemistry is a sub-science of chemistry that examines the chemical changes occurring at the interface of a chemical substance and a metallic conductor (such as metal, graphite, or semiconductor) [14]. Electroanalytical chemistry includes a group of quantitative analytical methods based on the electrochemical properties of the solution when the analyte solution is part of an electrochemical cell. The advantages of electrochemistry are that electrochemical measurements are often specific for a particular oxidation step of an element, while other used devices are relatively inexpensive. A third feature that can be seen as an advantage or a disadvantage is that electrochemical methods provide information about the activities rather than the concentration of chemical species [15].

ELECTROCHEMICAL CELLS

Electrochemical studies began in 1922 when Jaroslav Heyrovsky discovered polarography which is considered as the basis of today's electroanalytical chemistry. Electrochemical processes are carried out in a mechanism called electrochemical cell. The anode where the cathode reduction reaction occurs is the electrode where oxidation reactions occur in an electrochemical cell. It is necessary to provide

the external connections of the electrodes with a metal conductor, to allow ion exchange between the solutions, and an electron transfer reaction takes place in each of the electrodes in order to create a current in a cell. Electrochemical cells are classified as "galvanic" if they are used in electrical energy production and "electrolytic" if they use electricity from an external source. Both cells are used in analytical chemistry. Most cells can be operated for galvanic or electrolytic purposes by changing experimental conditions [16].

Ways of Mass Transfer in an Electrochemical Incident

The analyte in the buffer is transferred to the electrode surface by migration, diffusion, and convection when performing electrochemical analysis of a substance. One or more of these ways are used in mass transfer, depending on the experimental conditions. Migration is the act of moving particles by the electric field force. Diffusion is one of the ways of mass transfer based on the difference of density, as a result of the efforts of the substances to move from very dense to the less dense environment and eliminate the density difference. Convection, on the other hand, is the event that the substances that can be reduced or oxidized in solution are carried to the electrode surface by physical movements in the solution [17].

Electrochemical-Based Methods

Today, it is common to use electrochemical-based methods that provide fast, reliable, and selective measurement in hydrogen peroxide determination.

- Direct Electrochemical Methods: Hydrogen peroxide can be determined electrochemically by decomposing it into water and oxygen by applying certain potentials. In accordance with this purpose, measurements can be performed by using a reference electrode system, such as a working electrode made of materials such as saturated calomel electrode, silver-silver chloride electrode, silver, gold, and glassy carbon, where saturated hydrogen peroxide can be reduced. However, selectivity is lower in this method due to the occurrence of interventions. Sensitivity was tried to be increased by exposing the studied electrodes to processes such as surface wear.

- Biocomponent-Based Electrochemical Methods: In the method studied for this purpose, it is essential to monitor the electrochemical changes that occur due to the concentration of hydrogen peroxide in the environment by immobilizing proteins and enzymes containing elements such as iron and copper, which will react with hydrogen peroxide. The enzymes such as catalase, horseradish peroxidase, which provide the reduction of hydrogen peroxide to water and oxygen, and proteins such as cytochrome c and hemoglobin are the main biocomponents used in the determination of hydrogen peroxide. A wide variety of immobilization procedures can be applied, such as the use of carbon nanotubes for immobilization of these materials, retaining with cross-linked polymers, retaining with zeolites, DNA modification, and immobilization with spontaneous monolayers. Enzymes or proteins that will transform hydrogen peroxide are commonly immobilized on gold, silver, or glassy carbon electrodes.

Amperometric methods performed on the basis of monitoring the current changes in the conversion of hydrogen peroxide at a constant working potential and associating these changes with hydrogen peroxide concentration have a wide range of applications [3, 18]. In amperometric methods, current changes due to the reduction of oxygen or hydrogen peroxide formed as a result of the reaction are determined against a reference electrode. Recent studies have focused on amperometric observation of the direct effect of hydrogen peroxide on the electrochemistry of the protein of interest, rather than the reduction and oxidation changes of the reaction components. The chronoamperometry method, in which current variations are determined in accordance with time, is a preferred method due to its ease of application, real-time, and fast response time. In this method, the change of the current formed as a result of a fixed potential applied as a result of the addition of hydrogen peroxide is taken as a basis [19]. The cyclic **voltammetry** method is also widely used for the determination of hydrogen peroxide. Although it is similar to the principle of amperometry method, current changes can be determined by plotting in accordance with the potential changes.

Voltammetric Methods

Voltammetry includes a group of electroanalytical methods in which information about the analyte is obtained by using a measurement of the current as a function of potential applied under conditions where an indicator or working electrode is polarized [20]. Amperometry is the technique applied by measuring the current proportional to the analyte

concentration at a constant potential [21]. The limits of the potential range that can be applied to the electrode depend on the types of working electrodes, the solvent used, and electrolyte in order to study the electrochemical behavior of any substance in voltammetry. When non-electroactive ions are added to the solution in the voltammetric voltage range, these ions contribute more to the transportation of the electric charge. In this case, the contribution of the electroactive substance or an ionic type consisting of this substance to the migration flow becomes insignificant. Thus, only the current value consisting of the diffusion current value decreases. Another function of these ions, which are called support electrolytes, is to reduce the electrical resistance of the solution. In a case where the supporting electrolyte exists and the solution is not mixed, the transport of the electroactive type to the electrode is only possible through diffusion [22]. Voltammetry is based on measuring the current formed in an electrochemical cell under conditions of full concentration polarization. On the other hand, potentiometric measurements are performed under conditions where the current approaches zero and there is no polarization [23]. **Voltammetry** differs from electrogravimetry and coulometry in terms of taking the necessary measures to minimize or eliminate the effects of concentration polarization. Furthermore, while the analyte is minimized in voltammetry, almost all matter is transformed into another state in electrogravimetry and coulometry [24].

CYCLIC VOLTAMMETRY

The current-potential curve appears as a peak when a linearly increasing potential is applied to a micro electro in a stagnant solution containing an electroactive substance. In this method, if the potential scanning is reversed to decrease linearly after reaching a certain voltage value in the forward direction, the method is called alternating voltammetry [24]. In a CV experiment, a small stagnant electrode is applied to a current signal in a stagnant solution by applying a potential variation with the waveform similar to that shown in Figure 1. The triangle waveform represents potential scanning in the forward and in the reverse direction. The direction of the initial scan may be negative or vice versa depending on the composition of the sample. If scanning is done by going towards more negative potentials, this is called forward scanning, and in the other direction, it is called reverse scanning. Scanning times start from 1 ms or less and may increase to 100 s or longer. Cyclic voltammetry (CV) is one of the most preferred methods among electrochemical methods. It can be concluded about the potential of a system to be reduced and oxidized or whether the electrode reaction is related to a chemical reaction in solution, whether it is electrochemically reversible and the stability of the reaction products by examining the alternating voltammograms in detail. In a CV experiment, a single full cycle, a half cycle, or multiple cycles can be used. The current response of the solution to the alternating excitation signal is shown in Figure 2 [25].
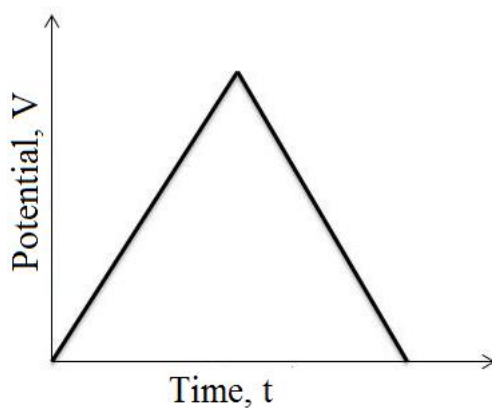
Figure 1. Cyclic voltammetry warning signal
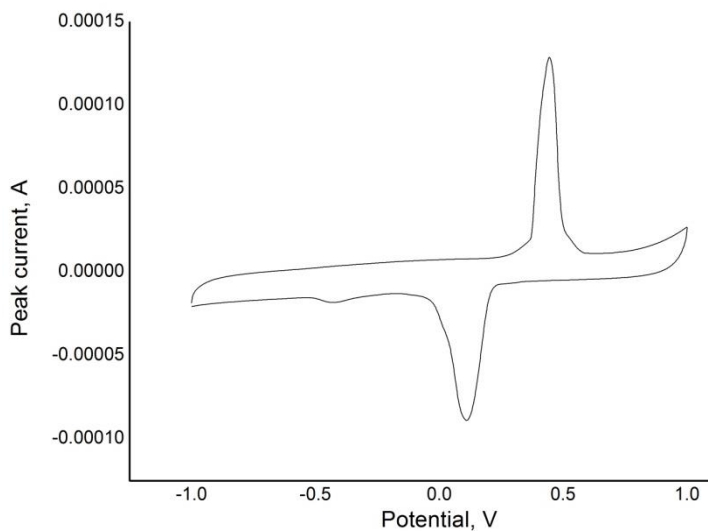
Figure 2. A typical cyclic voltammogram [11].

ELECTROCHEMICAL SENSORS

A sensor is an electrical motivating device that responds to a physical stimulus such as heat, light, sound, pressure, magnetism, or motion, and emerges as a means to change any particular property of the

constituent material. The word 'sensor' is derived from the Latin word 'sentient' which means to detect. Semantically, sensors have the ability to perceive the environment surrounding them [26]. A sensor (also called a detector) is a transducer that converts a physical quantity into a signal that can be made ready by the device that measures it. The sensor contains information that enables selective response to a specific analyte or an analyte group, thereby minimizing interference from other exemplary components [27]. A chemical sensor is an independent device that can provide real-time analytical information about a test sample. According to chemical information, the concentration of one or more chemical species can be understood in the sample. A target species is often called or determined analytically. Apart from the chemical species, microorganisms and viruses can be traced with the help of special bio-compounds such as nucleic acid or membrane components [28]. Specifically, electrochemical sensors are in the class of chemical sensors using an electrode as an element, a transducer in the presence of an analyte [26]. Electrochemical sensors convert information related to electrochemical reactions (the reaction between an electrode and analyte) into a viable qualitative or quantitative signal. Electrochemical sensors are often classified into three types: potentiometric, conductometric, and amperometric or voltammetric [29]. Electrochemical sensors can produce electronic outputs in digital signals for auxiliary analysis according to the steps demonstrated in Figure 3.
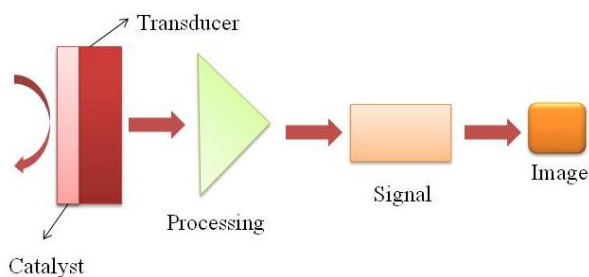
Figure 3. Working principle of the sensor [30]

Electrochemical sensors consist of heterogeneous catalysts that increase the speed of the reactions but do not react themselves. The stability of an electrocatalyst over time is one of the most important parameters to characterize it. Electrocatalysts are expected to operate for a long time at medium overvoltages. The most important factor that determines the electrocatalytic efficiency of such catalysts is adsorption energy. The weaker the binding force of the electrocatalyst with the reactant, the smaller the surface binding fraction. The main objectives of electrochemical studies include developing new strategies to increase the activity of metal catalysts [31].

METAL NANOPARTICLES

Metal nanoparticles can be defined as particles in the colloidal form with a particle size of 1-100 nm. Certain properties that nanoparticles should carry are listed below.

- The particle size must be less than 100 nm and the average standard deviation of the particle size must be less than 15%.

- Synthesizing the particles should be repeatable.

- The composition of the particles should be easily identifiable [32].

Although metal nanoparticles are reduced from metal to nanoscale, they are preferred because they exhibit different properties than the metals in bulk. It is especially useful as its catalytic life and catalytic activity increase as its size decreases. Metal nanoparticles are used in many areas due to their different properties. Transition metal nanoparticles are also suitable for use as catalysts because they are selective, active, and stable from their high surface area [33]. Metal nanoparticles are widely used in industrial products, machinery industry, consumer products, military applications, and especially in medicine, as they can be easily synthesized and chemically modified. Metal nanoparticles and their alloys, which have superior mechanical properties due to their crystal structures and very strong metallic bonds, are among the materials that best match the mechanical conditions of our skeletal-muscular system [34].

MODIFIED ELECTRODES

Modified electrodes are the electrodes obtained by attaching chemical substances spontaneously or externally to the electrode surface. Modified electrodes have usage areas in many different fields such as electrosynthesis, electrocatalysis, biosensor applications, drug release systems, corrosion, and energy applications. Especially modified electrodes coated with an electroactive polymer are highly preferred since their surface properties can be easily controlled. Modified electrodes are also used to achieve desired properties such as controlling the electrochemical reaction rate, and they provide various

advantages such as accelerating electron transfer reactions, selective and precise determination [35]. Modified electrodes are also used to achieve desired properties such as controlling the electrochemical reaction rate, and they provide various advantages such as accelerating electron transfer reactions and selective and precise determination. Materials used as modifiers can be both organic and inorganic. While organic materials are generally used in polymers; ligands, complexes or metal oxides can be used in inorganic materials [12, 36]. The difference of the modified electrodes from the unmodified electrodes is that they have a conductive substrate on their surface and have properties arising from this substrate. Modified electrodes can usually be obtained by attaching organic or inorganic compounds to the conductive substrate. Thus, electrodes with different properties can be prepared in accordance with the study. The basic rule is that the developed electrode system has superior properties than the unmodified electrode [37]. Voltammetric and amperometric measurements have emerged as well as disposable electrochemical devices as an advantage of the modification process applied to the electrodes. The advantages of modified electrodes are ease of use, low cost, and being able to be commercialized, being portable, and providing (bio) chemical modification possibilities [38]. Modified electrodes used in analytical chemistry possess several advantages. For example, the chemical substance used when modifying the electrode is unlimited. The electron transfer rate can be increased or decreased by changing the material and method used for the modification. For certain species, selective, highly sensitive, specific

surfaces can be created and it is possible to obtain surfaces resistant to external influences [39].

The most important and positive effect is the use of **support** material in terms of providing superior properties to the catalyst we will use in addition to the modification process.

SUPPORTED CATALYSTS

Assisted catalysts are heterogeneous catalysts prepared by storing the active ingredients on an inert porous support surface. The support materials increase the stability of the components and provide a more uniform distribution on a wider surface. The following interactions take place between the support material and the active ingredient [40].

- Physical (adhesive) forces: Van der Waals bonds,

- Chemical forces: Electron transfer,

- The formation of different phases on the boundary surface,

- The formation of reduced components on the catalyst (active metal) surface.

As support materials, large surface area, and porous materials such as activated carbon, clays, silica gels, and zeolite are used. The support material should have features such as high cation exchange capacity, swelling feature, expanding lattice structure, no layer stiffness in the structure [41] [42] [43]. The physical and chemical parameters that should be taken into account in the selection of the support substance are specified in Chart 1 [40].

Chart 1. Physical and chemical parameters affecting the choice of support material

Physical Properties	Chemical Properties
o Specific surface area (activity and active affects the distribution of the component)	o Specific activity
o Porosity (mass and heat transfer)	o Relationship with the active ingredient (selectivity, dual function catalysts)
o Particle size and shape (diffusion and pressure drop)	o With reactants or solvents reacting
o Thermal stability (catalyst life and regeneration)	
o Mechanical stability (wear and durability)	
o Mass density (active per unit volume component content)	
o Regain	

According to the abovementioned detailed information, an experimental study based on determining candidates for developing an enzyme-free hydrogen peroxide sensor was conducted by using supported metal nanoparticles as an electrocatalyst.

Accordingly, three different electrocatalysts were synthesized as Co-Ni-La/CNT, Co-Ni-La/Al$_2$O$_3$ and Co-Ni-La/Eupergit CM (Polymer) and the synthesis method is as follows;

La–Ni–Mo–B catalysts were prepared as previously described [44]. In the present study, we have optimised it as 0.21 and 0.30 molar ratio of La in the La/Ni/Mo catalyst. The following procedure was employed for testing the performance of La–Ni–Mo–B catalysts in H$_2$O$_2$ solution. Here, by 10 wt% metal content, 90 wt% support material was synthesized and the activity was examined.

The electrochemical behavior of the prepared electrodes was examined by using the cyclic voltammetry (CV) method.
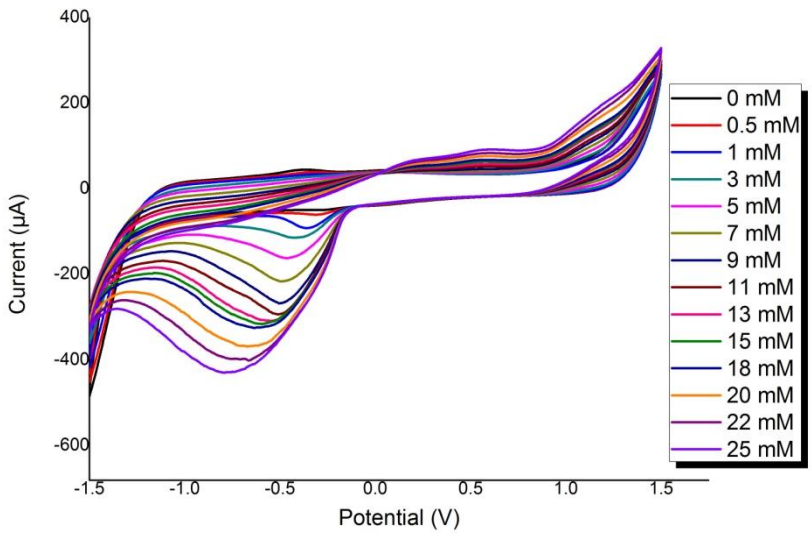
Figure 4. The effect of Co-Ni-La/CNT support material on peak current of H_2O_2 in 0.1 M PBS at 50 mVs $^{-1}$
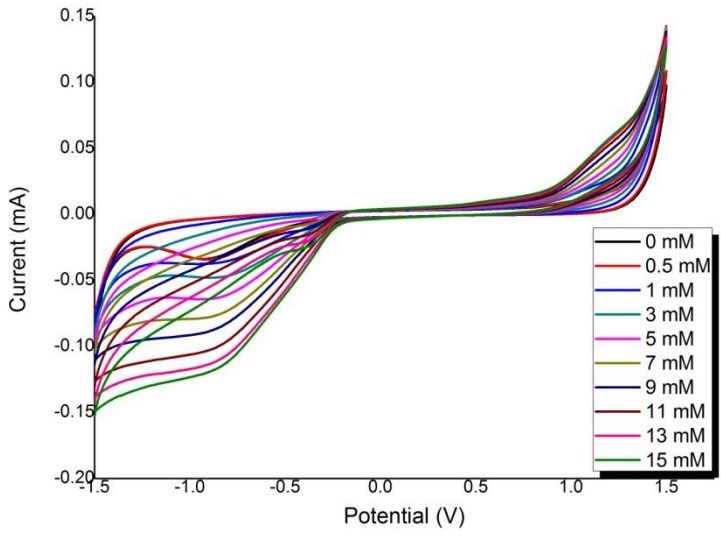
Figure 5. The effect of Co-Ni-La/Al$_2$O$_3$ support material on peak current of H_2O_2 in 0.1 M PBS at 50 mVs $^{-1}$
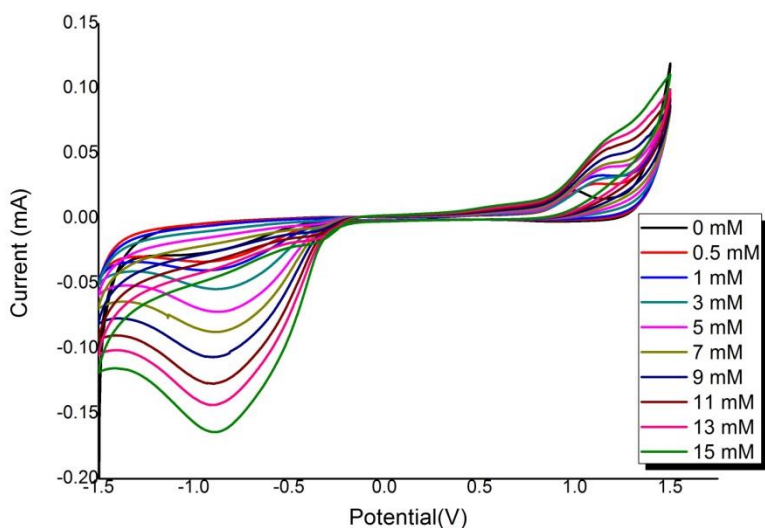
Figure 6. The effect of Co-Ni-La/Eupergit CM (polymer) support material on peak current of H_2O_2 in 0.1 M PBS at 50 mVs $^{-1}$

When the effect of the support materials on multi-metallic catalysts on the hydrogen peroxide sensor was examined, it was observed that the concentration range of the CNT-supported catalyst was 0-25 mM. Polymer and Al_2O_3 supported material have a concentration range of 0-25 mM. In addition, the reduction peak current was obtained as 400 µA in the catalyst with CNT supported material. It was observed that there were about 175 µA (Co-Ni-La/Eupergit CM (polymer)) and 120 µA (Co-Ni-La/Al_2O_3) in other catalysts. It is clear that multimetallic catalysts provide a nearly double increase in the reduction peak current with the support material.

REFERENCES

[1] S. H. Chen, R. Yuan, Y. Q. Chai, F. X. Hu, *Microchimica Acta* **2013**, *180*, 15-32.

[2] M. Di Carlo, D. Giacomazza, P. Picone, D. Nuzzo, P. L. San Biagio, *Free Radical Research* **2012**, *46*, 1327-1338.

[3] A. Caglar, H. C. Kazici, D. Alpaslan, Y. Yilmaz, H. Kivrak, N. Aktas, *Fullerenes Nanotubes and Carbon Nanostructures* **2019**, *27*, 736-745.

[4] O. Sahin, H. Kivrak, A. Kivrak, H. C. Kazici, O. Alal, D. Atbas, *International Journal of Electrochemical Science* **2018**, *13*, 2186-2192.

[5] H. C. Kazici, M. Yayla, B. Ulas, N. Aktas, H. Kivrak, *Electroanalysis* **2019**, *31*, 1118-1124.

[6] D. Duzenli, O. Sahin, H. C. Kazici, N. Aktas, H. Kivrak, *Microporous and Mesoporous Materials* **2018**, *257*, 92-98.

[7] F. Salman, H. C. Kazici, H. Kivrak, *Frontiers of Chemical Science and Engineering*.

[8] H. C. Kazici, M. Yayla, *Chemical Engineering Communications* **2019**, *206*, 1731-1742.

[9] C. Avci, F. Cicek, H. C. Kazici, A. Kivrak, H. Kivrak, *International Journal of Nano Dimension* **2018**, *9*, 15-23.

[10] H. C. Kazici, A. Caglar, T. Aydogmus, N. Aktas, H. Kivrak, *Journal of*

Colloid and Interface Science **2018**, *530*, 353-360.

[11] H. C. Kazici, F. Salman, A. Caglar, H. Kivrak, N. Aktas, *Fullerenes Nanotubes and Carbon Nanostructures* **2018**, *26*, 145-151.

[12] N. A. Ertas, E. Kavak, F. Salman, H. C. Kazici, H. Kivrak, A. Kivrak, *Electroanalysis*.

[13] H. C. Kazici, F. Salman, H. D. Kivrak, *Materials Science-Poland* **2017**, *35*, 660-666.

[14] G. Chang, M. Oyama, K. Hirao, *Journal of Physical Chemistry B* **2006**, *110*, 1860-1865.

[15] D. A. Skoog, *Abstracts of Papers of the American Chemical Society* **1992**, *204*, 115-ANYL.

[16] A. K. Samantara, S. Ratha, *Metal Oxides/Chalcogenides and Composites: Emerging Materials for Electrochemical Water Splitting* **2019**, 5-9.

[17] S. M. Jafari, A. F. Esfanjani, *Nanoencapsulation Technologies for the Food and Nutraceutical Industries* **2017**, 524-544.

[18] W. Chen, S. Cai, Q. Q. Ren, W. Wen, Y. D. Zhao, *Analyst* **2012**, *137*, 49-58.

[19] H. Shamkhalichenar, J. W. Choi, *Journal of the Electrochemical Society* **2020**, *167*.

[20] E. Noviana, C. P. McCord, K. M. Clark, I. Jang, C. S. Henry, *Lab on a Chip* **2020**, *20*, 9-34.

[21] M. A. Alonso-Lomillo, O. Dominguez-Renedo, M. J. Arcos-Martinez, *Biosensors: Properties, Materials and Applications* **2009**, 1-51.

[22] H. Nakajima, *Mass Transfer - Advanced Aspects* **2011**, 285-304.

[23] W. Munchgesang, U. Langklotz, *Electrochemical Storage Materials: from Crystallography to Manufacturing Technology* **2019**, 385-399.

[24] K. H. Lubert, K. Kalcher, *Electroanalysis* **2010**, *22*, 1937-1946.

[25] *Electroanalytical Methods: Guide to Experiments and Applications, Second Edition* **2010**, 1-359.

[26] F. R. Simoes, M. G. Xavier, *Nanoscience and Its Applications* **2017**, 155-178.

[27] M. A. Raj, S. A. John, *Graphene-Based Electrochemical Sensors for Biomolecules* **2019**, 1-41.

[28] R. M. Penner, *Annual Review of Analytical Chemistry, Vol 5* **2012**, *5*, 461-485.

[29] H. Ezoji, M. Rahimnejad, *Nanoparticle Design and Characterization for Catalytic Applications in Sustainable Chemistry* **2019**, *38*, 329-345.

[30] N. P. Shetti, D. S. Nayak, K. R. Reddy, T. M. Aminabhvi, *Graphene-Based Electrochemical Sensors for Biomolecules* **2019**, 235-274.

[31] T. Okada, M. Kaneko, *Molecular Catalysts for Energy Conversion* **2009**, *111*, 67-102.

[32] J. D. Aiken, Y. Lin, R. G. Finke, *Journal of Molecular Catalysis a-Chemical* **1996**, *114*, 29-51.

[33] H. L. S. Santos, J. A. Dias, M. A. S. Andrade, L. H. Mascaro, *Electrochemical Water Splitting: Materials and Applications* **2019**, *59*, 1-36.

[34] E. Kowalska, M. Endo, Z. S. Wei, K. L. Wang, M. Janczarek, *Nanoscale Materials in Water Purification* **2019**, 553-579.

[35] P. S. Adarakatti, S. K. Kempahanumakkagari, *Electrochemistry, Vol 15* **2019**, 58-95.

[36] H. C. Kazici, F. Salman, M. S. Izgi, O. Sahin, *Journal of Electronic Materials* **2020**, *49*, 3634-3644.

[37] M. Grden, M. Lukaszewski, G. Jerkiewicz, A. Czerwinski, *Electrochimica Acta* **2008**, *53*, 7583-7598.

[38] A. Dago, J. Navarro, C. Arino, J. M. Diaz-Cruz, M. Esteban, *Journal of Chromatography A* **2015**, *1409*, 210-217.

[39] J. F. Li, A. Rudnev, Y. C. Fu, N. Bodappa, T. Wandlowski, *Acs Nano* **2013**, *7*, 8940-8952.

[40] J. Hagen, *Industrial Catalysis: a Practical Approach* **2006**, 1-507.

[41] G. W. Brindley, T. C. Simonton, *Clays and Clay Minerals* **1984**, *32*, 235-237.

[42] M. L. Occelli, *Journal of Molecular Catalysis* **1986**, *35*, 377-389.

[43] S. R. Lee, Y. S. Han, M. Park, G. S. Park, J. H. Choy, *Chemistry of Materials* **2003**, *15*, 4841-4845.

[44] W. Y. Wang, Y. Q. Yang, H. A. Luo, W. Y. Liu, *Catalysis Communications* **2010**, *11*, 803-807.

CHAPTER 10

EFFECTS OF PESTICIDES ON HEMATOLOGICAL AND IMMUNOLOGICAL SYSTEM IN FISH

Dr. Selçuk DUMAN[1]

[1] Cukurova University, Imamoglu Vocational School, Department of Aquaculture, Adana, TURKEY. sduman@cu.edu.tr

INTRODUCTION

Nowadays, with the development of agriculture, the use of pesticides has increased and as a result, it has reached high contamination in aquatic environments. Although pesticide applications are intended to affect only target organisms, the toxicity of pesticides on non-target organisms poses an important potential risk (Harabawy & Ibrahim, 2014). After pesticide application which usually originates from intensive agriculture, with a surface flow and under-surface drainage in a few weeks, most pesticides reach the rivers, lakes, groundwaters, ponds and pollute the waters (Talebi, 1998; Nouri et al., 2000). The toxicity of different concentrations of pesticides for aquatic vertebrates is a major environmental problem (Van Der Kraak et al., 2014). Worry about the unfavorable effects of pesticides on fish and other aquatic organisms is increasing day by day, therefore so much research has been done on pesticides in the freshwater area (Sparling et al., 2001; Ramesh & Saravanan, 2008; Iwafune et al., 2011). Immunological, biochemical and hematological features are important factors in determining the physiological state of the fish (Luskova et al., 2002). It is quite probable that pesticides with different cytotoxic properties can disrupt multiple organ systems on fish and this situation can be visible on the immune system (Porter et al., 1999). Also, studies on the pathogenesis of diseases indicate that exposure to a chemical contaminant causes debilitation in the immune system that required to fight pathogens (Jobling & Tyler, 2003; Fatima et al., 2007). Fish blood is an indicator of all body functions pathophysiological. For this reason,

in fish exposed to a toxic substance, blood parameters are quite important in the diagnosis of their functional and structural conditions (Zutshi et al., 2010). Van Vuren 1986, reported that when water quality is damaged by toxic substances, any physiological change in fish will affect the amounts of one or more of the hematological parameters. In order to evaluate the physiology of the organism, the biochemical and hematological structure of the blood is important health indicators that provide to us precious information (Saravanan et al., 2011; Fazio et al., 2013). Fish is a food source of high nutritional value for both animals and humans. It also takes an important place in the food chain. However, fish are very responsive to environmental pollution and they are often used as a bio-indicator of environmental pollution in pesticide studies (Kaya et al., 2015).

HEMATO-IMMUNO ASSAYS

In the research by Velisek et al. (2010), the sub-chronic effects of terbutryn at concentrations 0.02, 2, 20 and 40 µg L^{-1} were determined in one-year-old common carp exposed for 28 days. Terbutryn is a herbicide used in fish ponds to control existing on the ground or free-floating weeds and algae as well as weeds in agricultural practices (Tomlin, 2009). The erythrocyte count increased significantly in fish exposed to 2, 20 and 40 µg L^{-1} terbutryn, while MCV and MCH values decreased significantly. There was no statistical change in Hb, PCV, MCHC, leukocyte and leukogram values among all groups. The hematological parameters in fish exposed to terbutryn are shown in Table 1. As a result of their studies, they stated that terbutryn may affect

biometric, biochemical and hematological profiles in carp, depletion of antioxidant defense mechanisms will cause oxidative stress that can cause deep damage to the organism.

Table 1: Hematological Values in Common Carp Following Sub-Chronic Exposure to Terbutryn (Velisek et al., 2010).

Fish group	Control	1	2	3	4
Terbutryn ($\mu g\,L^{-1}$)	–	0.02	2	20	40
	Mean±SD	Mean±SD	Mean±SD	Mean±SD	Mean±SD
RBC (T L^{-1})	1.05±0.03	1.08±0.07	1.61±0.24[*]	1.72±0.09[*]	1.60±0.25[*]
Hb (g L^{-1})	68.35±9.19	70.59±8.70	70.99±8.61	75.33±7.69	67.95±5.75
PCV (l L^{-1})	0.260±0.032	0.259±0.027	0.275±0.034	0.28370.039	0.252±0.020
MCV (fl)	248.07±36.01	236.05±33.50	176.45±36.63[*]	168.38±28.84[*]	168.12±26.28[*]
MCH (pg)	65.20±10.02	66.54±10.70	44.92±9.39[*]	43.99±5.54[*]	44.96±6.67[*]
MCHC (g L^{-1})	262.97±13.00	272.58±13.05	258.49±10.05	268.51±18.81	269.82±9.80
Leuko (G L^{-1})	85.38±15.45	85.08±8.64	82.67±20.93	90.33±41.12	71.25±12.66
Lymphocytes (G L^{-1})	74.72±14.13	73.69±13.85	75.29±14.81	75.03±11.06	59.68±23.09
Monocytes (G L^{-1})	0.37±0.35	2.22±1.78	0.47±0.30	0.94±0.68	0.98±0.56
Neutrophil granulocytes segments (G L^{-1})	9.84±6.13	8.06±5.81	5.62±4.73	15.88±10.21	8.23±5.84
Neutrophil granulocytes bands (G L^{-1})	0.45±0.44	1.11±0.85	0.71±0.52	0.16±0.23	0.13±0.24

Jayaprakash and Shettu (2013) examined changes in hematological parameters of freshwater fish *Channa punctatus* subjected to

deltamethrin toxicity. Deltamethrin is one of the insecticides commonly used for agricultural purposes as an insecticide and antiparasitic. Also it is highly toxic to fish and aquatic organisms (Mittal et al., 1994). *Channa punctatus* was exposed to synthetic pyrethroid pesticide deltamethrin 0.075 mg/L (low) and 0.15 mg/L (high) doses for 15, 30 and 45 days. In fish subjected to both doses for 45 days, there was a significant reduction in hemoglobin (Hb), total erythrocyte count (RBC), hematocrit (Hct), mean corpuscular volume (MCV), mean corpuscular hemoglobin (MCH), monocyte and basophil count compared to control group. Moreover, there was a significant increase in total leukocyte count (WBC), lymphocytes, neutrophils, eosinophils and mean corpuscular volume (MCV) in fish exposed to low and high deltamethrin concentrations for 30 and 45 days. Hematological parameters of *Channa punctatus* exposed to deltamethrin are given Table 2. As a result of this study, synthetic pyrethroid pesticide deltamethrin has been reported to negatively affect the hematology of freshwater fish *Channa punctatus*, and it has been recommended that limited and cautious use highly toxic pesticides such as deltamethrin.

Table 2: Mean Hematological Parameters of *Channa punctatus* Exposed to Sub Lethal Concentrations (0.075 mg/l and 0.15 mg/l) of Deltamethrin in 15, 30 and 45 Days (Jayaprakash and Shettu, 2013).

Parameter	Concentration (mg/l)	Control	Treated		
			15 days	30 days	45 days
TEC (x10^{6}mm^{-3})	0.075	3.165±0.023	2.833±0.023*	2.577±0.019*	2.272±0.027*
	0.15	3.139±0.019	2.753±0.028*	2.341±0.018*	1.873±0.028*
TLC (x10^{3}mm^{-3})	0.075	18.808±0.556	20.564±0.861*	19.784±0.520	17.639±0.542
	0.15	18.084±0.670	19.991±0.838*	17.259±0.420	14.793±0.596*
Hb (g/100ml)	0.075	12.537±0.309	10.536±0.280*	7.486±0.378*	5.724±0.296*
	0.15	12.603±0.273	9.447±0.280*	5.441±0.304*	2.691±0.127*
PCV (%)	0.075	34.366±0.236	31.143±0.038*	28.669±0.183*	25.757±0.205*
	0.15	34.343±0.213	30.669±0.280*	26.534±0.288*	21.699±0.175*
MCV (10^{-4}fl)	0.075	1.086±0.010	1.100±0.009	1.113±0.012	1.134±0.009*
	0.15	1.094±0.011	1.115±0.016	1.113±0.012	1.159±0.018*
MCH (10^{5}pg)	0.075	3.962±0.101	3.719±0.087*	2.906±0.150*	2.521±0.146*
	0.15	4.015±0.088	3.432±0.102*	2.324±0.129*	1.434±0.068*
MCHC (g%)	0.075	36.482±0.8800	33.831±0.918*	26.117±1.432*	22.227±1.201*
	0.15	36.700±0.913	30.781±1.139*	20.505±1.080*	12.480±0.671*
ESR (mm/hr)	0.075	5.071±0.189	7.000±5.000*	8.786±0.567	10.286±0.267*
	0.15	5.214±0.267	7.429±0.189*	10.429±0.534*	13.000±0.289*
CT (Sec.)	0.075	26.714±0.488	30.000±0.577*	35.000±0.577*	41.571±0.976*
	0.15	26.571±0.787	31.714±0.756*	40.571±0.787*	50.857±0.690*

Values are mean ± standard error of mean, n=7, *=Significant at p<0.01 level, TEC=Total erythrocytes count, TLC=Total leucocytes count, Hb=Haemoglobin, PCV=Packed cell volume, MCV=Mean corpuscular volume, MCH=Mean corpuscular Haemoglobin, MCHC= Mean corpuscular Haemoglobin concentration, ESR=Erythrocyte sedimentation rate, CT=Clotting time.

Girón-Pérez et al. (2006) investigated the effect of chlorpyrifos, an organophosphorus insecticide commonly used in agricultural activities and domestic, on the hematology and immunology of Nile tilapia (*Oreochromis niloticus*). They applied chlorpyrifos at different rates (0.422, 0.845, 1.69, and 3.38 mg/L) to Nile tilapia weighing approximately 80 g for 96 hours. Hematological parameters of Nile tilapia exposed to chlorpyrifos are shown Table 3. According to their result chlorpyrifos did not affect hemoglobin, hematocrit, red blood cell (RBC), mean corpuscular volume (MCV), mean corpuscular hemoglobin (MCH), and mean corpuscular hemoglobin concentration (MCHC) parameters. But, it has significantly affected the active phagocytic cells and the phagocytic index. They reported that phagocytic parameters against pesticides were more sensitive than hematological parameters in evaluating the acute toxic effect of chlorpyrifos in the Nile tilapia. Also, according to them, a reduction of phagocytic functions due to chlorpyrifos, it causes a negative effect on the natural immune mechanism and may have a weaker impact on the fight against infections.

Hematological parameters	Concentration of chlorpyrifos (mg/L)				
	3.38	1.69	0.845	0.422	Control
RBC (x10^6/μL)	1.65±0.24	1.62±0.27	1.62±0.37	1.46±0.32	1.46±0.32
Hemoglobin (g/dL)	7.12±0.89	7.12±1.2	7.12±1.4	7.30±0.97	6.44±0.81
Hematocrit (%)	25.59±3.09	25.25±3.71	25.61±4.79	26.66±3.64	22.67±3.8
MCV (fL)	157.6±24.5	157.6±23.0	161.4±17.7	162.6±19.4	159.4±30.6
MCH (pg)	43.3±6.92	44.54±7.95	45.25±10.64	44.38±3.78	45.0±8.49
MCHC (g/dL)	27.99±24.5	28.08±23.01	29.53±17.78	27.44±19.46	28.68±30.61

Kaya et al. (2015) investigated the effects of phosalone concentrations on serum biochemical, hematological, and immunological responses of carp (*Cyprinus carpio*). Phosalone is used as insecticides and acaricide to combat pests, and it is a pesticide that is toxic to fish (Çelik et al., 2012). They exposed fish to low (0.15 mg/L), medium (0.3 mg/L) and high (0.6 mg/L) phosalone concentrations throughout 7-14 days. They reported that phosalone concentrations were significantly affected hematological parameters such as RBC (red blood cell), WBC (white blood cell), Hct (hematocrit), Hb (hemoglobin), MCV (mean corpuscular volume), MCH (mean corpuscular hemoglobin) and MCHC (mean corpuscular hemoglobin concentration). They also informed that white blood cell (WBC) types such as neutrophil,

lymphocyte, and monocyte were affected by phosalone. Effect of different concentrations of phosalone on white blood cell types and hematological variables in *Cyprinus carpio* are given Table 4, Table 5. According to the results of Kaya et al. (2015) exposed to sublethal phosalone concentrations, the hematological and immunological parameters of the *Cyprinus carpio* were negatively affected. The alteration of these parameters is associated with oxidative stress damage and the immune system.

Table 4: White Blood Cell Types in *Cyprinus carpio* Exposed to Phosalone (Kaya et al., 2015).

Parameters/days	Experimental groups			
	Control (C)	Low (L)	Medium (M)	High (H)
LYMPHOCYTE (%) 0	82.50±3.56	82.50±3.56	82.50±3.56	82.50±3.56
7	83.00±4.31	63.00±3.56*	62.40±2.48*	61.60±2.34*
14	82.30±4.01	65.40±3.33*	59.20±3.56*	56.00±2.11*
NEUTROPHIL (%) 0	16.00±2.41	16.00±2.41	16.00±2.41	16.00±2.41
7	16.00±3.01	35.00±4.41*	36.00±3.56*	36.00±4.64*
14	16.50±2.78	32.00±3.11*	36.80±4.00*	39.00±4.89*
MONOCYTE (%) 0	1.50±0.34	1.50±0.34	1.50±0.34	1.50±0.34
7	1.00±0.11	2.00±0.43	1.60±0.18	2.40±0.61
14	1.20±0.13	2.60±0.22	4.00±0.40*	5.00±0.32*

Table 5: Hematological Parameters in *Cyprinus carpio* Exposed to Phosalone (Kaya et al., 2015).

Parameters/days	Experimental groups			
	Control (C)	Low (L)	Medium (M)	High (H)
RBC ($\times 10^6$/mm^3) 0	4.60±0.33	4.60±0.33	4.60±0.33	4.60±0.33
7	4.56±0.56	3.47±0.56	3.89±0.93	1.39±0.51*
14	4.29±0.54	0.79±0.05*	0.83±0.04*	0.87±0.04*
WBC ($\times 10^3$/mm^3) 0	54.00±1.87	54.00±1.87	54.00±1.87	54.00±1.87
7	55.00±1.73	46.67±2.03*	43.67±2.33*	40.00±0.58*
14	54.50±1.55	44.25±1.70*	35.75±2.21*	27.75±1.11*
Hct (%) 0	40.75±1.93	40.75±1.93	40.75±1.93	40.75±1.93
7	41.33±2.03	27.00±3.21*	27.00±2.52*	21.33±0.88*
14	36.50±2.60	31.25±1.38	25.25±1.25*	21.75±0.85*
Hb (g/dL) 0	9.88±0.54	9.88±0.54	9.88±0.54	9.88±0.54
7	8.04±0.42	9.38±0.52	9.30±0.20	11.61±0.97*
14	9.86±0.41	8.25±0.43*	7.43±0.32*	5.32±0.30*
MCV (μm^3) 0	88.48±12.64	88.48±12.64	88.48±12.64	88.48±12.64
7	92.27±6.63	66.40±15.04	81.37±26.97	237.50±63.78*
14	89.39±13.64	276.74±8.75*	310.68±30.89*	363.86±24.48*
MCH (pg) 0	21.60±2.09	21.60±2.09	21.60±2.09	21.60±2.09
7	18.04±1.82	34.50±3.12	26.64±5.99	82.63±20.49*
14	24.02±3.02	67.59±2.90*	91.24±7.76*	95.72±5.56*
MCHC (%) 0	24.57±2.33	24.57±2.33	24.57±2.33	24.57±2.33
7	19.48±1.01	35.34±2.64	35.07±3.54	54.96±6.63*
14	27.29±1.53	26.42±1.05	29.49±0.74*	24.43±0.77

Upadhyay et al., (2014) determined the acute toxicity of pesticide (Pyrazosulfuron-Ethyl which belongs to Sulfonylurea group) for freshwater fish *Oreochromis mossambicus* under laboratory conditions. Sulfonylurea herbicides are a significant class of herbicides commonly used to control weeds in agricultural products (Brown, 1990). Pyrazosulfuron-Ethyl was applied to the fish at rates of 50 mg / L, 100 mg / L, 200 mg / L and 400 mg / L for 96 hours. They identified hematological changes in *Oreochromis mossambicus*, a freshwater teleost fish that was acutely exposed to Pyrazosulfuron-Ethyl pesticide. Therefore, parameters such as RBC count, hemoglobin (Hb), hematocrit (PCV), mean corpuscular hemoglobin (MCH), mean corpuscular hemoglobin concentration (MCHC), mean corpuscular volume (MCV) and WBC count were examined to evaluate the effect of herbicide on hematological parameters. There was a significant increase in RBC count, HB, and PCV values in the group exposed to 50 and 100 mg / L doses in fish compared to the control group. While MCHC showed a significant decrease, no significant change was observed in MCV and MCH. The WBC count increased significantly compared to the control group. They reported that these changes could be used as non-specific biomarkers in the water ecosystems contaminated with herbicides. Hematological changes in *Oreochromis mossambicus* are given in Table 6.

Table 6: Hematological Changes in *Oreochromis mossambicus* Exposed to Pyrazosulfuron-Ethyl (Upadhyay et al., 2014).

Parameters	Concentration of Pyrazosulfuron-Ethyl (mg/l)				
	Control	50mg/l	100mg/l	200mg/l	400mg/l
RBC (10^6/µL)	1.04±0.025	1.90±0.027	1.69±0.023	1.40±0.028	1.28±0.022
Hb (g/dL)	5.3±0.154	9.7±0.159	8.6±0.152	6±0.157	5.80±0.162
PCV (%)	14.6±0.555	29.6±0.551	32.6±0.558	23.4±0.557	19±0.554
MCV (fL)	140.38±3.52	155.79±3.56	192.9± 3.54	144.44±3.57	142.42±3.51
MCHC (g/dL)	36.3±1.03	32.77±1.03	26.38±1.03	34.62±1.03	31.3±1.03
MCH (pg)	50.96±1.66	51.96±1.68	50.89±1.64	50±1.65	53.54±1.69
WBC (10^3/µL)	45,000± 655	151,600±653	109,500±653.64	79,600±657.89	76,800±652.23

Modesto and Martinez (2010) studied the effects of pesticide Roundup Transorb (RDT) on the Neotropical fish *Prochilodus lineatus*. RDT is widely used worldwide in agricultural applications. It is a herbicide containing a mixture of surfactants with glyphosate-based (Moreno et al., 2014). Juvenile fish (*Prochilodus lineatus*) with a mean weigh of 9.97±2.5 g were acutely exposed to 1 mg L^{-1} of RDT (RDT 1) and 5 mg L^{-1} of RDT (RDT 5) doses for 6, 24 and 96 hours. After 24 and 96 hours of exposure, the number of hematocrit and erythrocytes increased significantly in fish in the RDT 5 group. Also, leukocyte and lymphocyte levels were significantly increased in the same group fish after 96 hours of exposure. In addition, there was a reduction in the neutrophils values in the RDT 5 group after 96 hours of exposure. Hematological parameters and leukocyte cell types of *Prochilodus*

lineatus exposed to RDT were shown in Table 7, Table 8. There were no changes detected statistically for hemoglobin (Hb), monocyte, eosinophil and basophil values.

Table 7: Hematological Parameters of *Prochilodus lineatus* Exposed to RDT 1 (1 mg L^{-1}) and RDT 5 (5 mg L^{-1}) Doses for 6, 24 and 96 Hours Experimental Periods (Modesto and Martinez, 2010).

		Hemoglobin (g 100 mL^{-1})	Hematocrit (%)	RBC ($\times 10^6$ mm^{-3})	WBC ($\times 10^3$ mm^{-3})
6 h	Control	7.45 ± 0.47	32.2 ± 1.2	2.89 ± 1.40	201.3 ± 8.7
	RDT 1	8.05 ± 0.89	33.9 ± 0.9	2.88 ± 1.60	201.5 ± 6.4
	RDT 5	7.56 ± 0.74	32.5 ± 0.5	2.87 ± 1.04	202.7 ± 4.8
24 h	Control	7.85 ± 0.53	31.3 ± 0.7	2.29 ± 0.13	202.9 ± 5.1
	RDT 1	8.58 ± 0.62	34.6 ± 1.6	2.27 ± 0.10	203.4 ± 4.1
	RDT 5	6.96 ± 0.47	35.2 ± 1.0[*]	2.38 ± 0.11[*]	202.8 ± 6.8
96 h	Control	8.04 ± 0.78	33.5 ± 1.0	2.54 ± 0.85	201.7 ± 7.4
	RDT 1	8.21 ± 1.01	34.6 ± 1.9	2.53 ± 1.00	201.9 ± 6.7
	RDT 5	7.89 ± 1.04	36.9 ± 0.5[*]	2.65 ± 0.79[*]	220.1 ± 4.7 [*]

Table 8: Leukocyte cell types of *Prochilodus lineatus* Exposed to RDT 1 (1 mg L^{-1}) and RDT 5 (5 mg L^{-1}) Doses for 6, 24 and 96 Hours Experimental Periods (Modesto and Martinez, 2010).

		lymphocyte	neutrophil	monocyte	eosinophil	basophil
6 h	Control	54.9 ± 0.9	38.4 ± 1.7	5.1 ± 0.9	0.8 ± 0.4	0.8 ± 0.3
	RDT 1	55.1 ± 0.9	38.5 ± 1.4	5.0 ± 0.8	0.9 ± 0.8	0.6 ± 0.4
	RDT 5	55.2 ± 0.8	37.9 ± 1.8	5.1 ± 0.5	0.9 ± 0.7	0.9 ± 0.5
24 h	Control	54.5 ± 1.1	39.0 ± 1.1	4.9 ± 1.1	0.7 ± 0.5	0.9 ± 0.6
	RDT 1	54.8 ± 0.7	38.8 ± 0.7	5.0 ± 0.6	0.9 ± 0.7	0.5 ± 0.4
	RDT 5	55.0 ± 0.9	38.8 ± 1.0	4.8 ± 1.2	0.8 ± 0.6	0.6 ± 0.3
96 h	Control	54.7 ± 0.8	39.2 ± 0.9	4.8 ± 0.9	0.8 ± 0.4	0.5 ± 0.4
	RDT 1	54.1 ± 0.4	39.8 ± 0.8	4.8 ± 0.7	0.9 ± 0.6	0.4 ± 0.2
	RDT 5	60.1 ± 0.5[*]	34.9 ± 0.4 [*]	4.0 ± 0.5	0.4 ± 0.3	0.6 ± 0.3

Harabawy and İbrahim (2014) studied hematological parameters to determine the toxic effects of two sublethal carbofuran pesticide concentrations in African catfish (*Clarias gariepinus*) exposed to doses of 0.16 and 0.49 mg / L for 35 days. Carbofuran used as insecticide, acaricide and nematicide in agricultural areas, it is a widely used pesticide with a wide range of effects against many pests. Also, carbofuran has very high toxic effects on fish, invertebrates, birds and mammalian (Otieno et al., 2010). They reported that, a decrease in Hct (hematocrit), RBC (erythrocyte) count, Hb (hemoglobin) concentration, MCHC (mean corpuscular hemoglobin concentration) levels, and an increase MCH (mean corpuscular hemoglobin), MCV

(mean corpuscular volume) levels. Besides, there was an increase in WBC (white blood cell), neutrophil, eosinophil, basophil and monocyte levels from non-specific immune parameters while a decrease in lymphocyte level was detected. Hematological and non-specific immune parameters are indicated Table 9. According to current results, they expressed that *Clarias gariepinus* is a good bioindicator to reflect that determines the toxicity of carbofuran that might be released into aquatic ecosystems.

Ali et al., (2018) investigated hematological parameters to determine the toxic effect of atrazine on snow carp (*Schizothorax plagiostomus*) which an economically important fish species. Atrazine is a herbicide and it is widely used by farmers for weed control (Graymore et al., 2001). They exposed to fish 50, 100 and 150 mg/L of atrazine for 24, 48 and 72 hours respectively. In the study, RBC, Hb, MCH and MCHC values were found significant decline compared to the control group, whereas neutrophil and MCV increased. The lymphocyte count showed insignificant changes in all groups, Table 10. They said that atrazine affects hematological parameters in *Schizothorax plagiostomus* depending on dose and time, therefore, in areas close to natural water sources, farmers are recommended to use a minimum level of atrazine.

Table 9: Hematological and Non-Specific Immune Parameters in African Catfish (*Clarias gariepinus*) Exposed to Carbofuran (Harabawy and İbrahim, 2014).

Parameters	Control	T1=0.16 mg/L	T2=0.49 mg/L
RBCs (×10^6/ml)	2.537±0.05A	2.177±0.05B	1.517±0.08C
Hb (Mg/dl)	9.907±0.15A	7.947±0.17B	6.167±0.11C
HCT (%)	24.167±0.33A	20.637±0.45B	17.837±0.38C
MCV (mm^3)	134.287±3.16A	139.887±2.24B	143.327±0.99C
MCH (Pg)	48.087±0.98A	51.237±0.29B	56.007±0.624C
MCHC (%)	42.697±0.30A	40.827±0.75A	37.247±1.02B
WBCs (×10^3/ml)	27.567±1.65A	38.977±3.32B	52.137±8.67C
Neutrophil (%)	55.327±4.65A	60.787±4.98B	66.787±5.22C
Eosenophil (%)	3.767±1.32A	4.107±0.34B	5.627±0.87C
Basophil (%)	2.437±0.61A	3.957±0.93B	5.027±0.65C
Monocyte (%)	2.317±0.25A	2.377±0.46B	2.407±0.34C
Lymphocyte (%)	36.187±2.37A	28.807±2.13B	20.187±1.65C

Table 10: Hematological Parameters in *Schizothorax plagiostomus* Exposed to Different Atrazine Concentrations (Ali et al., 2018)

Exposure hours	Parameters	Atrazine dose (mg/l±SE)			
		Control	50	100	150
24	Hb	9.4 ±0.2	7.4 ±0.3	6.6 ±0.4	6.3 ±0.3
	RBCs	2.7 ±0.1	2.3 ±0.2	2 ±0.2	1.7 ±0.1
	WBCs	5.2 ±0.4	5.6 ±0.3	7.5 ±0.5	7 ±0.6
	Neutrophil	29.5 ±0.6	35.8 ±0.9	40.2 ±0.9	43.5 ±1.9
	Lymphocytes	51.9 ±2.3	52.7 ±2	56.3 ±1.2	52.4 ±1.7
	MCV	140.6 ±2	147.7 ±1.5	153 ±1.6	162.5 ±1.8
	MCH	43.1 ±1.1	38.7 ±0.5	35.5 ±1	32 ±1.8
	MCHC	30 ±0.6	30 ±1.2	25.1 ±1.3	20.9 ±0.8
	Total proteins	5.4 ±0.2	4.7 ±0.3	4±0.2	3.3 ±0.1
48	Hb	10.2 ±0.6	5.9 ±0.3	5.4 ±0.6	4.5 ±0.4
	RBCs	2.5 ±0.2	2.0 ±0.3	1.8 ±0.2	1.6 ±0.3
	WBCs	5 ±0.4	7.3 ±0.7	8.8 ±0.4	10.5 ±0.2
	Neutrophil	29.7 ±1.3	42.5 ±2.1	50.0 ±1.3	55.3 ±2.3
	Lymphocytes	45.1 ±2.2	58.9 ±1.1	48.9 ±1.1	47.7 ±1.1
	MCV	139.8 ±1.5	158.0 ±1.3	165.7 ±1.1	170.8 ±1.0
	MCH	40.4 ±1	29.8 ±0.5	25.3 ±1.6	20.1 ±1.9
	MCHC	30.6 ±0.6	25.0 ±1.2	19.9 ±0.7	19.0 ±0.8
	Total proteins	5.1 ±0.2	3.5 ±0.2	3.0 ±0.1	2.8 ±0.1
72	Hb	8.0 ±0.2	3.8 ±0.3	3.4 ±0.4	3.5 ±0.5
	RBCs	2.8 ±0.2	1.3 ±0.2	1.1 ±0.1	1.4 ±0.2
	WBCs	5.1 ±0.4	11.0 ±0.5	13.2 ±0.7	16.0 ±0.8
	Neutrophil	33.1 ±2.2	50.4 ±2.8	60.1 ±2.0	68.6 ±2.4
	Lymphocytes	45.2 ±1.2	48.3 ±2.0	48.4 ±0.7	43.8 ±1.0
	MCV	140.5 ±0.9	162.9 ±1.6	167.5 ±1.3	174.7 ±1.2
	MCH	40.8 ±1.7	29.6 ±1.4	20.9 ±1.1	17.0 ±1.2
	MCHC	32.4 ±1.3	20.2 ±0.4	16.7 ±0.3	13.6 ±0.8
	Total proteins	5.6 ±0.2	2.7 ±0.2	1.6 ±0.2	0.8 ±0.1

CONCLUSION

Pesticides used in agricultural struggle can destroy detrimental organisms and can cause an increase in crops, as well as causing damage to non-target creatures (Ahmet et al., 1998). Pesticides can affect hematological parameters and the leukocyte system in different ways in fish. Hematological parameters in fish are used as a health indicator to determine the functional status of fish exposed to pesticides (Upadhyay et al., 2014). Also, the examination of hematological parameters in fish as a result of pesticide exposure may provide an early sign to determine the acute toxic effect of the pesticide and their effects on the aquatic environment. Therefore, according to the current research results, it can be said that the stress caused by various pesticides in aquatic environments creates changes in hematological parameters, affect the immune system, and makes the fish undefended to diseases.

REFERENCES

Ahmed, M. T., Ismail, S. M., & Mabrouk, S. S. (1998). Residues of some chlorinated hydrocarbon pesticides in rain water, soil and ground water, and their influence on some soil microorganisms. *Environment International*, *24*(5-6), 665-670.

Ali, F., Khan, M. Q., Anjum, M. Z., & Khattak, I. (2018). Toxic effect of atrazine herbicide on the hematological indices of snow carp (Schizothorax plagiostomus): an indigenous fish species of economic importance. *Fresenius Environ Bull*, *27*, 3075-3080.

Brown, H. M. (1990). Mode of action, crop selectivity, and soil relations of the sulfonylurea herbicides. *Pesticide Science*, *29*(3), 263-281.

Çelik, E. S., Kaya, H., & Yılmaz, S. (2012). Effects of phosalone on mineral contents and spinal deformities in common carp (*Cyprinus carpio*, L. 1758). *Turkish Journal of Fisheries and Aquatic Sciences*, 12(2), 259-264.

Fatima, M., Mandiki, S. N. M., Douxfils, J., Silvestre, F., Coppe, P., & Kestemont, P. (2007). Combined effects of herbicides on biomarkers reflecting immune–endocrine interactions in goldfish: immune and antioxidant effects. *Aquatic Toxicology*, 81(2), 159-167.

Fazio, F., Faggio, C., Marafioti, S., Torre, A., Sanfilippo, M., & Piccione, G. (2013). Effect of water quality on hematological and biochemical parameters of *Gobius niger* caught in Faro lake (Sicily). *Iranian Journal of Fisheries Sciences*, 12(1), 219-231.

Girón-Pérez, M. I., Barcelos-Garcia, R., Vidal-Chavez, Z. G., Romero-Bañuelos, C. A., & Robledo-Marenco, M. L. (2006). Effect of chlorpyrifos on the hematology and phagocytic activity of Nile tilapia cells (*Oreochromis niloticus*). *Toxicology mechanisms and methods*, 16(9), 495-499.

Graymore, M., Stagnitti, F., & Allinson, G. (2001). Impacts of atrazine in aquatic ecosystems. *Environment international*, *26*(7-8), 483-495.

Harabawy, A. S., & Ibrahim, A. T. A. (2014). Sublethal toxicity of carbofuran pesticide on the African catfish *Clarias gariepinus* (Burchell, 1822): hematological, biochemical and cytogenetic response. *Ecotoxicology and environmental safety*, 103, 61-67.

Iwafune, T., Yokoyama, A., Nagai, T., & Horio, T. (2011). Evaluation of the risk of mixtures of paddy insecticides and their transformation products to aquatic organisms in the Sakura River, Japan. *Environmental toxicology and chemistry*, 30(8), 1834-1842.

Jaeger, J. W., Carlson, I. H., & Porter, W. P. (1999). Endocrine, immune, and behavioral effects of aldicarb (carbamate), atrazine (triazine) and nitrate (fertilizer) mixtures at groundwater concentrations. *Toxicology and Industrial health*, 15(1-2), 133-151.

Jayaprakash, C., & Shettu, N. (2013). Changes in the hematology of the freshwater fish, *Channa punctatus* (Bloch) exposed to the toxicity of deltamethrin. *Journal of Chemical and Pharmaceutical Research*, 5(6), 178-183.

Jobling, S., & Tyler, C. R. (2003). Endocrine disruption, parasites and pollutants in wild freshwater fish. *Parasitology*, 126(7), S103-S107.

Kaya, H., Çelik, E. Ş., Yılmaz, S., Tulgar, A., Akbulut, M., & Demir, N. (2015). Hematological, serum biochemical, and immunological responses in common carp (*Cyprinus carpio*) exposed to phosalone. *Comparative Clinical Pathology*, 24(3), 497-507.

Luskova, V., Svoboda, M., & Kolářová, J. (2002). Effect of diazinon on blood plasma biochemistry in carp (*Cyprinus carpio* L.). *Acta Veterinaria Brno*, 71(1), 117-123.

Mittal, P. K., Adak, T., & Sharma, V. P. (1994). Comparative toxicity of certain mosquitocidal compounds to larvivorous fish, Poecilia reticulata. *Indian journal of malariology*, 31(2), 43-47.

Modesto, K. A., & Martinez, C. B. (2010). Effects of Roundup Transorb on fish: hematology, antioxidant defenses and acetylcholinesterase activity. *Chemosphere*, *81*(6), 781-787.

Moreno, N. C., Sofia, S. H., & Martinez, C. B. (2014). Genotoxic effects of the herbicide Roundup Transorb® and its active ingredient glyphosate on the fish Prochilodus lineatus. *Environmental toxicology and pharmacology*, *37*(1), 448-454.

Nouri, J., Arjomandi, R., & Bayat, H. (2000). Ecological investigation of application of pesticides in rice fields. *Iranian Journal of Public Health*, 29(1-4), 137-146.

Otieno, P. O., Lalah, J. O., Virani, M., Jondiko, I. O., & Schramm, K. W. (2010). Carbofuran and its toxic metabolites provide forensic evidence for Furadan exposure in vultures (Gyps africanus) in Kenya. *Bulletin of environmental contamination and toxicology*, *84*(5), 536-544.

Ramesh, M., & Saravanan, M. (2008). Haematological and biochemical responses in a freshwater fish *Cyprinus carpio* exposed to chlorpyrifos. *International Journal of Integrative Biology*, 3(1), 80-83.

Sparling, D. W., Fellers, G. M., & McConnell, L. L. (2001). Pesticides and amphibian population declines in California, USA. *Environmental Toxicology and Chemistry*, 20(7), 1591-1595.

Saravanan, M., Kumar, K. P., & Ramesh, M. (2011). Haematological and biochemical responses of freshwater teleost fish *Cyprinus carpio* (Actinopterygii: Cypriniformes) during acute and chronic sublethal exposure to lindane. *Pesticide Biochemistry and Physiology*, 100(3), 206-211.

Talebi, K. (1998). Diazinon residues in the basins of Anzali Lagoon, *Iran. Bulletin of environmental contamination and toxicology*, 61(4), 477-483.

Tomlin, C. D. (2009). *The pesticide manual: A world compendium* (No. Ed. 15). British Crop Production Council.

Upadhyay, A., Pandya, P., & Parikh, P. (2014). Acute exposure of pyrazosulfuron ethyl induced haematological and blood biochemical changes in the freshwater teleost fish Oreochromis mossambicus. *International Journal of Advanced Research in Biological Sciences*, *1*(2), 79-86.

Van Der Kraak, G. J., Hosmer, A. J., Hanson, M. L., Kloas, W., & Solomon, K. R. (2014). Effects of atrazine in fish, amphibians, and reptiles: An analysis based on quantitative weight of evidence. *Critical reviews in toxicology*, 44(sup5), 1-66.

Van Vuren, J. H. (1986). The effects of toxicants on the haematology of *Labeo umbratus* (Teleostei: Cyprinidae). *Comparative biochemistry and physiology - Part C: Toxicology & pharmacology*, 83(1), 155.

Velisek, J., Sudova, E., Machova, J., & Svobodova, Z. (2010). Effects of sub-chronic exposure to terbutryn in common carp (*Cyprinus carpio* L.). *Ecotoxicology and Environmental Safety*, 73(3), 384-390.

Zutshi, B., Prasad, S. R., & Nagaraja, R. (2010). Alteration in hematology of *Labeo rohita* under stress of pollution from Lakes of Bangalore, Karnataka, India. *Environmental monitoring and assessment*, 168(1-4), 11-19.

214 CURRENT STUDIES AT POSITIVE SCIENCES

CHAPTER 11

FOOD COLORANTS AND THEIR TOXIC EFFECTS

Res. Asst. Salih DİKİLİTAŞ[1], Assoc. Prof. Dr. Özlem AKSOY[2]

[1] Biology, Kocaeli University, Kocaeli, Turkey. salih.dikilitas@kocaeli.edu.tr
[2] Biology, Kocaeli University, Kocaeli ,Turkey, ozlem.aksoy@kocaeli.edu.tr

INTRODUCTION

Food colorants are type of food additives which are used in food industry. These synthetic colorants have a wide range of usage because of their properties like, stability, uniformity and low cost. Synthetic food colorants have been used in food products to give an attractive appearance to them. They are used in several forms such as gels, powders and liquid food products. The color, flavor, texture and nutritive value are the main criteria for the quality of food for consumers, so the use of synthetic food colorants has recently increased considerably. It has been known that most of these food colorants have properties similar to the mutagenic chemicals and they are originally derived from coal tar, containing the azo group. There are many studies about the cytotoxic and genotoxic effects of food colorants such as mitotic index reduction, chromosomal aberration, DNA fragmentation, morphological abnormalities in spermatozoids. Most of these studies report that these colorants have cytotoxic and genotoxic effects on organisms after long-term and repeated use. It can be suggested that the use of these synthetic food colorants should be limited or banned and the use of the natural food colorants obtained from plants should be increased. In this review, it is aimed to investigate the usage of food colors and their effects on organisms.

1. FOOD COLORANTS

Food Protection Committee of the Food and Nutrition Board, defined the food additives as "*a substance or mixture of substances, other than a basic foodstuff, which is present in a food as a result of any aspect of production, processing, storage, or packaging''*. The use of food additives has become inevitable because of their great importance for long-term preservation of foods. In present, more than 2500 additives are used in food products to protect their properties or to extend shelf life, but some of these food additives have toxic effects on organisms (Pandey and Upadhyay, 2007; Türkoğlu, 2009) and so they have been banned in all parts of the world or only in some countries throughout the years. (Branen *et al.*, 2001). For instance, tartrazine was banned in the United Kingdom, Quinoline yellow was banned in United States and amaranth was banned in Canada. (Stevens *et al.*, 2013).

Acceptable daily intake (ADI) value was determined for each food additives by FAO/WHO Expert Committee on Food Additives (JECFA, 1981).

ADI which expressed on the basis of body weight, can be defined as the amount of additives that can be taken for a lifetime without a significant health risk (WHO, 1987). Food additives can be divided into four groups based on safety data (Table 1) (Branen *et al.*, 2001)

Table 1. Toxicological Classification of Food Additives Based on Available Safety Data (Branen *et al.*, 2001)

Group A	Additives with an established ADI value
Group B	Additives generally considered safe
Group C	Additives with no sufficent data
Group D	Flavoring components
Group E	Natural additives with no scientific safety data or with insufficient data

Three categories of additive intake was suggested by Joint FAO/WHO Food and Animal Feed Contamination Monitoring Programme (JFCMP);

- Additives below 30% of the ADI are accepted safe for whole population.
- Additives between 30 % and 100 % of the ADI indicate concern for the safety of extreme consumers, children in particular.
- Additives greater than 100% of the ADI are accepted unsafe for the whole population.

Food additives can be classified into six major groups: coloring agents, preservatives, texturizing agents, flavoring agents, nutritional additives and miscellaneous additives.

Food colorants are used to color the drinks and foods and to strengthen the original color or to give the lost color of the product during the manufacturing process (Mekkawy, Ali and El-Zawahry, 1998; Frick,

2003). From jellies to jams, from drinks to desserts, food colorants are used in many food products. It is reported that more than 800,000 tons of dyestuffs are produced annually and 60-70 % of these are azo dyes (Anliker, 1977; Combes and Haveland-Smith, 1982). An international numbering system developed by Codex Alimentarius Commission (2001) for food additives based on ''E'' system. All of the colorants have ''E'' codes between E100 and E180, which are used in European Union and Switzerland. Food colorants with E numbers listed in Table 2 (*EU Approved additives and E Numbers*, 2018).

Table 2. E Numbers for colorants (*EU Approved additives and E Numbers*, 2018)

Codes	Names	Color	Natural or Nature Identical	Status (Approved in)
E100	Curcumin	Yellow-orange	Yes	EU and US.
E101i	Riboflavin	Yellow-orange	Yes	EU and US.
E101ii	Riboflavin-5'-phosphate	Yellow-orange	Yes	EU.
E102	Tartrazine	Lemon yellow		EU and US.
E104	Quinoline yellow	Dull or grenish yellow		EU.
E110	Sunset Yellow FCF; Orange Yellow S	Yellow-orange		EU and US.

E120	Cochineal; Carminic acid; Carmines	Crimson	Yes	EU and US.
E122	Azorubine;Carmoisine	Red to maroon		EU.
E123	Amaranth	Dark red		EU.
E124	Ponceau 4R; Cochineal red A	Red		EU.
E127	Erythrosine	Red		EU and US.
E129	Allura Red AC	Red		EU and US.
E131	Patent Blue V	Dark blue		EU.
E132	Indigotine	Indigo		EU and US.
E133	Brilliant Blue FCF	Reddish blue		EU and US.
E140	Chlorophylls and chlorophyllins	Green	Yes	EU.
E141	Copper complexes of chlorophyll and chlorophyllins	Green	Yes	EU and US.
E142	Green S	Green		EU.
E150a	Plain caramel	Brown	Yes	EU and US.
E150b	Caustic sulphite caramel	Brown		EU and US.
E150c	Ammonia caramel	Brown		EU and US.
E150d	Sulphite ammonia caramel	Brown		US.
E151	Brilliant Black BN; Black PN	Black		EU.
E153	Vegetable carbon	Black	Yes	EU.
E155	Brown HT	Brown		EU.
E160a	Carotenes	Yellow-orange to brown	Yes	EU.

E160b	Annatto; Bixin; Norbixin	Orange	Yes	EU and US.
E160c	Paprika extract; Capsanthian; Capsorubin	Red	Yes	EU and US.
E160d	Lycopene	Bright to deep red	Yes	EU and US.
E160e	Beta-apo-8'-carotenal (C30)	Orange-red to yellow	Yes	EU and US.
E161b	Lutein	Orange-red to yellow	Yes	EU.
E161g	Canthaxanthin	Violet	Yes	EU and US.
E162	Beetroot Red; Betanin	Red	Yes	EU and US.
E163	Anthocyanins	Red, green and purple ranges	Yes	EU.
E170	Calcium carbonate	White		EU.
E171	Titanium dioxide	White		EU and US.
E172	Iron oxides and hydroxides	Brown		EU and US.
E173	Aluminium	Silver to grey		EU.
E174	Silver	Silver		EU.
E175	Gold	Gold		EU.
E180	Litholrubine BK	Red		EU.

In general, food colorants are classified into two groups; synthetic and natural colorants. Natural colorants are extracted from plant, insect or fungi. However, these colorants have some disadvantages like easy degradation, high cost, sensitivity to pH, light and temperature. Unlike the natural colorants, synthetic colorants are more reliable and economic. Synthetic colorants have important characteristics like high

stability to pH, oxygen, light, color uniformity, low cost and less microbiological contamination (Llamas *et al.*, 2009; Wu *et al.*, 2013).

Synthetic colorants are basicly included as azo, indigotine triphenylmethane, quinolone and xanthene colorants. Azo colorants which contained azo groups (-N=N-) is the largest group of colorants. An approximately 65% of azo colorants are used as food colorants (Rebane *et al.*, 2010).

It is reported that, the amounts of AFCs (Artificial Food Colorants) certified in the United States has increased fivefold, from 12 to 62 mg/capita/day from 1955 to 2010 (Figure 1) (Stevens *et al.*, 2013).
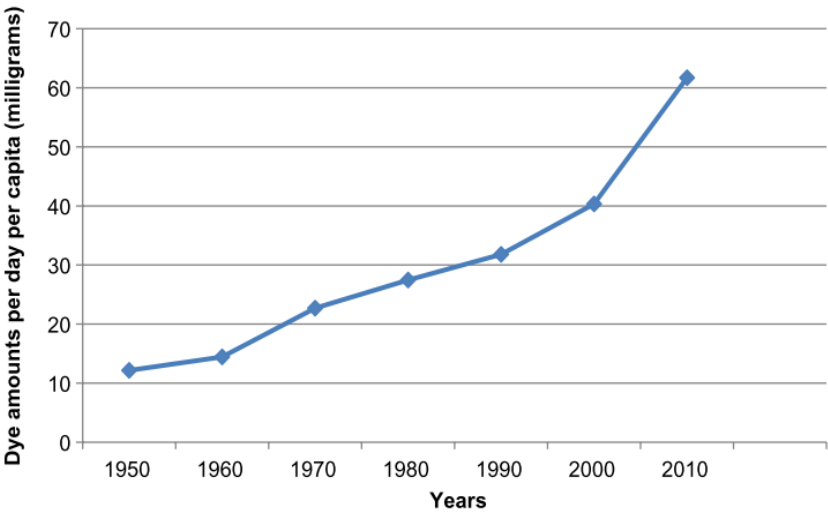

Figure 1 Per Capita Per Day Certification of Food Dyes (in mg) Between 1950 and 2010 (Stevens et al., 2013)

These dyes and their breakdown products such as arylamines and free radicals which are released into the environment, have toxic,

carcinogenic and mutagenic effects on humans and aquatic life (Spadaro, Gold and Renganathan, 1992; Chung, 2000; Pinheiro, Touraud and Thomas, 2004; Seesuriyachan *et al.*, 2007; Mpountoukas *et al.*, 2010). Furthermore, wastewater from plants are applied to agricultural fields and this may result in considerable concentrations of colorants in soils (Zhou, 2001), thus fertility of the soil will be reduced (Topac-Sağban *et al.*, 2010).

2. LITERATURE

Recently there has been an increasing atention to toxicity of food additives, especially to azo-dyes. Azo dyes are the most widely used group of food colorants. Azoreduction of these group of dyes results into carcinogenic metabolites by intestinal microbiota, thereby the use of these dyes has been limited (Feng, Cerniglia and Chen, 2012).

Al-Shabib *et al.*, (2017) investigated the effects of tartrazine on myoglobin protein at the pHs 2.0 and 7.4. Several spectroscopic techniques (Rayleigh light scattering (RLS), Congo Red, turbidity, intrinsic fluorescence, and far-UV CD) and microscopy techniques like atomic force microscopy (AFM) and transmission electron microscopy (TEM) was used to characterize the tartrazine-induced aggregation in myoglobin. According to RLS results, the higher concentrations resulted to formation of bigger size aggregates in myoglobin at pH 2.0. In turbidity measurement, the myoglobin-solvent interaction was disturbed, and tartrazine-myoglobin interaction increased which ultimately led to aggregation in myoglobin. It is concluded that

tartrazine resulted to stimulation of amorphous aggregation in myoglobin at pH 2.0.

Sasaki *et al.* (2002) investigated the effect of tartrazine in model mice and concluded that tartrazine directly affected the nuclear DNA migration in vivo.

In a study conducted by Mpountoukas *et al.*, (2010), in which effects of tartrazine, erythrosine and amaranth on human peripheral blood cells (HPBC) was investigated. 0.02-8 mmol/L$^-$1 of food colorants were used and their cytotoxic, genotoxic and cytostatic potential was tested. According to results, Amaranth showed a genotoxic effect in all concentrations that may lead to break on chromosomes. Amaranth lead to cytostaticity at the highest concentrations (4-8 mmol/L$^-$1) and strong positive correlation was found between mitotic index and proliferation rate index.

Dikilitas and Aksoy (2018) investigated the effects of carmoisine and sunset yellow on *Zea mays* and reported that high doses of carmoisine and sunset yellow decreases the alfa amylase activity and total chlorophyll content. Also as a result of RAPD analysis, higher polymorphism percentages were observed in the treatment group when compared to the control groups, and it is concluded that they have genotoxic effects on *Zea mays* in high concentrations.

Khan et. al. (2020) investigated the effects of carmoisine on root meristematic cells of *Allium cepa*. They used four different

concentrations (0.25 %, 0.50 %, 0.75 % and 1.0 %) and tested the effects of carmoisine after 24 h and 48 h of exposure period. Some genotoxicity parameters like chromosomal aberrations and mitotic indices studied. It was found that carmoisine led to a significant decrease in mitotic index and also caused different chromosomal aberrations like metaphase stickiness, disorientation at metaphase, anaphase bridge, anaphase stickiness, c-mitosis and chromosome breaks.

Al Reza et. al. (2018) conducted a study to assess the toxic effects and relation to carcinogenicity of carmoisine. Four different doses of carmoisine (0, 4, 200, and 400 mg/kg bw) administered into mice orally for 120 days. Within this study, some parameters including animal body weight, organ weights, were observed and also biochemical, hematological, and molecular parameters were investigated. The body weights of the mice which were administered 200 and 400 mg/kg bw carmoisine, decreased significantly compared to control group. Serum cholesterol level was decreased while other biochemical parameters such as total protein, serum alanine aminotransferase, alkaline phosphatase, aspartate aminotransferase, creatinine, urea, and globulin levels were significantly increased when compared to control. According to RT-PCR results, expression of p53 gene was decreased while PARP and Bcl-x gene was dramatically increased in the liver tissues of mouse which treated with carmoisine. This study revealed that 400 mg/kg bw concentration of carmoisine may led to hepatoxicity and renal failure.

Hashem *et al.*, (2010) investigated the effects of azo colorants in albino rats immunologically. 47 mg/kg synthetic colorants were administratied orally during 4 weeks. All animals are immunostimulated by intra peritoneal injection of sheep RBCs (Red Blood Cells) 10 % after 2 weeks. The percentage of monocytes and neutrophils were significantly reduced.

In another study conducted by Sarikaya, Selvi and Erkoç (2012), potential genotoxicity of amaranth on *Drosophila melanogaster* was investigated with somatic mutation and recombination test (SMART). Positive results were observed with different concentrations of amaranth. The lowest concentration (1 mg/mL) of amaranth lead to formation of small single spots with total multiple wing hair (mwh) and spots but higher concentration (50 mg/mL) of amaranth lead to an increase of the frequency of all mutation types which showes the genotoxic potantials of amaranth.

Mpountoukas *et al.*, (2010) conducted an in vitro study about the genotoxicity and cytotoxicity of tartrazine with human peripheral blood lymphocytes. Sister chromatid exchanges (SCEs) analysis was used to test safety of tartrazine. Moreover, the effects of tartrazine on mitotic index and proliferation rate index were studied. According to the results, it was shown that tartrazine has toxic potential because of its ability to bind directly to DNA and damage human lymphocytes. However, no genotoxic effects were observed at doses of 0.02-8 mM. In contrast to this study, Soares *et al.* (2015), reported that tartrazine showed genotoxicity only at higher doses between 0.25-64.0 mM,

however no cytotoxicity was seen. According to these results, it can be concluded that tartrazine may result carcinogenesis at a very high dose or cumulative.

Tsuda *et al.*, (2001) has been studied the effects of another food colorant, amaranth, on DNA. Amaranth induced by oral administration to male and pregnant mice and effects of this colorant was measured using comet assay. According to the results, it was found that amarant has negative effects in the colon 3h after administration. In another study conducted by Sasaki *et al.* (2002), effects of several food colorants on mouse was investigated. Allura red, amaranth, tartrazine and new coccine starting at 10 mg/kg, dose-related DNA damage was observed in the colon 3 h after administration. Other organs like glandular stomach, urinary bladder, gastrointestinal organ, liver, kidney and lung was effected negatively from different food colorants ranging doses between 10mg/kg-100 mg/kg. In addition to these, Shimada *et al.*, (2010) showed that 10 mg/kg new coccine, allura red and amaranth also induced colon specific DNA damage in mice.

Furthermore, in anorher study effect of quinoline yellow has assessed on the DNA damaging at doses ranging from low 0.5-20 ug mL$^-$1 and reported there has been dose dependent genotoxic effect (Chequer *et al.*, 2015).

Kus and Eroglu, (2015) assessed the cytotoxic and genotoxic effects of brilliant blue and sunset yellow in lymphocyte cell cultures using replication index, mitotic index and mcronucleus assay. The results

showed that replication index and mitotic index were decreased significantly (p<0.05) micronucleus fruquency was increased with increasing concentrations of brilliant blue and sunset yellow. According to the results, brilliant blue and sunset yellow may have genotoxic and cytotoxic potential. Similar results were reported by Chequer *et al.*, (2009). Disperse orange 1 and disperse red 1 increased the micronucleus (MN) frequencies in HepG2 in cells and human lymphocytes in a dose dependent manner.

Mehedi *et al.*, (2013) showed that a significant increase in serum ALT, AST, and alkaline phosphatase activities in 2.5 % tartrazine treated groups in swiss mice. Also, these results are in compatible with those of Aboel-Zahab *et al.*, (1997) who revealed that liver enzymes ALT, alkaline phosphatase and AST levels were increased in rats whose diets were supplemented with chocolate colors A and B.

The same results were also reported by Amin et al. (2010). Within that study, high dose of tartrazine (500 mg/kg bw) was given to rats in their diet for 30 days and resulted significant increase in serum AST, ALT and alkaline phosphatase activities. Similar results were obtained by Mekkawy, Ali and El-Zawahry, (1998) who reported that two doses (low or high doses) of tartrazine and carmoisine lead to a significant increase in serum ALT, AST, and alkaline phosphates activities. Himri *et al.*, (2011) also revealed that the rats which consumed 7.5, 10 mg/kgbw of tartrazine showed a significant increase in serum total protein concentrations compared to control rats. Serum creatinine concentration was also increased significantly and in parallel to dose

concentration, when the rats were exposed to tartrazine for 90 days. El-Wahab and Moram, (2013) investigated the effects of food colorants on male rats and reported a considerable increase in serum AST, ALP, ALT activities and total bilirubin for all groups treated with synthetic colorants compared with the control group. Furthermore, a significant increase was observed in creatinine, serum urea, albumin, and total protein in all of the treated groups when compared with the control group. GSH content and SOD activities in blood and the liver were also reduced significantly compared with the control. Helal, Zaahkouk and Mekkawy, (2000) tested the effects of carmine and sunset yellow and showed that total serum protein was significantly decreased in treated groups after 30 days of treatment. In order to test the oral administration of carmine and sunset yellow on liver functions, enzyme levels were investigated. It is revealed that remarkable increase in the serum AST level in all the treated groups after 30 days of treatment.

Various doses of azorubine were administirated orally to rats for 30 days, and the effects of this food colorant were investigated on reproductive organs and hormones. Reproductive hormone levels like follicular stimulation hormone, luteinizing hormone, estrogen hormone and progesterone hormone, were decreased significantly ($P<0.05$) in groups of rats treated with 5, 10 and 20 mg/kg doses of azorubine when compared to control group. Additionally, 20 mg/kg doses of treatment resulted immature Graffian follicle with many atretic and shrunk follicles. According to results, it can be concluded that azorubine led to

hormonal disturbances, infertilities and irregular estrus cycle in the female rats (Muhamad Amin, F.A.S. 2018).

Iheanyichukwu et al (2019) investigated the effects of tartrazine and erythrosine on cholesterol, serum glucose and triglycerides. They used wistar rats and administered 5, 10, 15 and 20 mg/kgbwt erythrosine and tartrazine for 21 days. According to results, it was concluded that there was a significant increase for glucose level in rats which administired 15 and 20 mg/kgbwt colorants when compared to control group. Also higher chlosterol concentration was observed in the rats which were administired 15 mg/kgbwt colorants. This result revealed that colorants increased cholesterol and glucose level in a dose-dependent manner.

Food colorants can show antimitotic properties and lead to chromosomal aberrations. Ishidate, Sofuni and Yoshikawa (1981) exposed Chinese hamster cells to 2.5 mg/ml concentration of tartrazine and observed that tartrazine can induce chromosomal aberrations. In another study conducted by Patterson and Butler (1982), tartrazine concentrations ranging from 5-20 mg/ml induced chromosomal aberrations in Muntiacus muntjac fibroblasts when compared to the control. Also, Giri *et al.*, (1990) showed that chronic exposure to high doses of the tartrazine induced SCE and chromosomal aberrations in bone marrow cells of mouse and rat.

Effects of tartrazine was tested in human peripheral blood cells for 72 h between 0.02 to 8 mM concentrations. It is reported that 4 and 8 mM concentrations of tartrazine had a significant toxic effects on the

chromesemes. Moreover, 4 and 8 mM concentrations of tartrazine resulted to a significant delay in cell division and decrase in mitotic index compared to control group (Mpountoukas *et al.*, 2010).

Similarly, tartrazine led to significant damage in human lymphocytes at the concentrations of 0.25-64 mM. DNA damage was dose-related so higher concentrations resulted to higher effect. It is also reported that tartrazine had capable of strong binding to linear double stranded DNA (Soares *et al.*, (2015).

Prajitha and Thoppil, (2016) investigated the cytotoxicity of lemon yellow and orange red on *Allium cepa*. They concluded that these food colorants led to formation of giant cells. Furthermore, number of giant cells were increased with the concentration and duration of treatment of the colorants. It has been shown that these giant cells contain aberrations like binucleate and bridged condition, double nuclear lesion, nuclear lesion, nuclear erosion, unequal condensation in early metaphase and macro and microcell formation. Treatment of *A. cepa* root meristem with these food colorant solutions resulted to decrease in mitotic index. Mitotic index was found to be higher than negative and lower than positive control. Mitotic index values were inversely proportional to duration of treatment and concentration of colorants. Motta el al., (2019), studied the effects of cochineal red, ponceau red, tartrazine and blue patent on the three different organisms namely *Danio rerio*, *Artemia salina* and *Cucumus sativus*. All of the colorants caused different physiological, biochemical and developmental effects. Germination rate of *C. sativus* was increased by tartrazine while

root/shoot ratio was ~20 % reduced by tartrazine, cochineal red and ponceau red. Total chlorophylls and carotenoids contents were increased between 15-20 % by cochineal red and blue patent while total antioxidant activity was reduced nearly 25 % by all of the colorants. Tartrazine, ponceau red and blue patent increased up to 50 % the mortality and low mobility of *A. salina* nauplii, and cochineal red altered significantly the nauplii phototactic response. Tartrazine, ponceau red and blue patent increased hatching percentages at 48 h up to two to four-fold on *Danio rerio* and caused to developmental defects were observed in the 20 % of embryos.

Joshi and Kathi (2018), investigated the effects of tartrazine on the embryonic development of *Danio rerio*. They concluded that tartrazine is not teratogenic up to a dose level of 10 mM concentration. However, between 20 to 30 mM of tartrazine concentration, caused, cardiac and yolk sac edema and tail bending in 50% of larvae. The embryos which exposed to tartrazine between 30 to 50 mM of concentration, resulted to decline of heart rates with the above mentioned deformities and resulted to mortality within 96 to 144 hours postfertilization. Concentaration of tartrazine between the 75-100 mM caused to developmental cease completely. Similar results were obtained the study conducted by Joshi and Kathi (2018) who investigated the effects of sunset yellow on *Danio rerio*. Gupta et al. (2019) also reported similar results who investigated the effects of erythrosine and tartrazine on *Danio rerio*. Additionally, they also reported that both of these

colorants significantly increased SOD activity, and caused to upregulated SOD mRNA transcripts.

Ameur F.Z. et. al. (2020) assessed the effect of tartrazine on the enzymatic activity of lipase, amylase, and proteases after 13 weeks ingestion in Swiss mice. Two different concentrations (0.005 % and 0.05%) of tartrazine and tap water (control group) were treated to mice. According to results, no observed adverse effects on body weight gain and on lipase or amylase activities. However, 0.05 % dose of tartrazine led to a significant decrease in trypsin and chymotrypsin enzymatic activities. According to study, it can be colcluded that excessive consumption of tartrazine may alter the enzymatic activity of proteases and which have deleterious consequences on digestion. Although lower doses of tartrazine do not appear to affect enzymatic activities, high consumption of tartrazine should be strictly controlled, especially in foods consumed by children.

CONCLUSION

Unfortunately, food colorants that are very popular in use today and used in all kinds of pastries, biscuits, ice cream products are not usually obtained from the plants that are named after. Their consumption can cause health problems that are very dangerous for humans, and should be avoided whenever possible. They are made up of chemicals, even though they are called food colorants, it is revealed that they cause many problems in overdose intake. Synthetic colorants are not the only

way to create brightly colored foods; it will be better to use vegetable-based colorants to achieve the same effect.

REFERENCES

Aboel-Zahab, H. (1997). Physiological effects of some synthetic food colouring additives on rats. Bollettino chimico farmaceutico, 136(10), 615–27. Available at: http://www.ncbi.nlm.nih.gov/pubmed/9528169 (Accessed: 30 August 2018).

Al Reza, Md. S. et al. (2018). Study of a common azo food dye in mice model: Toxicity reports and its relation to carcinogenicity. Food Science & Nutrition. 7:667–677.

Al-Shabib, N. A. (2017). Synthetic food additive dye "Tartrazine" triggers amorphous aggregation in cationic myoglobin. International Journal of Biological Macromolecules. Elsevier B.V., 98, 277–286. doi: 10.1016/j. ijbiomac.2017.01.097.

Ameur, F.Z. et. al. (2020). Effect of tartrazine on digestive enzymatic activities: in vivo and in vitro studies. Toxicological Research, 36, 159–166.

Anliker, R. (1977). Color chemistry and the environment. Ecotoxicology and Environmental Safety, Academic Press, 1(2), 211–237. doi: 10.1016/0147-6513(77)90037-9.

Arakawa, H., Ahmad, R. and Naoui, M. (2000). A Comparative Study of Calf Thymus DNA Binding to Cr (III) and Cr (VI) Ions. 275(14), 10150–10153.

Arvin, M. et al., (2013). Spectroscopic and Electrochemical Studies on the Interaction of Carmoisine Food Additive with Native Calf Thymus DNA. Spectroscopy Letters, 46(4), 250–256. doi: 10.1080/00387010.2012.723663.

Basu, A. and Kumar, G. S. (2014). Targeting proteins with toxic Azo dyes: A microcalorimetric characterization of the interaction of the food colorant amaranth with serum proteins. Journal of Agricultural and Food Chemistry,

62, 7955–7962. doi: 10.1021/jf5025278.

Basu, A. and Kumar, G. S. (2015). Binding of carmoisine, a food colorant, with hemoglobin: Spectroscopic and calorimetric studies. Food Research International, Elsevier Ltd, 72, 54–61. doi: 10.1016/j.foodres.2015.03.015.

Basu, A. and Kumar, G. S. (2016). Studies on the interaction of the food colorant tartrazine with double stranded deoxyribonucleic acid. Journal of Biomolecular Structure and Dynamics. Taylor & Francis, 34(5), 935–942. doi: 10.1080/07391102.2015.1057766.

Branen, A. L. et al., (2001). Food Additives. Secon Edit. Edited by A. L. Branen et al. New York: Taylor&Francis. Available at: http://ariefm.lecture.ub. ac.id/files/2012/10/A._Larry_Branen_P._Michael_Davidson_Seppo_SalmiB ookFi.org-FOOD-ADDITIVES.pdf.

Chequer, F. M. D. et al. (2009). The azo dyes Disperse Red 1 and Disperse Orange 1 increase the micronuclei frequencies in human lymphocytes and in HepG2 cells. Mutation Research - Genetic Toxicology and Environmental Mutagenesis, 676(1), 83–86. doi: 10.1016/j.mrgentox.2009.04.004.

Chequer, F. M. D. (2012). Genotoxic and mutagenic effects of erythrosine B, a xanthene food dye, on HepG2 cells. Food and Chemical Toxicology. Elsevier Ltd, 50, 3447–3451. doi: 10.1016/j.fct.2012.07.042.

Chequer, F. M. D. et al. (2015). The cosmetic dye quinoline yellow causes DNA damage in vitro. Mutation Research - Genetic Toxicology and Environmental Mutagenesis, Elsevier Ltd, 777(1), 54–61. doi: 10.1016/j.mrgentox. 2014.11.003.

Chung, K. T. (2000). Mutagenicity and carcinogenicity of aromatic amines metabolically produced from azo dyes. Journal of Environmental Science and Health - Part C, 18(1), 51–74. doi: 10.1080/10590500009373515.

Codex Alimentarius Commission (2001). Class names and the International Numbering System for Food Additives, Codex Alimentarius. doi: 10.1017/CBO9781107415324.004.

Combes, R. D. and Haveland-Smith, R. B. (1982). A review of the genotoxicity of food, drug and cosmetic colours and other azo, triphenylmethane and xanthene dyes. Mutation Research/Reviews in Genetic Toxicology. Elsevier, 98(2), pp. 101–243. doi: 10.1016/0165-1110(82)90015-X.

Dikilitaş, S. and Aksoy Ö. (2018): The genotoxic effects of some food colorants on *Zea mays* L. var. saccharata Sturt, Caryologia, 71(4), 438-445. DOI: 10.1080/00087114.2018.1503494

El-Wahab, H. M. F. A. and Moram, G. S. E. D. (2013). Toxic effects of some synthetic food colorants and/or flavor additives on male rats. Toxicology and Industrial Health, 29(2), 224–232. doi: 10.1177/0748233711433935.

EU Approved additives and E Numbers (2018). Available at: https://www.food.gov.uk/print/pdf/node/847 (Accessed: 25 July 2018).

Feng, J., Cerniglia, C. E. and Chen, H. (2012). Toxicological significance of azo dye metabolism by human intestinal microbiota. Frontiers in Bioscience, (67), 568–586.

Frick, D. (2003). The Coloration of Food', Review of Progress in Coloration and Related Topics, 33, 15–32. doi: 10.1111/j.1478-4408.1973.tb00198.x.

Giri, A. K. et al. (1990). Sister chromatid exchange and chromosome aberrations induced by curcumin and tartrazine on mammalian cells in vivo. Cytobios, 62(249), 111–117. Available at: http://www.ncbi.nlm.nih.gov/pubmed/2209081 (Accessed: 9 August 2018).

Gupta, R. et al. (2019). Toxic Effects of Food Colorants Erythrosine and Tartrazine

on Zebrafish Embryo Development, Current Research in Nutrition and Food Science. 7(3). 876-885

Hashem, M. M. et al. (2010). Immunological studies on Amaranth, Sunset Yellow and Curcumin as food colouring agents in albino rats. Food and Chemical Toxicology. Elsevier Ltd, 48(6), 1581–1586. doi: 10.1016/j.fct.2010.03.028.

Helal, E. G. E., Zaahkouk, S. A. M. and Mekkawy, H. A. (2000). Effect of Some Food Colorants (Synthetic and Natural products) of Young Albino Rats I-Liver and Kidney Functions. The Egyptian Journal of Hospital Medicine. 1, 103–113.

Himri, I. et al. (2011). A 90 day oral toxicity study of tartrazine, asynthetic food dye, in wistar rats. International Journal of Pharmacy and Pharmaceutical Sciences, 3(3). 160–169.

Iheanyichukwu, W., Uwaezuoke, C. A., and Amanda I. (2019). The Effect of Some Synthetic Food Colorants on Selected Biochemical Indices of Male Wistar Rats. European Journal of Nutrition & Food Safety. 10(2). 149-155.

Ishıdate, M. J., Sofuni, T. and Yoshikawa, K. (1981). Chromosomal aberration tests in vitro as a primary screening tool for environmental mutagens and/or carcinogens. in Inui, N., Kuroki, T., and Yamada, M.A. Heidelberger, C. (eds) Mutation, promotion and transformation in vitro . Tokyo: Japan Scientific Societies Press, 95–108. Available at: https://hero.epa.gov/ hero/index.cfm/reference/details/reference_id/9083 (Accessed: 9 August 2018).

JECFA (1981). Evaluation of certain food additives. Geneva.

Joseph, N. and Siril, E. A. (2010). Cytotoxic Evaluation of Annatto (Bixa orellana L.) Dye Compared with Orange Red. Cytologia, 75(2), 163–167. doi: 10.1508/cytologia.75.163.

Joshi, V. and Katti, P. (2018). Developmental Toxicity Assay for Food Additive Tartrazine Using Zebrafish (*Danio rerio*) Embryo Cultures. International Journal of Toxicology, 37(1), 38–44. doi: 10.1177/1091581817735227.

Joshi, V. and Katti, P. (2018). Food colorant Sunset Yellow (E110) intervenes developmental profile of zebrafish (*Danio rerio*). Jounal of Applied Toxicology. 39:571–581.

Kashanian, S. and Zeidali, S. H. (2011). DNA Binding Studies of Tartrazine Food Additive. DNA and Cell Biology, 30(7), 499–505. doi: 10.1089/dna.2010.1181.

Khan, I.S. (2020). Genotoxic effect of two commonly used food dyes metanil yellow and carmoisine using *Allium cepa* L. as indicator. Toxicology Reports. 7, 370–375.

Kus, E. and Eroglu, H. E. (2015). Genotoxic and cytotoxic effects of sunset yellow and brilliant blue, colorant food additives, on human blood lymphocytes. Pakistan Journal of Pharmaceutical Sciences. 28(1).

Llamas, N. E. et al. (2009). Second order advantage in the determination of amaranth, sunset yellow FCF and tartrazine by UV‑vis and multivariate curve resolution-alternating least squares. Analytica Chimica Acta, 655, 38–42. doi: 10.1016/j.aca.2009.10.001.

Ma, Y., Zhang, G. and Pan, J. (2012). Spectroscopic studies of DNA interactions with food colorant indigo carmine with the use of ethidium bromide as a fluorescence probe. Journal of Agricultural and Food Chemistry, 60(43), 10867–10875. doi: 10.1021/jf303698k.

Mehedi, N. et al. (2013). A thirteen week ad libitum administration toxicity study of tartrazine in Swiss mice. 12(28), 4519–4529. doi: 10.5897/AJB2013.12125.

Mekkawy, H. Ali, M. and El-Zawahry, A. (1998). Toxic Effect of Synthetic and Natural Food Dyes on Renal and Hepatic function in Rats. Toxicology Letters. Elsevier Science, 95(1), 155. Available at: https://elibrary.ru/ item.asp?id=39010 (Accessed: 26 July 2018).

Motta C. M. et al. (2019). Effects of four food dyes on development of three model species, *Cucumis sativus, Artemia salina* and *Danio rerio*: Assessment ofpotential risk for the environment. Environmental Pollution. 253. 1126-1135.

Mpountoukas, P. et al. (2010). Cytogenetic evaluation and DNA interaction studies of the food colorants amaranth, erythrosine and tartrazine. Food and Chemical Toxicology. Elsevier Ltd, 48(10), 2934–2944. doi: 10.1016/j.fct.2010.07.030.

Muhamad Amin F. A. S. (2018). Effects of Azorubine food additive on female reproductive organs and hormones in Sprague Dawley rat. The Iraqi Journal of Veterinary Medicine. 42(2):67-72.

Pandey, R. M. and Upadhyay, S. (2007). Impact of Food Additives on Mitotic Chromosomes of Vicia. Caryologia, 60(4), 309–314. doi: 10.1080/00087114.2007.10797952.

Patterson, R. M. and Butler, J. S. (1982). Tartrazine-induced chromosomal aberrations in mammalian cells. Food and chemical toxicology : an international journal published for the British Industrial Biological Research Association, 20(4), pp. 461–465. Available at: http://www.ncbi.nlm.nih.gov /pubmed/6890025 (Accessed: 9 August 2018).

Pinheiro, H. M., Touraud, E. and Thomas, O. (2004). Aromatic amines from azo dye reduction: Status review with emphasis on direct UV spectrophotometric detection in textile industry wastewaters. Dyes and Pigments, 61(2), 121–139. doi: 10.1016/j.dyepig.2003.10.009.

Prajitha, V. and Thoppil, J. E. (2016). Induction of giant cells by the synthetic food colorants viz. lemon yellow and orange red. Cytotechnology. Springer Netherlands, 68(3), 443–450. doi: 10.1007/s10616-014-9797-x.

Rebane, R. et al. (2010). A review of analytical techniques for determination of Sudan I-IV dyes in food matrixes. Journal of Chromatography A. Elsevier B.V., 1217(17), 2747–2757. doi: 10.1016/j.chroma.2010.02.038.

Sarikaya, R., Selvi, M. and Erkoç, F. (2012). Evaluation of potential genotoxicity of five food dyes using the somatic mutation and recombination test. Chemosphere, 88(8), 974–979. doi: 10.1016/j.chemosphere.2012.03.032.

Sasaki, Y. F. et al. (2002). The comet assay with 8 mouse organs: Results with 39 currently used food additives. Mutation Research - Genetic Toxicology and Environmental Mutagenesis, 519(1–2), 103–119. doi: 10.1016/S1383-5718(02)00128-6.

Seesuriyachan, P. et al. (2007). Metabolism of azo dyes by Lactobacillus casei TISTR 1500 and effects of various factors on decolorization. Water Research, 41(5), 985–992. doi: 10.1016/j.watres.2006.12.001.

Shimada, C. et al. (2010). Differential colon DNA damage induced by azo food additives between rats and mice. The Journal of toxicological sciences, 35(4), pp. 547–54. doi: 10.2131/jts.35.547.

Soares, B. M. et al. (2015). Effects on DNA repair in human lymphocytes exposed to the food dye tartrazine yellow. Anticancer Research, 35, 1465–1474.

Spadaro, J. T., Gold, M. H. and Renganathan, V. (1992). Degradation of azo dyes by the lignin-degrading fungus Phanerochaete chrysosporium. Applied and Environmental Microbiology, 58(8), 2397–2401. doi: 0099-2240/92/082397-05$02.00/0.

Stevens, L. J. et al. (2013). Mechanisms of behavioral, atopic, and other reactions to artificial food colors in children. Nutrition Reviews, 71(5), 268–281. doi: 10.1111/nure.12023.

Topac-Sağban, F. O. et al. (2010). Biostimulation of azo dye-contaminated soils by food industry sludge. Soil and Sediment Contamination, 19(4), 436–454. doi: 10.1080/15320383.2010.486055.

Tsuda, S. et al. (2001). DNA damage induced by red food dyes orally administered to pregnant and male mice. Toxicological sciences : an official journal of the Society of Toxicology, 61(1), 92–99. Available at: http://www.ncbi.nlm.nih. gov/pubmed/11294979 (Accessed: 6 August 2018).

Türkoğlu, Ş. (2009). Genotoxic effects of mono- , di- and trisodium phosphate on mitotic activity, DNA content , and nuclear volume in *Allium cepa* L. Caryologia, 62(3), 171–179.

WHO (1987). Principles for the safety assessment of food additives and contaminants in food. Geneva: Geneva : World Health Organization. Available at: http://apps.who.int/iris/handle/10665/37578 (Accessed: 26 July 2018).

Wu, D. et al. (2015). Characterisation of interaction between food colourant allura red AC and human serum albumin: Multispectroscopic analyses and docking simulations. Food Chemistry, 170, 423–429. doi: 10.1016/j.foodchem. 2014.08.088.

Wu, H. et al. (2013). A rapid shaking-based ionic liquid dispersive liquid phase microextraction for the simultaneous determination of six synthetic food colourants in soft drinks, sugar- and gelatin-based confectionery by high-performance liquid chromatography. Food Chemistry. Elsevier Ltd, 141, 182–186. doi: 10.1016/j.foodchem.2013.03.015.

Zhang, G. and Ma, Y. (2013). Mechanistic and conformational studies on the

interaction of food dye amaranth with human serum albumin by multispectroscopic methods', Food Chemistry. Elsevier Ltd, 136(2), 442–448. doi: 10.1016/j.foodchem.2012.09.026.

Zhou, Q. (2001). Chemical pollution and transport of organic dyes in water-soil-crop systems of the Chinese Coast. Bulletin of environmental contamination and toxicology, 66(6), 784–793. Available at: http://www.ncbi.nlm.nih.gov /pubmed/11353382 (Accessed: 6 August 2018).

CHAPTER 12

STRUCTURE AND FUNCTION OF PROTON PUMPS

Res. Asst. Dr. Serap ÇETİNKAYA[1],
Prof. Dr. Ali Fazıl YENİDÜNYA[2]

[1] Department of Molecular Biology and Genetics, Science Faculty, Sivas Cumhuriyet University, Sivas, Turkey, e-mail: serapcetinkaya2012@gmail.com
[2] Department of Molecular Biology and Genetics, Science Faculty, Sivas Cumhuriyet University, Sivas, Turkey, e-mail: alifazilyenidunya@gmail.com

INTRODUCTION

Hydrogen ion transport systems are present in bacterial membrane vesicles, mitochondria, and chloroplasts. It has also been shown in artificial vesicles containing oxidation-reduction enzymes or mitochondria ATPase. In these examples, the pump is electrogenic and the hydrogen ion gradient is indispensable in energy transfer and ion transport (Malonev et al., 1974).

A eukaryotic microorganism *Neurospora crassa* plasma membrane has a transmembrane electric potential. Experimental work on the membrane of this organism has demonstrated the presence of an electrogenic ATPase. The ATPase produces the membrane electric potential, approximately 200mV, generated by ATP hydrolysis. This ATPase also acts as the proton pump. It produces a pH gradient for the functioning of Ca^{+2}/H^+ antiporter (Scarborough, 1977).

The gastric proton pump has been studied for a very long time. In a microsomal fraction, the presence of ATP-dependent H^+ intake has been discovered. This pump performs an electroneutral H^+: K^+ exchange, at the expense of ATP hydrolysis. Therefore, it is not electrogenic (Sachs et al., 1976).

Upon food intake, gastric H^+/K^+-ATPase reduces stomach pH to approximately 1. This high acidity has two main functions: it is necessary for digestion, and it serves a natural barrier for pathogens. It can, on the other hand, also cause serious ulcers, and, surprisingly,

Helicobacter pylori infections are often treated with antibiotics which inhibit the secretion of gastric acid (Sachs et al., 1996).

Pumping H^+ into the pH 1 medium is a particularly difficult task because the pKa of the free carboxyl groups of the enzyme range from 3 to 5. The molecular mechanism underlying the transport of the proton to the stomach is determined by analysing the crystal structures of the gastric H^+/K^+-ATPase at 2.8 Å resolution. Thus, the molecular interaction between potassium-competitive acid inhibitor (P-CAB) and H^+/K^+-ATPase is defined and how H^+/K^+-ATPase pumps the proton into the stomach, even at pH 1, is understood (Wolosin, 1985).

Two hydrogen ions are released in return for two potassium ions at neutral pH. However, theoretically, under acidic conditions, only one proton can be transported and only one K^+ transport is achieved by one ATP hydrolysis (Robon et al., 1982). This discrepancy implied that H^+/K^+-ATPase should have two distinct proton binding sites, having different pKa values (Robon et al., 1982; Abe et al., 2012). The proton binding region should also involve a lysine residue. The pig H^+/K^+-ATPase, used in the crystallography study, had a glutamic acid, Glu820, in the centre of the cation binding region. This glutamate residue was flanked by Asn792, Glu795, and Lys791, and by some other polar amino acids. Mutation studies has suggested that one of the glutamates, (Glu795 or Glu820), was protonated.

In this section, the components of the gastric acid secretion mechanism, the structure and functioning of H^+/K^+-ATPase, the types of α-subunit, kidney H^+/K^+-ATPase, H^+ release and K^+ back absorption, H^+/K^+-

ATPase signal pathways, and the structural features of H^+/K^+-ATPase are introduced. A short pharmacological perspective is also provided.

1. COMPONENTS OF THE GASTRIC ACID SECRETION MECHANISM

The parietal cells in the gastric gland are responsible for the secretion of gastric hydrochloric acid. The release of the acid is regulated by the transfer of the primary proton pump (H^+/K^+-ATPase) from the cytoplasmic tubulovesicles to the apical plasma membrane (Fig. 1). In response to the stimulation of acid secretion, intracellular canaliculi expand and apical microvilli extend, and their number is increased. Tubulovesicles enriched with membrane H^+/K^+-ATPases are then taken into the apical canalicular membrane by fusion. There are a number of proteins in the parietal cell that are involved in the targeting, insertion, and fusion. These include the synaptosomal-associated protein receptor (SNARE) proteins which bind the soluble N-ethylmaleimide sensitive factor, the Rab GTPases, and the secretion-bearing carrier membrane proteins (SCAMPs). When the acid release ends, the parietal cells return to their initial (resting) conformation (Forte and Zhu, 2010; Yao and Forte, 2003; Chalhoun and Goldenring, 1997).
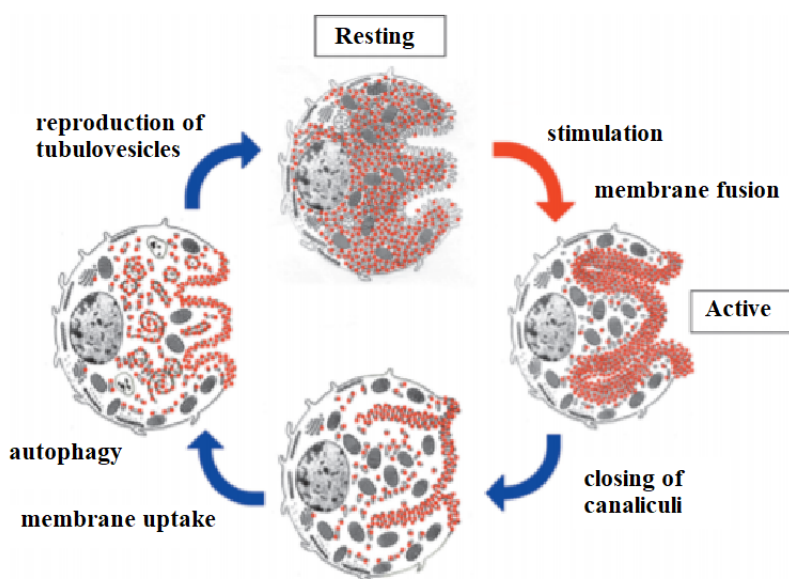
Figure 1. A schematic representation of H^+/K^+-ATPase transfer within a parietal cell (Aoyama and Sawaguchi, 2011).

In the apical membrane, the H^+/K^+-ATPase pump and the chlorine (Cl^-) flow are both required for the production of hydrochloric acid in the glandular lumen. The channels involved may be the intracellular chlorine channel-6 (CLIC-6 or Parkorin), the cystic fibrous transmembrane regulator (CFTR), SLC26A9 (a Cl^-/HCO_3-exchanger), and the K^+-Cl^- cotransporter-4 (KCC4) (Aoyama and Sawaguchi, 2011).

CLIC-6 is mostly found at rest in the cytosol of gastric parietal cells. In the active state, it is transferred to the apical membrane. CFTR is a chlorine channel, regulated by cAMP, and it is predominantly located in the tubulovesicles. In mice, inhibition of this channel with a drug or by mutation significantly reduces the secretion of hydrochloric acid.

This might be taken as an evidence that CFTR participates in the regulation mechanism of normal gastric acid secretion. SLC26A9 is found in the tubulovesicles. Its deletion appears to disrupt gastric hydrochloric acid secretion. KCC4 is found only in the apical canalicular membrane. It has been suggested that KCC4 could act as a K^+ supplier to H^+/K^+-ATPase and that it might be a Cl^- carrier in the basal hydrochloric acid secretion. KCC4 can also act together with other Cl^- channels, CFTR, CLIC-6, and SLC26A9, at elevated acid secretion levels (Aoyama and Sawaguchi, 2011).

Hydrochloric acid secretion also requires the return of potassium ion to the lumen, because the action of H^+/K^+-ATPase has been linked to K^+ intake through the potassium channels of apical canalicular membrane. In the excited state, the apical K^+ channels open up in order to maintain the cytosolic K^+ level, and this provides sufficient substrate for mutual H^+ extrusion by H^+/K^+-ATPase. So far, two candidates have been reported for luminal K^+ channels in gastric parietal cells: the heart K^+ channel KCNQ1 and lumen K^+ channel subunit KCNE2. They both are found in the tubulovesicles and in the apical canalicular membrane (Heitzmann et al., 2004). In mice, their dysfunction in these channels causes gastric hyperplasia, hypochlorhydria and high gastrin concentrations (Lee et al., 2000).

It has been known that translocation of KCNQ1 to apical canalicular membrane occurs independently of H^+/K^+-ATPase translocation. Another luminal K^+ channel candidate has been Kir4.1. Translocation

of this channel to the apical canalicular membrane seems to occur together with H^+/K^+-ATPase (Kaufhold et al., 2008).

In mice, the absence of H^+/K^+-ATPase α- or β-subunit reduces the length and the number of the canalicular microvilli, and it leads to the development of atypical tubulovesicles which are enlarged and shortened. The lack of chlorine carrier SLC26A9, on the other hand, gives rise to the loss of parietal tubulovesicles. Although the tubulovesicular system fully develops in KCNQ1 knockout mice, acid release seems to be compromised. Intracellular canaliculi of mice lacking KCNE2 appear to be vacuolated and the cell is surrounded by less microvilli. In these mice, stomach mucosa hyperplasia has also been reported (Roepke et al., 2006).

1.1. Structure and Functioning of Gastric H^+/K^+-ATPase

Gastric H^+/K^+-ATPase has been included into the family of P2 type ATPases. A mutual property of the family members is their transient high-energy phosphorylated state. Therefore, they are known as P type ATPases. In gastric H^+/K^+-ATPase the alpha chain (~ 100kDa) is the catalytic subunit. It spans across the cell membrane ten times; hence it has ten transmembrane (TM) segments. It also contains an intramembrane carboxylic amino acid cluster. The catalytic α-subunit consists of 1,033 or 1,034 amino acids and shows 98% homology among species. It displays approximately 63% similarity to Na^+/K^+-ATPase and 25% similarity to sarco/endoplasmic reticulum Ca^{+2}-ATPase (SERCA Ca^{+2}-ATPase) (Sweadner and Donnet, 2001). The beta subunit, on the other hand, has only one transmembrane segment,

and its N-terminal faces to the cytoplasm. The extracellular domain of the beta subunit can be glycosylated at its six or seven residues. This modification seems to be necessary for the formation and transport (targeting) of the enzyme assembly. Its precise placement, however, remains to be explored, since a refined crystal structure is as yet not made available for the H^+/K^+-ATPase (Shin et al., 2009).

A refined crystal structure of sarco-endoplasmic reticulum calcium-ATPase (SERCA Ca-ATPase) made it possible to understand the catalytic cycle of P2-type enzymes. The crystal structure of SERCA Ca-ATPase, computer aided homology models, and analysis with region-specific mutations have also provided an understanding of the ionic transport and proton pump inhibition mechanisms of gastric H^+/K^+-ATPase (Melle-Milovanovic et al., 1998).

In the alpha subunit, the intramembrane carboxylic amino acid cluster contains the ion binding domain of the enzyme. Lysine, at position 791, of the fifth transmembrane segment plays a very important role in the extrusion of the hydronium ion (Fig. 2, Yamamato et al., 2019).

The accurate three-dimensional structure of the gastric H^+/K^+-ATPase and its transfer to the apical membrane requires the presence of a second subunit (~ 30kDa). This β-subunit is made up of 291 amino acids and its six, sometimes seven, residues are glycosylated. These *N*-glycosylation sites are thought to be responsible for the adhesion of the enzyme to the membrane (Reuben et al., 1990). The tertiary structure of gastric H^+/K^+-ATPase is formed during its translation in the

endoplasmic reticulum and it is targeted to the apical membrane as oligomers of a heterodimer.

After Mg-ATP binding and phosphorylation, the H^+/K^+-ATPase acid pump assumes either of the two structural states, E1 and E2. In the E2P configuration, the extrusion of the proton at 160mM (pH 0.8) occurs when the lysine at position 791 passes into the ion-binding region. The intake of potassium into the lumen depends on the activation of the potassium and chlorine channels. In the E2P configuration, potassium ions, flowing through the luminal channel, cause the lysine residue to return to its initial position. Subsequent dephosphorylation returns the enzyme to its E1 configuration. The enzyme releases protons at pH 6.1 with a stoichiometry ranging from 1H/1K/ATP to 2H/2K/ATP and retains potassium ion in return (Shin et al., 2009).
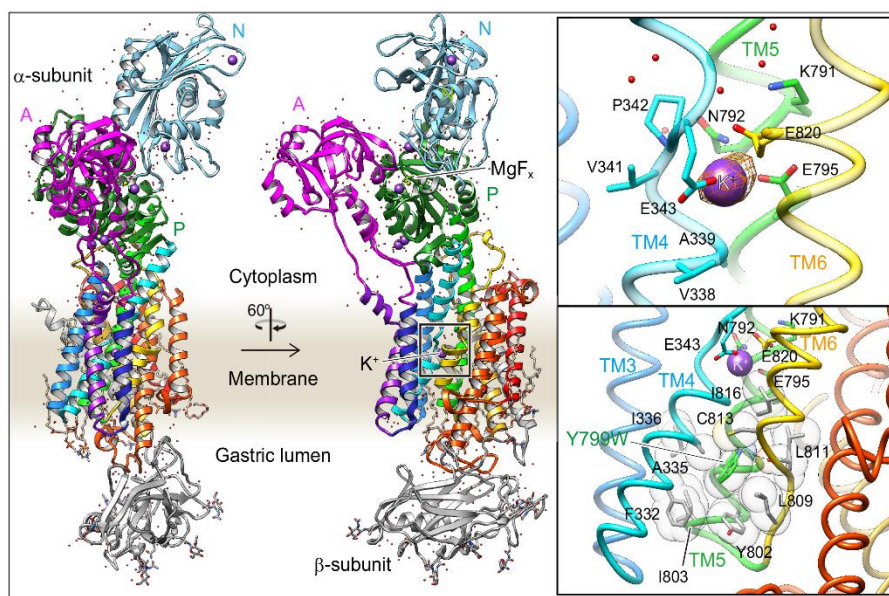

Figure 2. Spatial Organisation of Gastric H^+/K^+-ATPase (Yamamato et al., 2019).

1.2. H$^+$/K$^+$ ATPase α-Gene Products

So far it has been known that four different types of alpha subunits are expressed in mammalian kidneys for H$^+$/K$^+$-ATPase. HK α1, the α-unit of gastric H$^+$/K$^+$-ATPase, was first identified in the rat stomach (Shull and Lingrel, 1986). This ion pump appears to be the main agent of the increased levels of acid in the stomach. Activity analyses, immunohistochemistry, and molecular probes have demonstrated that HK α1 was also expressed in the kidneys (Silver and Soleimanim, 1999). The gene produces a 3,500 bases long transcript and encodes a protein with 1,033 amino acids (Shull and Lingrel, 1986). It has been shown that the HK α2 subunit is the product of another gene, and in some species three alternative transcripts were produced. Although their size and function were similar to HK α1, HK α2 proteins had only 67% homology with HK α1 subunits and were therefore considered as different subtypes. The first transcript, copied from the HK α2 gene, encodes the HK α2a subunit of the column H$^+$/K$^+$-ATPase. HK α2a has initially been found in the rat colon and later shown to be expressed in the rat kidney (Kone and Higham, 1998). A 3,900 bases long transcript produced a protein with 1,036 amino acids, and was the predominant product of the HK α2 gene. Similar transcripts and proteins have been found in the kidneys of many other mammal species, including guinea pigs, humans, mice, and rabbits (Madyanov et al., 1995). In rabbits and rats, the HK α2 gene produced alternative transcripts. A short form of HK α2b mRNA, with unknown function, has also been detected in rats. Another mRNA, copied from the same gene, produced HK α2c protein, lacking the first two amino acids of HK α2a and having additional 63

amino acids at its N-terminal (Codina and Dubose, 2006). The HK α2c subunit has initially been identified in rabbits and later shown to be expressed in rats as well. Studies on the sequence of the first intron in the human HK α2 gene (ATP1AL1) have suggested that there was no alternative transcript, comparable to rabbit- or rat HK α2c.

1.3. Renal H^+/K^+-ATPase

In rabbit kidney, H^+/K^+-ATPase has been found at low K^+ in the collection channels of outer medullary (OMCD). Later on, two renal H^+/K^+-ATPases, containing the HK1 or HK2 catalytic subunit, have been identified. These were HK1 H^+/K^+-ATPase and HK2 H^+/K^+-ATPase. HK2 H^+/K^+-ATPase has been named as non-gastric or colonic H^+/K^+-ATPase, since it was copious in the colon. HK1 H^+/K^+-ATPase appeared to be sensitive to imidazopyridine, 2-methyl-8-(phenylmethoxy) imidazole [1,2a] -pyridine-3-acetonitrile and seminaftoquinoline at micromolar concentrations. Ouabain is a typical Na^+/K^+-ATPase inhibitor at relatively higher concentrations (Wallmark et al., 1987). In some studies, omeprazole sensitive total CO_2 and K^+ flow was recorded as a measure of H+ secretion.

Studies with laboratory animals on the localization of HK1 and HK2 mRNAs and proteins have been available. Consistent data have been found for the localization of renal HK1 and HK2 across mice, rabbits, and rats, while their activity and ion affinity profiles slightly differed. Specifically, HK1 has been detected in the OMCD cells of rats and rabbits. HK2 was expressed in the CD of rats, rabbits and mice (Gumz et al., 2010).

The rabbit and rat CDs displayed K^+ induced ATPase activity. K^+-ATPase activity has been found in rat nephron and it was sensitive to Sch-28080. This has indicated the activity of an HK1 H^+/K^+-ATPase. K^+-dependent ATPase activity on CD has been of two types, type I or type III. The former was sensitive to Sch-28080 and not susceptible to ouabain. It existed in the cortical collection channel (CCD) and in OMCD of the rats, kept on the normal K diet. It had a similar activity to K^+-ATPase from microsomes of the gastric mucosa. Type I and type III activities have also been found in mice and HK1 or HK2 H-K-ATPase-null mice. Type I activity could not be determined in HK1-nul mice, while type III activity was maintained. These data together have indicated that type I activity might require the expression of the HK1 subunit. Type III activity could also not be detected in HK2-nul mice, while type I activity was maintained. These findings might argue that the expression of the HK2 subunit is necessary for type III activity (Gumz et al., 2010).

Another type II K^+-ATPase activity has been detected in the early proximal tubule (PT) and TAL (thick ascending limb) in rats. Its activity was sensitive to Sch-28080 and ouabain, and significantly lessened upon potassium diminution. Type II activity was pharmacologically comparable to that of the type III. However, type II activity was lost due to K^+ exhaustion and it was not compensated by Na^+. Type II activity appeared to be absent in HK1- or HK2-null mice (Gumz et al., 2010).

1.4. The Role of H^+/K^+-ATPase and Acid-Base Fluctuations in H^+ Secretion and K^+ Back-Absorption

H^+/K^+-ATPase takes part in the transport of either of the cations in CD segments. Upon acute acid load, the CD exhibited an important acid secretion mechanism that was sensitive to Sch-28080 or to K^+. Here, H^+/K^+-ATPase has been found in the apical region. This finding might imply that the enzyme functioned both in the absorption of K^+ and in the secretion of H^+ (Campbell et al., 1999).

In isolated CDs, measurements of HCO_3-flow, mediated by H^+/K^+-ATPase, have suggested that the activity of the enzyme could be controlled with barium. Under conditions where potassium was limited, barium prevented the reabsorption of HCO_3 in the CCD. Potassium reabsorption was also inhibited with peritubular barium when potassium was limited. These data have been exploited to produce a model in which H^+/K^+-ATPase cooperated with apical and basolateral channels. This model suggested a synchronized H^+ secretion with the return of K^+ to the apical membrane, and the reabsorption of K^+ by the basolateral K^+ channels. Since ammonia induced the net HCO_3-flow, sensitive to Sch-28080 and ouabain in the lumen, it could be thought that both H^+/K^+-ATPase isoforms participated in the creation of this response (Gumz et al., 2010).

Ammonia also induces CCD H^+/K^+-ATPase through the inclusion of a membrane vesicle to the apical plasma membrane. Therefore, this activity requires intracellular calcium, microtubule, and a process associated with the transport of a Golgi vesicle. These findings, together

with those found on the induction of K^+ absorption, could imply that ammonia prompted the calcium-dependent H^+ expelling mechanism via an H^+/K^+-ATPase (Gumz et al., 2010).

1.5. H^+/K^+-ATPase Activity in the Context of Na^+ and NH_4 Transport

Diets low in potassium may drive both healthy and hypertensive individuals to NaCl sensitive hypertension. On the other hand, diets with rich potassium have been shown to have a relieving effect on systemic hypertension. Potassium and sodium ions could race for the same absorption itinerary, and for binding on H^+/K^+-ATPase. This has been confirmed using various H^+/K^+-ATPase inhibitors. For example, Sch-28080 and A80915A prevented only the Na^+ absorption in CCDs in rabbits, fed with sodium-free diet (Zhou et al., 1998).

Beside sodium, potassium ions can also support the phosphorylation of H^+/K^+-ATPase, containing HK1, and one or more H^+/K^+-ATPase isoforms can be induced with a sodium-free diet. These findings advocate that H^+/K^+-ATPase could be involved in the reabsorption of sodium ions. H^+/K^+-ATPase could also be seen in a compensatory mechanism against other kidney disorders. The amount of HK2 H^+/K^+-ATPase increased after ischemia-reperfusion injury or with acetazolamide therapy. This increase has been thought to recompensate the negative regulation of cortical and medullary NHE-3. NHE-3 is an apical Na^+/H^+ modifier and it provides more than half of the acid secretion, normally taking place in PT (Wang et al., 1997).

Diets devoid of potassium caused a form of sodium-based hypertension, although the plasma aldosterone levels decreased. This result indicated that some H^+/K^+-ATPase isoforms could participate in NaCl intake. There have been laboratory confirmations suggesting that H^+/K^+-ATPase might work on the CCD with an apical Cl/HCO_3 exchanger. Luminal and cytosolic cation binding regions of different H^+/K^+-ATPase isoforms could be involved in both absorption and reabsorption events (Gumz et al., 2010).

HKα1-null mice developed achlorhydria, hypergastrinemia, gastric epithelial metaplasia, and abnormal gastric mucosa. It seems that similar lines of research are also required in order to elucidate the role of H^+ pumps in the transport of other ions. Some studies have shown that HK2 H^+/K^+-ATPase, besides being a hydrogen pump, could play a very important role in balancing of the colon potassium and act as a Na^+-K^+-ATPase in the column and in sodium absorption of the kidney (Spicer et al., 2000).

1.6. Signal Pathways in the Regulation of H^+/K^+-ATPase

The acute activity of gastric H^+/K^+-ATPase depends on the transport of the enzyme from the intracellular vesicles to the apical membrane of gastric parietal cells. The signals required for this traffic are the secondary messengers such as cAMP, Ca^{+2}, and diacylglycerol. Protein kinases acting in related pathways are protein kinases A and C (PKA, PKC). PKC can phosphorylate HK1 protein at the N-terminal (in Ser 27), and PKA at the C terminal. The first phosphorylation causes an increase in HK1 ATPase activity, and this may play a role in the

transition from E1P to E2-P. Thus, the phosphorylation of the N-terminal can serve as a conformational switch (Cornelius and Mahmmoud, 2003).

In laboratory, phosphorylation of HK1 ATPase with PKA takes place through the tyrosine kinase-Ras-Raf-1-MEK-ERK cascade. Consensus phosphorylation sites for PKA have also been found in HK2 protein. For activation of HK2 H^+/K^+-ATPase through PKA, a protein must be placed on the plasma membrane. Serine 955 in the enzyme may be the region where phosphorylation was performed. Phosphorylation of PKA to HK2 could contribute to the transfer of the enzyme to the plasma membrane (Laroche-Joubert et al., 2003).

1.7. Conformational Features of H^+/K^+-ATPase

Both H^+/K^+-ATPase conformations, E1P and E2-P, are important for the understanding of its pharmacological properties. The crystal structure of Ca^{+2}-ATPase, studied in both conformations, has been used to create models for other P-type ATPases. In these models, in the case of E1, the ion binding regions facing the cytoplasm have been demonstrated to have higher affinity for H^+ than K^+. In E2, however, the ion-binding region, facing the extracellular lumen, had a lower affinity for H^+ than K^+. In its E1 form, H^+/K^+-ATPase is phosphorylated on the cytoplasmic face (E1P). The energy produced by the phosphorylation reaction is used in switching to the E2 state. Here H^+ is extruded into the lumen and phosphorylation is required for K^+ binding. These two events return the enzyme to E1 state. In kidney cells, K^+ binding inhibits the self-phosphorylation of the HKα-subunit by

neutralizing a negative charge. This makes K^+ mandatory for the activity cycle of H^+/K^+-ATPase (Zies et al., 2007).

CONCLUSION: A PHARMACOLOGICAL PERSPECTIVE

Drugs that can strongly suppress gastric proton secretion are favourable agents in the treatment of gastric acid- (Burget et al., 1990) and *Helicobacter pylori* associated (Marshall, 1995) diseases. In humans, the main stimulant of gastric acid secretion is histamine (Black et al., 1972), the H2 receptor antagonists, a well-known therapeutic agent. A certain number of patients however can clinically develop some degree of tolerance; (Smith et al., 1990) for example, 5 to 10% of duodenal ulcer patients may be resistant to H2-receptor antagonists (Bianchi et al., 1988). Proton pump inhibitors (PPIs) are benzimidazoles and they obstruct the gastric proton pump through covalent bonding (McTavish et al., 1991) and thus challenge the problem of tolerance. Since the action of these drugs are required in the acid channel (canaliculus) of the parietal cells, the absolute pH rise effect develops in the stomach within 2-3 days. In fact, parietal cells in resting state are unaffected by the drug; hence, an immediate relieve in the symptom should not expected (Glise et al., 1991). In contrast, it requires covalent bonding to neither proton pump antagonists (PPAs) nor SH groups of the proton pump (Pope and Parsons, 1993). Proton pump antagonists disturb the transport cycle of the proton pump (Mendlein and Sachs, 1990), as they contest for potassium with the domains of the catalytic α-subunit on the surface of the cell. These antagonist compounds can attach to the

unstimulated (resting) pump, i.e., in the absence of ATP (Munson and Sachs, 1988).

Vanadate is a phosphate analogue and irreversibly binds to all P-type ATPases and inactivates. The affinity of the enzyme for vanadate also depends on the conformation of the enzyme. Dephosphorylated H^+/K^+-ATPases have a higher affinity for vanadate in the case of E2. Typical IC50 values for Vanadate were measured in the presence of K^+, and these values range from 10 to 20μM (Zies et al., 2007).

Ouabain is a typical inhibitor of Na^+/K^+-ATPases. The concentrations needed for inhibition vary greatly according to the isoform and species. To illustrate, human Na^+/K^+-ATPases is very sensitive to ouabain; the rodent enzyme is resistant and is completely insensitive to HK α1 ouabain. The sensitivity of HK α2 Na^+/K^+-ATPases to ouabain may depend on the cell type used and the expression system. HK α2 Na^+/K^+-ATPase is sensitive to ouabain in *Xenopus* oocytes; however, it is insensitive to SF9 or HEK 293 cell lines. These findings indicate that the cell environment can alter the sensitivity of HK α2 to ouabain and lead to the expression of an alternative HK α2 transcript with different pharmacological properties (Zies et al., 2007).

In the HK α1 knockout mouse, HK α2 H^+/K^+-ATPase activity has been demonstrated to be sensitive to ouabain. Ouabain sensitive binding site is the cysteine residue at the 8th position. In HK α1 and HK α2 region there is a phenylalanine at this position. This difference may be the reason for their relatively less sensitivity (Zies et al., 2007).

REFERENCES

Abe, K., Tani, K., Friedrich, T. and Fujiyoshi, Y. (2012). Cryo-EM structure of gastric H^+, K^+-ATPase with a single occupied cation-binding site, *Proc. Natl Acad. Sci. USA,* 109, 18401–18406.

Aoyama, F. and Sawaguchi, A. (2011). Functional transformation of gastric parietal cells and intracellular trafficking of ion channels/transporters in the apical canalicular membrane associated with acid secretion, *Biol. Pharm. Bull.*, 34, 813–16.

Bianchi Porro, G. and Parente, F. (1988). Duodenal ulcers resistant to H2 blockers: An emerging therapeutic problem, *Scand J Gastroenterol,* 23(153), 81–88.

Black, J. W., Duncan, W. A. M., Durant, C. J., Ganellin, C. R., Parsons, E. M. (1972). Definition and antagonism of histamine H2-receptors, *Nature*, 236, 385–390.

Burget, D. W., Chiverton, S. G., Hunt, R. H. (1990). Is there an optimal degree of acid suppression for healing of duodenal ulcers? A model of the relationship between ulcer healing and acid suppression, *Gastroenterology*, 99, 345–351.

Campbell, W. G., Weiner, I. D., Wingo, C.S., Cain, B.D. (1999). HK-ATPase in the RCCT-28A rabbit cortical collecting duct cell line, *Am J Physiol Renal Physiol.*, 276, 237–245.

Chalhoun, B. C and Goldenring, J. R. (1997). Two Rab proteins, vesicle-associated membrane protein 2 (VAMP-2) and secretory carrier membrane proteins (SCAMPs), are present on immunoisolated parietal cell tubulovesicles, *Biochem. J.*, 325, 559-564.

Codina, J. and Dubose, T. D. (2006). Molecular regulation and physiology of the H^+, K^+-ATPases in kidney, *Semin. Nephrol.*, 26(5), 345 -351.

Cornelius, F. and Mahmmoud, Y. A. (2003). Direct activation of gastric H,K-ATPase by N-terminal protein kinase C phosphorylation. Comparison of the acute regulation mechanisms of H,K-ATPase and Na,K-ATPase. *Biophys J.*, 84, 1690–1700.

Forte, J. G. and Zhu, L. (2010). Apical recycling of the gastric parietal cell H, K-ATPase *Annu. Rev. Physiol.*, 72, 273-296.

Glise, H., Martinson, J., Solhaug, J. H., Carling, L., Unge, P., Engström, G, Hallerbäck, B. (1991). Two and four weeks' treatment for duodenal ulcer, Symptom relief and clinical remission comparing omeprazole and ranitidine. *Scand J Gastroenterol*, 26, 137–145.

Gumz, M. L., Lynch, I. J., Greenlee, M. M., Cain, B. D., Wingo, C. S. (2010). The renal-ATPases: physiology, regulation, structure, *Am J Physiol Renal Physiol,* 298, 12–21.

Heitzmann, D., Grahammer, F., von Hahn, T., Schmitt-Gräff, A., Romeo, E., Nitschke, R, Gerlach, U., Lang, H. J., Verrey, F., Barhanin, J., Warth, R. (2004). Heteromeric KCNE2/KCNQ1 potassium channels in the luminal membrane of gastric parietal cells, *J. Physiol,* 561, 547-557.

Kaufhold, M. A., Krabbenhöft, A., Song, P., Engelhardt, R., Riederer, B., Fährmann M, Klöcker, N. Beıl, W., Manns,M., Hagen, S. J., Seıdler, U. (2008). Localization, trafficking, and significance for acid secretion of parietal cell Kir4. 1 and KCNQ1 K^+ channels, *Gastroenterology*, 134, 1058-1069.

Kone, B. C. and Higham, S. C. (1998). A novel *N*-terminal splice variant of the rat H^+-K^+-ATPase α 2 subunit. Cloning, functional expression, and renal adaptive response to chronic hypokalemia, *J. Biol. Chem.*, 273 (5), 2543-2552.

Laroche-Joubert, N., Marsy, S., Luriau, S., Imbert-Teboul, M., Doucet, A. (2003). Mechanism of activation of ERK and H-K-ATPase by isoproterenol in rat cortical collecting duct, *Am J Physiol Renal Physiol*, 284, 948–954.

Lee, M. P., Ravenel, J. D., Hu, R. J., Lustig, L. R., Tomaselli, G., Berger, R. D., *et al.* (200). Targeted disruption of the Kvlqt1 gene causes deafness and gastric hyperplasia in mice, *J. Clin. Invest.,* 106, 1447-1455.

Malonev, P. D., Kashket, E. R. and Wilson, T. H. (1974). A Protonmotive Force Drives ATP Synthesis in Bacteria, *Proc. Natl. Acad. Sci. U. S. A.*, 71, 3896–3900.

Marshall, B. J. (1995). Managing acid peptic disease in the *Helicobacter pylori* era, *J Clin Gastroenterol*, 21(1), 155–159.

McTavish, D., Buckley, M. M. T., Heel, R. C. (1991). Omeprazole. An updated review of its pharmacology and therapeutic use in acid-related disorders, *Drugs*, 42, 138–170.

Melle-Milovanovic, D., Milovanovic, M., Nagpal, S., Sachs, G., Shin, J. M. (1998). Regions of association between the alpha and the beta subunit of the gastric H,K-ATPase, *J Biol Chem.,* 273, 11075–11081.

Mendlein, J. and Sachs, G. (1990). Interaction of a K+- competitive inhibitor, a substituted imidazo[1,2a]pyridine, with the phospho- and dephosphoenzyme forms of H^+,K^+-ATPase, *J Biol Chem.,* 265, 5030–5036.

Modyanov, N. N., Mathews, P. M., Grishin, A.V., Begui,n P., Beggah, A. T., Rossier, B. C., *et al.* (1995). Human ATP1AL1 gene encodes a ouabain-sensitive H-K-ATPase, *Am. J. Physiol.,* 269 (4), 992 -997.

Munson, K. B. and Sachs, G. (1988). Inactivation of H^+,K^+- ATPase by a K+- competitive photoaffinity inhibitor, *Biochemistry*, 27, 3932–3938.

Pope, A. J. and Parsons, M. E. (1993). Reversible inhibitors of the gastric H^+/K^+-transporting ATPase: A new class of anti-secretory agent, *Trends Pharmacol Sci.,* 14, 323–325.

Rabon, E. C., McFall, T. and Sachs, G. (1982). The gastric [H,K]ATPase:H^+/ATP stoichiometry, J. *Biol. Chem.*, 257, 6296–6299.

Reuben, M. A., Lasater, L. S., Sachs, G. (1990). Characterization of a beta subunit of the gastric H+/K(+)-transporting ATPase, *Proc Natl Acad Sci U S A.,* 87, 6767–6771.

Roepke, T. K., Anantharam, A., Kirchhoff, P., Busque, S. M., Young, J. B., Geibel, J. P., *et al.*(2006). The KCNE2 potassium channel ancillary subunit is essential for gastric acid secretion. *J. Biol. Chem.*, 281, 23740-23747.

Sachs, G., Chang, H. H., Rabon, E., Schackman, R., Lewin, M., Saccomani, G. (1976). A non-electrogenic H' pump in plasma membranes of hog stomach. *J Biol Chemt.,* 251, 7690-8.

Sachs, G., Meyer-Rosberg, K., Scott, D. R., Melchers, K. (1996). Acid, protons and Helicobacter pylori, *Yale J. Biol. Med*., 69, 301–316.

Scarborough, G. A. (1977). Properties of the *Neurospora crassa* plasma membrane ATPase, *Arch. Biochem. Biophys.,* 180, 384-393.

Shin, J. M., Munson, K., Vagin, O., Sachs, G. (2009). The gastric HK-ATPase: structure, function, and inhibition, *Pflugers Arch.,* 457, 609–22.

Shull, G. E. and Lingrel, J. B. (1986). Molecular cloning of the rat stomach (H^++K^+)-ATPase, *J. Biol. Chem.*, 261(36), 16788 -16791.

Silver, R. B. (1999). Soleimanim M. H^+ -K^+ -ATPases: regulation and role in pathophysiological states, *Am. J. Physiol.*, 276 (6), 799 -811.

Smith, J. T. L., Gavey, C., Nwokolo, C.U., Pounder, R.E. (1990). Tolerance during 8 days of high-dose H2- blockade: Placebo-controlled studies of 24- hour acidity and gastrin, *Aliment Pharmacol Ther,* 4(1), 47–63.

Spicer, Z., Miller, M. L., Andringa, A., Riddle, T. M., Duffy, J. J., Doetschman, T., Shull, G. E. (2000). Stomachs of mice lacking the gastric H,K-ATPase alphasubunit have achlorhydria, abnormal parietal cells, and ciliated metaplasia, *J Biol Chem.*, 275, 21555–21565.

Sweadner, K. J. and Donnet, C. (2001). Structural similarities of Na,KATPase and SERCA, the Ca($^{2+}$)-ATPase of the sarcoplasmic reticulum. *Biochem J.*, 356, 685–704.

Wallmark, B., Briving, C., Fryklund, J., Munson, K., Jackson, R., Mendlein, J., *et al*. (1987). Inhibition of gastric H$^+$,K$^+$-ATPase and acid secretion by SCH 28080, a substituted pyridyl(1,2a)imidazole, *J Biol Chem.,* 262, 2077–2084.

Wang, Z., Rabb, H., Craig, T., Burnham, C., Shull, G. E., Soleimani, M. (1997). Ischemic-reperfusion injury in the kidney: overexpression of colonic H$^+$-K$^+$-ATPase and suppression of NHE-3, *Kidney Int.*, 51, 1106–1115.

Wolosin, J. M. (1985). Ion transport studies with H+-K+-ATPase-rich vesicles: implications for HCl secretion and parietal cell physiology, *Am. J. Physiol. Gastrointest. Liver Physiol.,* 248, 595–607.

Yamamoto, K., Dubey, V., Irie, K., Nakanishi, H., Khandelia, H., Fujiyoshi, Y., Abe, K. (2019). A single K-binding site in the crystal structure of the gastric proton pump, Elife 8, undefined. doi: 10.7554/eLife.47701

Yao, X. and Forte, J. G. (2003). Cell biology of acid secretion by the parietal cell, *Annu. Rev. Physiol.*, 65, 103-131.

Zhou, X., Xia, S. L., Wingo, C. S. (1998). Chloride transport by the rabbit cortical collecting duct: dependence on H,K-ATPase, *J Am Soc Nephrol*., 9, 2194–2202.

Zies, D. L., Gumz, M. L., Wingo, C. S., Cain, B. D. (2007). The renal H,K-ATPases as therapeutic targets, *Expert Opin Ther Targets,* 11, 881– 890.